The Islamic University–Gaza

Research and Postgraduate Affairs

Faculty of Engineering

Master of Electrical Engineering

Communication Systems

الجامعـــــــة الإســـلاميـة – غـزة

شئون البحث العلمي والدراسات العليا

كليـــة الـهنـــدســـــــــــــة

ماجستيـر الـهندســة الكهربائيـــة

أنظـــمة اتصـــــــــــــالات

Design of Reconfigurable Microstrip Filtering Antenna

تصميم مرشح هوائي باستخدام الشرائح الرقيقة مع خاصية اعادة التشكيل للمواصفات

Salem khames Alothmani

Supervised by

Dr. Talal Skaik

Assistant prof. of Electrical Engineering

A thesis submitted in partial fulfillment
of the requirements for the degree of
Master of Electrical Engineering – Communication Systems Engineering

April/2017

إقـــــرار

أنا الموقع أدناه مقدم الرسالة التي تحمل العنوان:

Design of reconfigurable microstrip filtering antenna

تصميم مرشح هوائي باستخدام الشرائح الرقيقة مع خاصية اعادة التشكيل للمواصفات

أقر بأن ما اشتملت عليه هذه الرسالة إنما هو نتاج جهدي الخاص، باستثناء ما تمت الإشارة إليه حيثما ورد، وأن هذه الرسالة ككل أو أي جزء منها لم يقدم من قبل الاخرين لنيل درجة أو لقب علمي أو بحثي لدى أي مؤسسة تعليمية أو بحثية أخرى.

Declaration

I understand the nature of plagiarism, and I am aware of the Uuniversity's policy on this. The work provided in this thesis, unless otherwise referenced, is the researcher's own work, and has not been submitted by others elsewhere for any other degree or qualification.

Student's name:	سالم خميس العثماني	اسم الطالب:
Signature:	سالم العثماني	التوقيع:
Date:	17/7/2017	التاريخ:

بسم الله الرحمن الرحيم

الجامعة الإسلامية غزة
The Islamic University of Gaza

مكتب نائب الرئيس للبحث العلمي والدراسات العليا هاتف داخلي 1150

الرقم: ج س غ/35/ Ref:

التاريخ: 2017/06/14م Date:

نتيجة الحكم على أطروحة ماجستير

بناءً على موافقة شئون البحث العلمي والدراسات العليا بالجامعة الإسلامية بغزة على تشكيل لجنة الحكم على أطروحة الباحث/ **سالم خميس ابراهيم العثماني** لنيل درجة الماجستير في **كلية *الهندسة*** قسم **الهندسة الكهربائية – أنظمة الاتصالات** وموضوعها:

تصميم مرشح هوائي باستخدام الشرائح الرقيقة مع خاصية اعادة التشكيل للمواصفات

Design of Reconfigurable Microstrip Filtering Antenna

وبعد المناقشة التي تمت اليوم الأربعاء 19 رمضان 1438هـ، الموافق 2017/06/14م الساعة الحادية عشر والنصف صباحاً، اجتمعت لجنة الحكم على الأطروحة والمكونة من:

د. طلال فايز سكيك	مشرفاً و رئيساً	.....
د. عمار محمد أبو هدروس	مناقشاً داخلياً	.....
د. مصطفى حسن أبو نصر	مناقشاً خارجياً	.....

وبعد المداولة أوصت اللجنة بمنح الباحث درجة الماجستير في كلية *الهندسة*/ قسم **الهندسة الكهربائية – أنظمة الاتصالات.**

واللجنة إذ تمنحه هذه الدرجة فإنها توصيه بتقوى الله ولزوم طاعته وأن يسخر علمه في خدمة دينه ووطنه.

والله ولي التوفيق،،،

نائب الرئيس لشئون البحث العلمي والدراسات العليا

أ.د. عبدالرؤوف علي المناعمة

شئون البحث العلمي والدراسات العليا
Research & Graduate Affairs

Abstract

This thesis presents antenna with pattern and frequency reconfiguration characteristic. The antenna structure proposed here is a bow tie antenna combined with a microstrip bandpass filter. Pattern reconfiguration is achieved by switches and microstrip triangular segments added to the antenna, and frequency reconfiguration can be obtained by the bandpass filter integrated within the feeding line of the antenna. The filter is designed using open loop resonators with variable varactors to choose the required center frequency. The operating band of antenna is from 1.80 GHz to 2.75 GHz and thus recovering Global System Mobile (GSM), Universal Mobile Telecommunication System (UMTS), Wireless Fidelity (Wi-Fi) and Long Term Evolution (LTE) frequencies. The antenna is designed using CST simulation software. The frequency and the pattern reconfiguration are achieved successfully.

Keywords: Bow tie antenna, microstrip filter, resonators, pattern reconfigurable, frequency reconfigurable, band width from 1.80 GHz to 2.75 GHz and CST Microwave Studio.

ملخص البحث

تقدم هذه الأطروحة هوائي بخصائص إعادة تشكيل التردد والنمط الاشعاعي ، والهوائي المقترح هنا هو (ربطة القوس) جنبا الى جنب مع مرشح التغيير الدقيق.

إعادة تشكيل النمط الإشعاعي يتم بواسطة مفاتيح وقطع تضاف الى تصميم الهوائي من جهة الأرضي ، وإعادة تشكيل التردد يتم بواسطة مرشح التغيير الدقيق مصمم من حلقة مفتوحة من كاشفات موجات هرتزيه مزود بمكثفات متغيرة من أجل اختيار التردد المطلوب ضمن نطاق تشغيل الهوائي.

نطاق تشغيل الهوائي يعمل من 1.8 جيجاهرتز الى 2.75 جيجاهرتز وهذا يغطي النظام العالمي للاتصالات المتنقلة (الجيل الثاني) ، النظام العالمي للاتصالات المتنقلة (الجيل الثالث) ، الاتصال اللاسلكي للشبكات المحلية ونظام تطور طويل الأمد ، النتائج المحاكاة بواسطة برنامج رسام الموجات الدقيقة تظهر شكل ، اتجاه وقوة الطاقة للنمط الاشعاعي واداء مرشح التغيير الدقيق في اختيار التردد المطلوب.

Dedication

This thesis is dedicated firstly to my mother who stand with me on all my life stages, to my wife who encourages me to complete my high studies, to my children who increase my life beauty and to all my family

Acknowledgment

First, I would like to thank my God for giving me the strength to complete this work, I am grateful to my supervisor Dr. Talal Skaik for his advices , guidance , standing with me in all stages in this research.

Also I would thank my thesis discussion members, Dr. Ammar Abu- Hadrous and Dr. Mustafa Abu Nasser for their advices and constructive notes which leading me to complete my work.

Thanks to all people who motivated and supported me to complete this work .

Table of Contents

List of Tables

List of Figures

List of Abbreviations

CST	Computer System Technology
dB	decibel
dBi	decibel isotropic
EGP	Electromagnetic Band Gap
VSWR	Voltage Standing Wave Ratio
CPW	Co-Planar Wave guide
WLAN	Wireless Local Area Network
WIMAX	Worldwide Interoperability for Microwave
ITU	International Telecommunication System
IEEE	Institute of Electrical and Electronics Engineers
RF-MEMs	Radio Frequency Micro ElectroMechanical systems
ASA	Annular Slot Antenna
BPF	Band Pass Filter
MSA	Microstrip Antenna
HPBW	Half Power Beam Width
FNBW	First Null Beam Width
RH	Right Hand
LF	Left Hand
Wi-Fi	Wireless Fidelity
GPR	Ground Penetrating Radar
RFID	Radio Frequency Identification
MoM	Method of Moment
FBW	Fractional Beam Width

Chapter 1
Introduction

Chapter 1

Introduction

1.1 Background

With the development in the wireless communications , there is big demand to antennas that are smart and their characteristics can be tuned (pattern, frequency, polarization) according to system requirements. Reconfigurable antennas have been studied at last two decades and this type of antennas contains switching elements to change electrical properties of antenna. Electrically reconfigurable antennas use PIN diodes, or varactors to perform the required tunability in the antenna functionality. The activation/deactivation of these switching elements requires the incorporation of biasing lines in the radiating plane of the antenna.

Smart antenna differs from reconfigurable antennas because the reconfiguration lies inside the antenna rather than the external beam forming the network . The capability of reconfigurable antennas is used to improve and maximize the antenna performance to satisfy changing in operating requirements.

1.2 Types of Antenna Reconfiguration

The reconfiguration of the antenna can be sorted based on antenna parameters , radiation pattern , frequency of operation and polarization.

- Pattern reconfiguration
- Frequency reconfiguration
- Polarization reconfiguration
- Compound reconfiguration

1.2.1 Pattern Reconfiguration

Pattern reconfigurable is based on the modification of distribution of radiation pattern. The most common application for this reconfiguration is beam steering which consists of steering of the direction of maximum radiation to maximize the antenna gain. Pattern reconfigurable is used in rotating structures and almost including switchable and parasitic elements.(Aboufoul, Alomainy, Chen and Parini (2013).

1.2.2 Frequency Reconfiguration

Frequency reconfigurable is used in antenna to adjust their frequency of operation , and this reconfiguration can be used in several communication systems converge because the multiple antennas required can be replaced by a single reconfigurable antenna. Frequency reconfiguration is implemented by using RF switches (Panagamuwa, Chauraya, and Vardaxoglou. 2006). Impedence loading (Erbil, Tonally, Ulna, Civil, and Akin, 2007).Or tunable materials(Liu, and Langley, 2008).

1.2.3 Polarization Reconfiguration

The polarization reconfigurable is switching between different modes of polarization such as switching between vertical , horizontal and elliptical polarization. The capability of switching between horizontal, vertical and circular polarizations can be used to reduce polarization mismatch losses in portable devices. (Simons, Donghoon, and Katehi, 2002).

1.2.4 Compound Reconfiguration

Compound reconfiguration is the combination of multi-mode of reconfigurable characteristics . The most common mode of compound reconfigurable is the combination between the frequency and pattern to improve the operating characteristic of antenna. Compound reconfigurable can be achieved by combining

between different single reconfiguration technique. (Aboufoul , Chen, Parini, and Alomainy, 2014)

1.3 Advantages and Disadvantages of Reconfigurable Antenna

Advantage of reconfigurable antenna :

1. Antenna can operate in many bands and this is very useful for different applications.
2. Easy to integrate with switching devices and control circuit.
3. Small in size.

The disadvantage of reconfigurable antenna are:

1. The reconfigurable antenna is largely depend on RF switches techniques.
2. More complex for some devices like mobile phone.
3. In some applications it decreases the efficiency.(Christodoulou, Tawk , Lane and Erwin , 2012)

1.4 Thesis Motivation

Many wireless systems use reconfigurable antenna for many reasons such as low power consumption , low construction cost. For normal antenna without reconfiguration there are some problems occur like rapidly changing of propagation channel and this need multiple antenna to force that problem , so reconfigurable antenna can be used to solve that problem without need to multiple antenna (Costantine and Christodoulou , 2012). Most research concentrated on frequency or radiation pattern reconfigurable ,but the combination of reconfigurable frequency and pattern in one antenna is the main motivation for the current work on this topic. A bow-tie antenna is used here and frequency reconfiguration is achieved by

adding a tunable filter within the feeding line for the antenna as shown in figure 1.1. Moreover, pattern reconfiguration is achieved by using PIN diodes to connect some parasitic elements in the antenna structure.

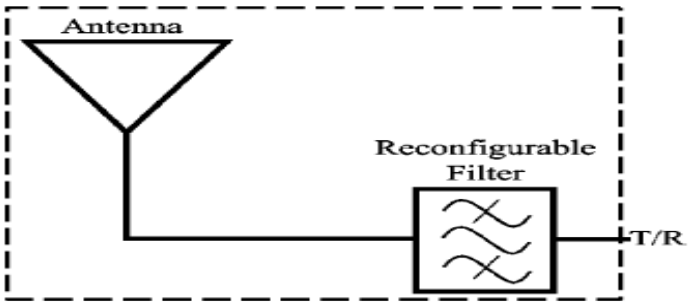

Figure(1.1): Antenna system with reconfigurable filter

1.5 Contribution

The main target for this thesis is a design a bow tie antenna with reconfigurable characteristic in frequency and pattern . Most of studies presented reconfigurability in one parameter , pattern , frequency or polarization. The combination of frequency and pattern reconfiguration are presented in this work to improve the features of antenna. Moreover , reconfigurable antennas that had been reported in literature were certain types of patch antenna and didn't use bow tie antenna as reconfigurable antenna. Here in this work the antenna structure is bow tie antenna with combination of frequency and pattern reconfigurable. A novel bow-tie reconfigurable structure is presented in this thesis.

1.6 Literature Review

1.6.1 Pattern Reconfigurable

There are many of the studies on pattern re-configurable antenna**:**

In (Sarrazin, Mahe, Avrillon and Toutain 2014), the pattern reconfiguration is achieved with PIN diode switches by short-circuiting slots in their center. A prototype of the antenna, including PIN diodes and operating in the 5 GHz band, has been built to demonstrate the feasibility of the concept.

Measurements have been conducted and three-dimensional radiation patterns are provided. Diversity performances are evaluated by calculating the envelope correlation coefficient. However, this design only introduced pattern reconfiguration.

However this design can be operated only for 5 GHz without extension in the bandwidth.

In (Majid, Rahim, Hamid, Murad, Samsuri, Kamarudin and Yosof 2014), a radiation pattern reconfigurable monopole antenna using Electromagnetic Band-Gap (EBG) Structure is proposed.. The EBG characteristic can be manipulated by controlling the state of switch. The switch is positioned between the EBG's via and the ground plane. By controlling the state of EBGs, the radiation pattern can be reconfigured to an omni-directional pattern and four directional pattern with different angles. this design only introduced pattern reconfiguration.

The proposed structure is operated on (EBG) principle and it is difficult compared to other structures.

In (Nasrabadi and Rezaei 2013), a novel radiation pattern reconfigurable antenna using a central circular patch and four parasitic patches. The radiation pattern of the proposed antenna can changed into three modes. Changing the mode of antenna is done by four pin diode switches that are located in gaps of parasitic rectangular patch .by means of simple electrical arrangement a short or open circuit can be provided in the gap. The designed antenna works in 5.8GHz frequency band and its bandwidth is 2.2 GHz.

However the pin diode switches that are located in gaps of parasitic rectangular patch are added more complexity in the design.

In (Li 2012), a pattern reconfigurable antenna is designed , its performance is testified by the simulation results, 0°,25°,40°and 50°beam direction can be achieved by the antenna, Voltage Standing Wave Ratio (VSWR) under each

of these four different states is less than 2 from 2.5 GHz to 3.25 GHz except for part frequency points .this design is important for beam scanning of phased array antenna in satellite communication.

The band width of proposed antenna is seemed narrow compared with other antennas which are operated in this field.

In (Bai, Xiao, Tang, Liu and Wang 2011), a novel pattern reconfigurable patch antenna with a microstrip configuration is proposed. The antenna consists of a disc patch, a ring and eight radially symmetrically distributed microstrip monopoles .The patterns are reconfigured by shifting the states of the eight switches and eight reconfigurable states are available. Each conical pattern around the broadside of the antenna has a wide beam width in the azimuth plane and the eight reconfigurable patterns can cover continuously the space in the horizontal plane. The performance is very advantageous for smart antenna applications on future mobile terminals.

The disadvantage for this design is a wide beam width which it can be reduced the directivity in the given direction.

In (John, Shynu and Ammann 2010), the design and operating principle of a pattern reconfigurable multi-mode slot antenna with a hybrid feed. The slot antenna is excited by an orthogonal arrangement of a Co-Planar Waveguide (CPW) fed circular disc and a microstrip fed square patch. The design objective is to be able to change the direction of the main lobe by feeding the two orthogonal elements with different phases. However, this design only introduced pattern reconfiguration.

However the pattern reconfigurable by hybrid feed is added more complexity in the operation of proposed antenna.

1.6.2 Frequency Reconfigurable

There are many of the studies on frequency re-configurable antenna**:**

In (Zou, Shen and Pan 2016)**,** a circularly polarized frequency-reconfigurable water antenna with high radiation efficiency is proposed based on the design concept of combining a frequency-reconfigurable radiating structure with a frequency-independent feeding structure. A resonator made of distilled water and an Archimedean spiral slot are employed as the radiating and feeding structures, respectively. The operating frequency of the antenna can be continuously tuned over a very wide range while maintaining good impendence matching and circular polarization by changing the dimensions of the water resonator.

However this design is considered advanced design which operated by Archimedean spiral slot.

In (Liu, Yang and Kong 2015), a frequency-reconfigurable coplanar-waveguide (CPW) fed monopole antenna using switchable stubbed ground structure is presented. Four PIN diodes are employed in the stubs stretching from the ground to make the antenna reconfigurable in three operating modes: a single-band mode (2.4-2.9 GHz), a dual-band mode (2.4 to 2.9 GHz/5.09-5.47 GHz) and a triple-band mode (3.7 to 4.26 GHz/5.3-6.3 GHz/8.0-8.8 GHz). The monopole antenna is resonating at 2.4 GHz, while the stubs produce other operating frequency bands covering a number of wireless communication systems, including Wireless Local Area Network (WLAN), Worldwide Interoperability for Microwave Access (WiMAX), Cband, and International Telecommunication Union (ITU).

The proposed structure can be operated in different bands covering a number of wireless communication systems and it is a good advantage for this design.

In (Majid, Rahim, Hamid, and Ismail 2014), frequency reconfigurable slot-patch antenna with reflector at the back of an

antenna is presented. The proposed antenna consists of a microstrip patch antenna and a microstrip slot antenna where the slot antenna is positioned at the ground plane underneath the patch. Three switches are placed in the slot. The antenna is capable to reconfigure up to six different frequency bands from 1.7 GHz to 3.5 GHz.

However the design depend on two antennas and it is better if the design depend on one antenna in this kind of structure.

In (Perma and Gayatri 2013), the reconfigurable antenna consists of five different antenna patches on the same circular substrate. The frequency reconfigurable is achieved by rotating the antenna patch. The rotational motion is brought about by the stepper motor attached at the back of the circular substrate. The two antennas are fabricated on the same substrate and fed at the opposite edges of the substrate. However the advantage of this antenna is that there is no need of bias lines as in the case of Radio Frequency Micro Electromechanical System (RF-MEMS), pin-diodes or lumped elements.

In (Cheng, Wang, Liu and Zhu 2013), a novel microstrip antenna with the frequency reconfiguration characteristic is proposed. A U-slot has been introduced in the square patch. The slot is switched on and off by using three PIN diodes, which realizes the frequency reconfiguration characteristics. The antenna can operate at six different frequencies with similar radiation patterns. The antenna has 2 dB gain flatness with the maximum gain being 5 dB over the whole range. However the gain of this antenna is small and it is needing to rise up.

1.6.3 Pattern and Frequency Reconfigurable

There are many of the studies on pattern and frequency re-configurable antenna**:**

In (Trong, Hall and Fumeaux 2016), a frequency- and pattern-reconfigurable antenna based on a center-shorted microstrip patch is presented. The novel design utilizes two resonance modes of a microstrip

antenna with shorting at the patch center. To set up the antenna tuning mechanism, two groups of varactors with a measured tuning range of [0.149, 1.304] pF are placed at two opposite sides of the antenna, followed by open-circuited loading stubs. For a particular bias voltage configuration, the structure operates as a dual-band antenna with broadside radiation at the upper resonance frequency and monopole-like radiation at the lower band. By varying the dc bias voltage, both resonance frequencies can be changed simultaneously. Based on the proposed concept, a demonstration antenna has been designed so that the two types of aforementioned patterns can be reconfigured across a continuous fractional frequency range of more than 20%. However , the patterns are reconfigured over fractional frequency range by 20% is considered small ratio for operation.

In (Li, Bao, Si and Yingsong 2014), a dielectric embedded antenna with hybrid reconfigurable characteristics is proposed for portable wireless terminal applications, which is used as frequency or radiation reconfigurable antenna. The proposed hybrid reconfigurable antenna consists of a driven element, two parasitic elements and eight switches. By controlling the ON/OFF states of these switches set on the driven element, the proposed antenna can operate at two different frequencies, namely, 0.85 GHz and 1.9 GHz. The radiation reconfigurable characteristic is achieved by switching six switches installed on the parasitic elements.

In (Majid, Rahim, Hamid and Ismail 2012), a novel frequency and pattern microstip reconfigurable Yagi antenna is proposed. The antenna is formed by a driver, a reflector and two directors. The introduction of switches using a PIN diode at the arms of the driver element produces three switchable frequencies at 1.25 GHz, 1.85 GHz and 2.45 GHz. By controlling the switches at the directors and reflector, the radiation pattern can be configured to near Omni-directional pattern or directional pattern at those three frequencies.

The proposed antenna can be operated at other frequency bands by controlling the switches at the directors and reflectors.

In (Yang, Wang, Xiao and man 2008), the microstrip Yagi antenna is fabricated on the top side of a grounded substrate and is fed by a coaxial probe. By using switches to reconfigure the silts etched on the driven patch, the antenna can operate at two frequencies of 8.175 and 9.31 GHz. By changing the states of the slots etched on different parasitic element patches, directions of the radiation pattern can be changed. However , the proposed antenna is fed by coaxial probe and it is introduced more complexity of matching process.

In (Nikolaou, Bairavasubramanian, Lugo, Carrasquillo, Thompson, Ponchak, Papapolymerou and Tentzeris 2006), the planar antenna is fabricated on one side of a Duroid substrate and the microstrip feeding line with the matching network is fabricated on the opposite side of the board. The central frequency is 5.8 GHz and, by reconfiguring the matching circuit, the antenna was also designed to operate at 5.2 and 6.4 GHz. Pin diodes are also used to short the Annular Slot Antenna(ASA) in preselected positions along the circumference, thereby changing the direction of the null in the plane defined by the circular slot changes. Two pin diodes are placed 45 on both sides of the feeding line along the ASA and the direction of the null is shown to align with the direction defined by the circular slot center and the diode. Consequently, a design that is reconfigurable in both frequency and radiation pattern is accomplished. However the reconfiguration through the matching circuit caused more difficult in operation of proposed antenna.

1.6.4 Reconfigurable Filtering Antenna

There are many of the studies on reconfigurable filtering antenna :

In (Zainuddin, Mat and Roslan 2016), design of integrated filter antenna for 2.4GHz microwave applications. Open loop resonator bandpass filter is designed to increase the bandwidth of the antenna by producing the range of frequencies that can be accepted by the antenna structure. However direct connection between the filter structure and antenna may cause impedance mismatch and deteriorates the performance of both antenna and

filter. Thus, by integrating both filter and antenna into a single module, the overall performance can be improved and increase the efficiency of the system with improved bandwidth .

In (Vijayashanthi, Jayanandan, and Roshini 2015), a new compact filter and a microstrip antenna is proposed for Institute of Electrical and Electronics Engineers IEEE 802.11 applications. Here the size of the three pole hair pin Band Pass Filter (BPF) is approximately reduced from 6.83 cm to 5.81 Cm, The three pole hair pin BPF designed at center frequency 1.97 GHz achieves an impedance bandwidth of 5.16 % (over 1.6 – 2.4 GHz) at a reflection coefficient $|S_{11}| < -20$ dB and has a gain of 0.44 dB. Also the size of the designed antenna is nearly 45 mm x 35 mm on TRF substrate with relative permittivity of 4.1 dB. The antenna has a resonance frequency of 2.14 GHz with a gain of 0.15 dB. However the gain of proposed antenna is small and the size is big.

In (Muthu, Dhivyaa and Thenmozhi 2014), multiband antenna can be reconfigured for five different frequencies without any changes in resonant modes is proposed. This reconfigurability is done by band-pass filter that is integrated on the feed line of the antenna. Filter is of T- shaped defected structure with switches which helps in switching the frequency. This structure consists of dual sided tapered antenna which helps in remaining very less distortion. This type of antenna can be used for application like cognitive radios which makes use of free white space available on the spectrum .

In (Zuo, Wu and Zhang 2013), a simple microstrip filtering-antenna with compact size for WLAN application. The T-shape resonator through an inset coupling structure can be treated as the admittance inverter and the equivalent circuit of the filtering-antenna is exactly the same as the bandpass filter prototype. With a little extra circuit area, the proposed filltering-antenna has almost twice wider bandwidth, good skirt selectivity and high

suppression in the stopband compared to the conventional microstrip antenna. However if U-shape resonators are used may be reduced the size of proposed structure.

In (Lugo and Papapolymerou 2006), a six-state reconfigurable band-pass filter intended to add frequency tunability to antenna systems is presented. The present topology produces filter responses with center frequencies of f_o= 9, 10, and 11 GHz and achieves independent bandwidth control with an average tunable passband ratio of 1.73:1 between the wideband configurations ranging from 13.4% and 14.7% and the narrowband configurations ranging from 7.7% and 8.5%. PIN diodes are implemented as switching elements and the distinct states are discretely accomplished by the connection and isolation of strategically placed transmission line sections. The insertion loss of the filter ranges between 1.74 and 1.92 dB.

All the previous structures doesn't use the bow tie antenna for the pattern or frequency reconfiguration.

1.7 Structure of the Thesis

Chapter 1: presents introduction , types of antenna reconfiguration , advantages and disadvantages of reconfigurable antenna , motivation , contribution , literature Review .

Chapter 2: presents antenna Theory , and it contains background , antenna types, Maxwell's equations , antenna parameters and design equations for microstrip bow-tie antennas.

Chapter 3: shows filter theory , including types of filters ,low pass prototype , frequency and element transformation and design procedures of microstrip filters..

Chapter 4: presents design of reconfigurable antenna , design of Bow-tie antenna , design of filter , design of frequency reconfigurable filtering antenna , design of pattern reconfigurable antenna , design of pattern and frequency reconfigurable filtering antenna.

Chapter 5: presents conclusions and comments on the results of the simulations and provides a summary of the main contributions and findings of the study and concludes the accomplished work packages. It also introduces suggestions for future research activities.

Chapter 2

Antenna Theory

Chapter 2

Antenna Theory

In this chapter a theory of antennas is introduced, allowing the comprehension of its main features, types and parameters. Finally, a study of the Bow-Tie antennas and their advantages and disadvantages will be presented .

2.1 Background

If two people want to communicate who are at longer distances, then we have to convert these waves into electromagnetic waves. The device, which converts the required information signal into electromagnetic waves, is known as an Antenna. An antenna is a transducer, which converts electrical power into electromagnetic waves and vice versa. An antenna can be used either as a transmitting antenna or a receiving antenna.

- A **transmitting antenna** is one, which converts electrical signals into electromagnetic waves and radiates them.
- A **receiving antenna** is one, which converts electromagnetic waves from the received beam into electrical signals.
- In two-way communication, the same antenna can be used for both transmission and reception.

The function of an antenna is power radiation or reception as shown in figure 2.1. Antenna (whether it transmits or receives or does both) can be connected to the circuitry at the station through a transmission line. The functioning of an antenna depends upon the radiation mechanism of a transmission line.

A conductor, which is designed to carry current over large distances with minimum losses, is termed as a transmission line. For example, a wire, which is connected to an antenna. A transmission line conducting current with uniform velocity, and the line being a straight one with infinite

extent, radiates no power. For a transmission media, to become a waveguide or to radiate power, has to be processed as such.

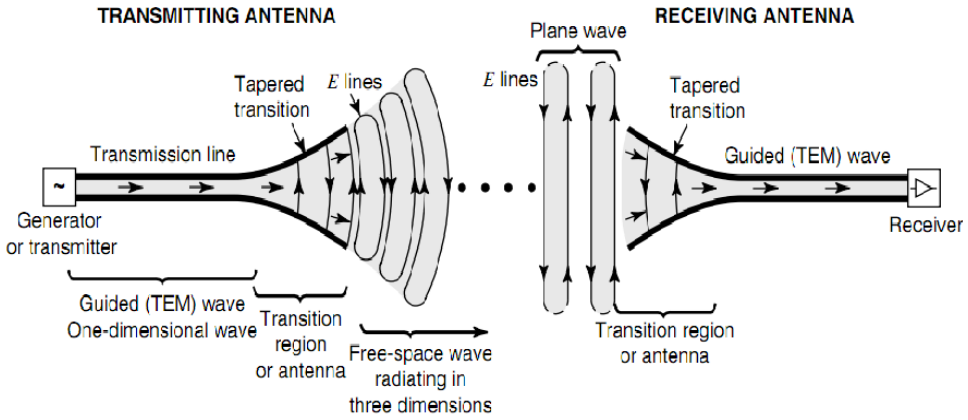

Figure (2.1) : The antenna as a transition structure for a transmitting antenna and for a receiving antenna

2.2 Basic Types of Antennas

1. **Wire antennas** which are the most famous and popular kind of antennas to people that it can be seen almost everywhere (cars, buildings, ships, TVs, radios, some mobiles and so on. It can be in different shapes like straight wire (dipole), loop, and helix as shown in Figure 2.2. (Balanis, 2005).

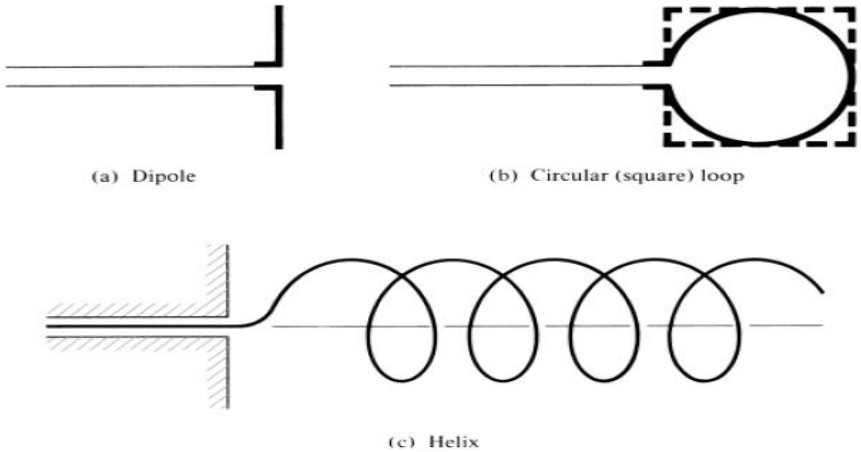

Figure (2.2): Wire antenna configurations

2. **Aperture antennas** that are developed because of the need to more complex forms and usage for higher frequencies than wired antennas as shown in Figure 2.3. These antennas are very useful in aircraft and spacecraft applications because they can be covered with a dielectric material to protect them from dangerous conditions from high speed environment. (Balanis, 2005).

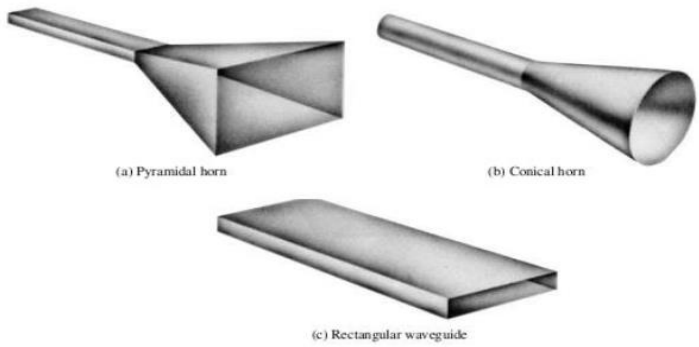

Figure (2.3): Aperture antenna configurations

3. **Microstrip antennas** or patched antenna. A microstrip antenna (MSA) basically consists of two metallic sheets "patches" that are separated by a substrate, one of them is the ground and the other acts as a radiator as shown in Figure 2.4. This antenna becomes widely used because of low cost, easy to analyze and fabricate and their small size . It can be used on the surface of high performance aircraft, satellites, mobiles, missiles, and space crafts . (Huang and Boyle, 2008).

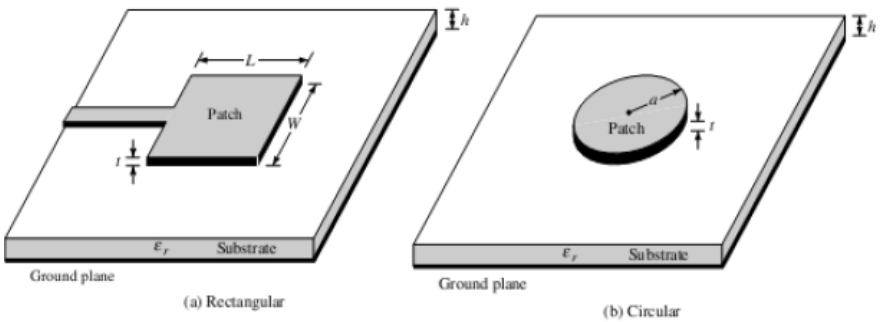

Figure (2.4) : Rectangular and circular microstrip (patch) antennas.

4. **Array antennas** are a group of radiating elements arranged in a certain electrical and geometrical arrangement (an array) as shown in Figure 2.5 to

achieve a certain radiation characteristic which may not be achieved in a single radiating element. This array also may give the radiation increased to maximum in a particular direction or directions and decreasing in others as desired. (Balanis, 2005).

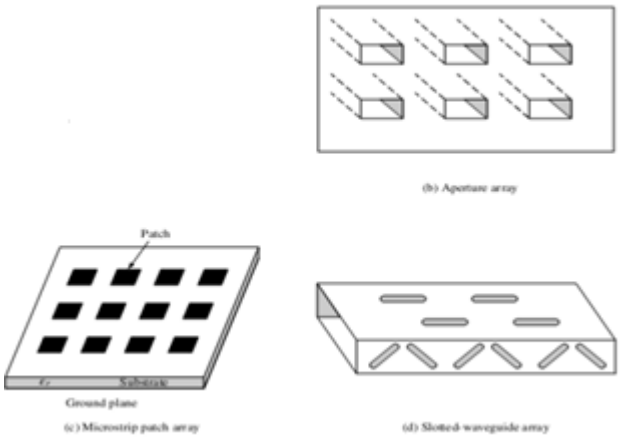

Figure (2.5): Typical wire, aperture, and microstrip array configurations. (Balanis, 2005)

5. **Reflector antennas** are primary used for satellite communications because of the great distances. The parabolic antenna (reflector) is the most popular form for this type of antennas. In this type as large the antenna diameter as high gain can be achieved for transmitting and receiving. Their shapes are shown in Figure 2.6. (Balanis, 2005) .

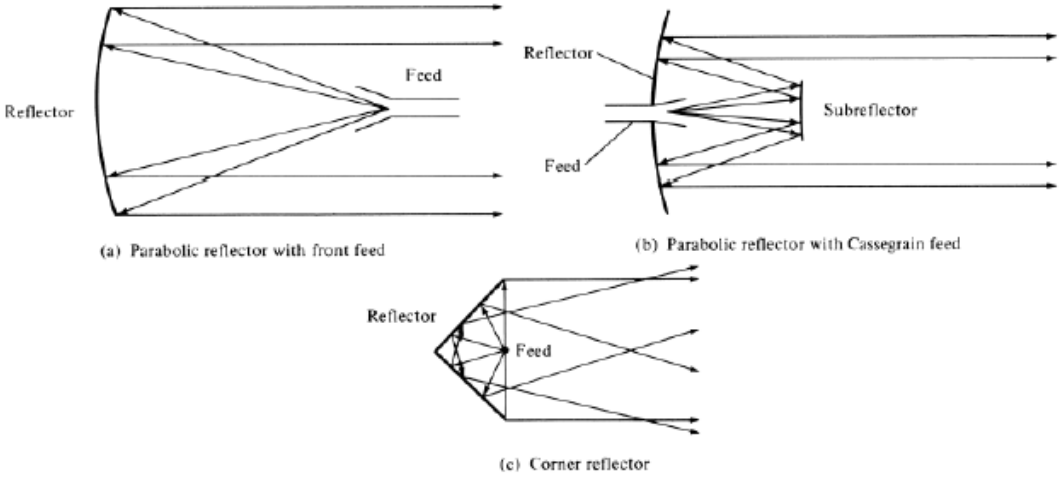

Figure(2.6): Typical reflector configurations. (Balanis, 2005)

6. **Lens antennas** are constructed of a dielectric material and can be used as a reflector antenna, to concentrate radiated energy in a certain direction or directions. They can be placed in front of a dipole on horn antenna to increase their directivity in the desired direction. They can be classified according to their material or their shapes. They are mostly used for high frequencies. Some forms are shown in Figure 2.7. (Balanis, 2005).

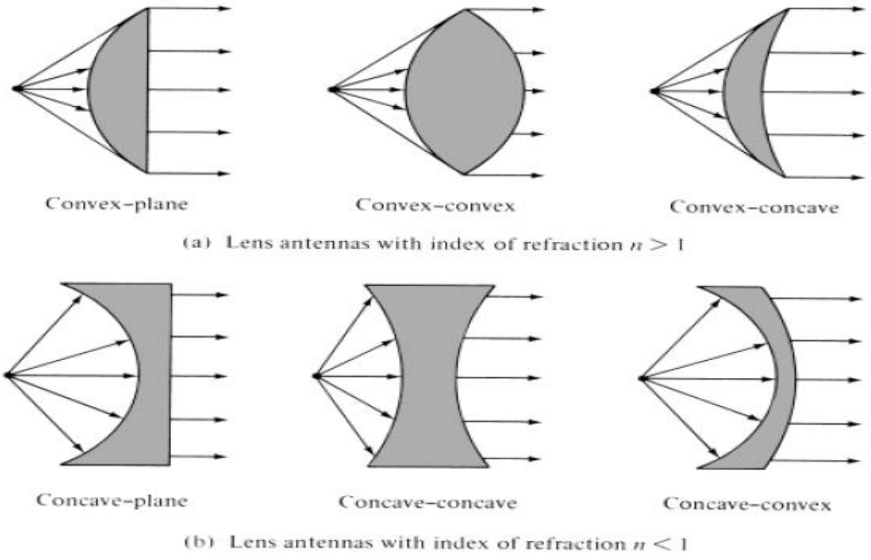

Figure (2.7) : Typical lens antenna configurations. (Balanis, 2005)

2.3 Maxwell's Equations

Maxwell's four equations describe the electric and magnetic fields arising from distributions of electric charges and currents, and how those fields change in time. It made evident for the first time that varying electric and magnetic fields could feed off each other , these fields could propagate indefinitely through space, far from the varying charges and currents where they originated. (Balanis, 2005).

Here are the equations as integral form:

1. Gauss' Law for electric fields: (The integral of the outgoing electric field over an area enclosing a volume equals the total charge inside, in appropriate units.)

$$\int \mathbf{E}.\mathbf{dA} = q/\varepsilon_{\circ} \qquad (2.1)$$

2. The corresponding formula for magnetic fields: (No magnetic charge exists:

no "monopoles".) $$\int \mathbf{B}.\mathbf{dA} = 0 \qquad (2.2)$$

3.Faraday's Law of Magnetic Induction:

$$\oint \mathbf{E}.\mathbf{dl} = -\frac{d}{dt}\int (\mathbf{B}.\mathbf{dA}) \qquad (2.3)$$

The first term is integrated round a closed line, usually a wire, and gives the total voltage change around the circuit, which is generated by a varying magnetic field threading through the circuit.

4.Ampere's Law plus Maxwell's displacement current:

$$\oint \mathbf{H}.\mathbf{dl} = \int \left(\mathbf{J} + \frac{\partial \mathbf{D}}{\partial \mathbf{t}}\right).\mathbf{dA} \qquad (2.4)$$

where

E : electric field intensity (V/m)

q : electric charge (C)

B : magnetic flux density (Wb/m²)

D: electric flux density (C/m²)

ε : permittivity (F/m)

dA: differential area (m²)

dl : differential length (m)

H: magnetic field intensity (A/m)

J : current density (A^2/m)

Maxwell's equations as differential forms **:**

1. Gauss's Law

$$\nabla . \mathbf{E} = q/\varepsilon_{\circ} \tag{2.5}$$

- There are two types of charge, positive and negative, just as there are two types of real numbers, positive and negative.
- Electric field lines diverge from positive charge and converge on negative charge.

2. No One's Law

$$\nabla . \mathbf{B} = 0 \tag{2.6}$$

- There is no magnetic monopole
- Magnetic field lines neither converge nor diverge (have no beginning or end)

3. Faraday's law

$$\nabla \times \mathbf{E} = -\frac{\partial \mathbf{B}}{\partial t} \tag{2.7}$$

- Electric field lines don't curl except when the magnetic field changes.

4. Ampère's law

$$\nabla \times \mathbf{H} = \mathbf{J} + \frac{\partial \mathbf{D}}{\partial t} \tag{2.8}$$

- Magnetic field lines curl around electric current and also curl when the electric field changes.

Maxwell's Equations are critical in understanding antenna parameters. The Maxwell's equations (Faraday's law and Ampere's law) are responsible for electromagnetic radiation. The curl operator represents the spatial variation of the fields, which are coupled to the time variation.

2.4 Antenna Parameters

2.4.1 Radiation Pattern

An antenna radiation pattern or antenna pattern is defined as a mathematical function or a graphical representation of the radiation properties of the antenna as a function of space coordinates. (Balanis, 2005). Defined for the far-field as a function of directional coordinates , there can be field patterns (magnitude of the electric or magnetic field) or power patterns (square of the magnitude of the electric or magnetic field). Often normalized with respect to their maximum value. The power pattern is usually plotted on a logarithmic scale or more commonly in decibels (dB) as shown in figure 2.8.

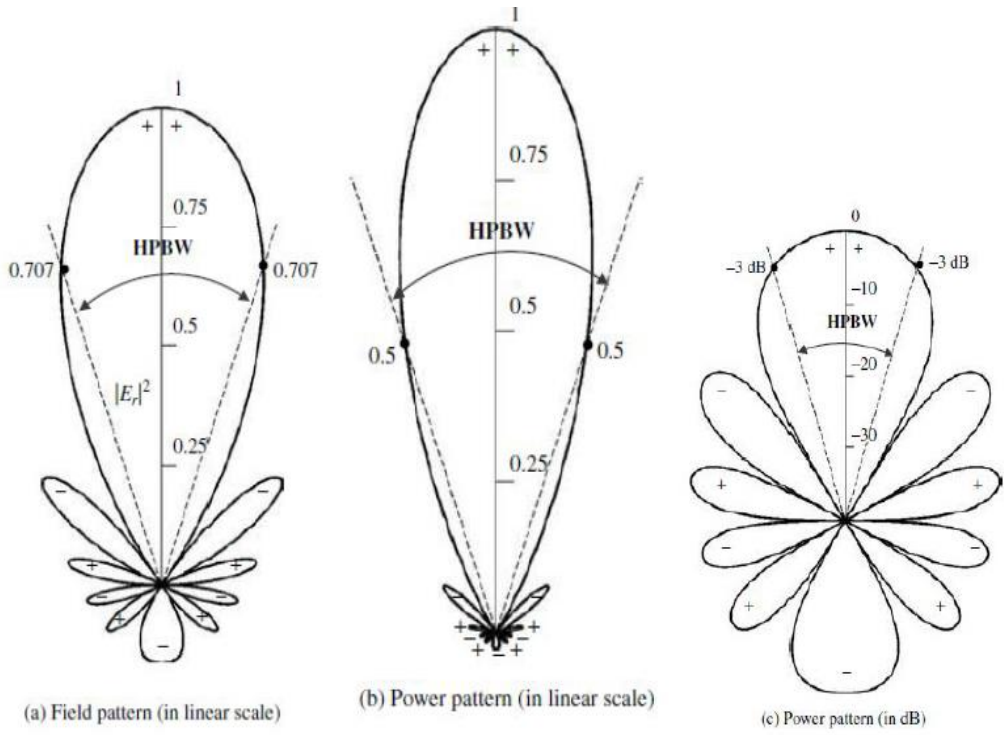

Figure (2.8): Radiation pattern .(Balanis 2005)

2.4.2 Radiation Pattern Lobes :

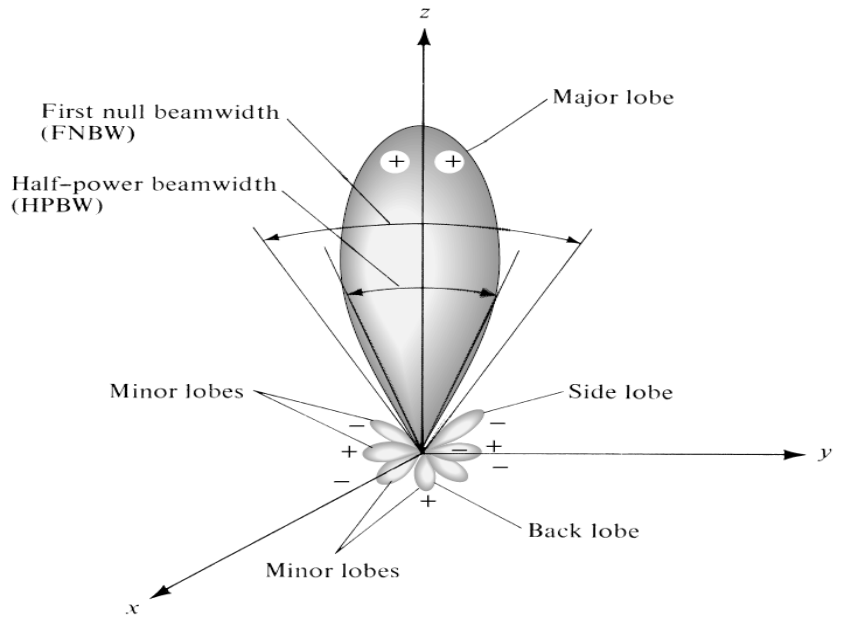

Figure(2.9) : Pattern lobes .(Balanis 2005)

As shown on in figure 2.9, radiation lobe is a portion of the radiation pattern bounded by regions of relatively weak radiation intensity. The pattern consist of main lobe , minor lobes ,side lobes , back lobes

The main lobe (or main beam or major lobe) is the lobe containing the direction of maximum radiation. There is also usually a series of lobes smaller than the main lobe. Any lobe other than the main lobe is called a minor lobe. Minor lobes are composed of side lobes and back lobes. Back lobes are directly opposite the main lobe, or sometimes they are taken to be the lobes in the half-space opposite the main lobe (Stutzman, Thiele, 1998).

2.4.3 Isotropic, Omnidirectional and Directional Patterns

An isotropic radiator is a hypothetical lossless antenna having equal radiation in all directions. An omnidirectional radiator is having an essentially nondirectional pattern in a given plane (e.g., in azimuth) and a directional pattern in any orthogonal plane. An directional radiator is having

the property of radiating or receiving more effectively in some directions than in others. Usually the maximum directivity is significantly greater than that of a half-wave dipole. (Balanis 2005).

2.4.4 Beam Width

The beam width of an antenna is a very important figure of merit and often is used as a trade-off between it and the side lobe level; that is, as the beam width decreases, the side lobe increases and vice versa. The beam width of the antenna is also used to describe the resolution capabilities of the antenna to distinguish between two adjacent radiating sources or radar targets.

(Half-Power Beam Width (HPBW))**.** In a plane containing the direction of the maximum of a beam, the angle between the two directions in which the radiation intensity is one-half value of the beam. .(Balanis 2005).

(First-Null Beam width (FNBW))**.** Angular separation between the first nulls of the pattern as shown in figure 2.10.

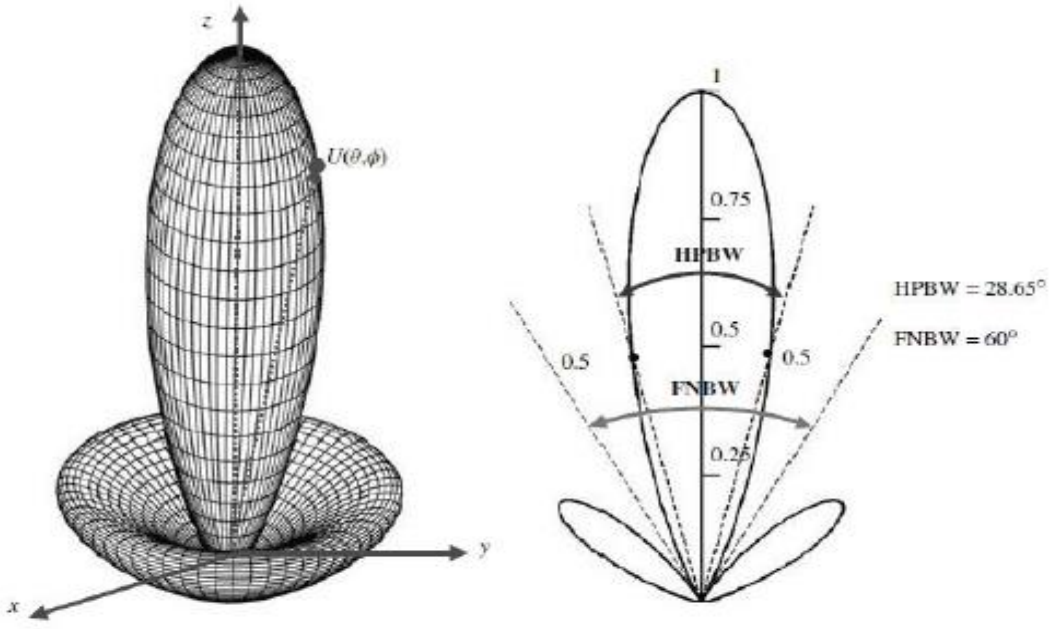

Figure(2.10): beam widths of a directional antenna power pattern.(Balanis 2005).

2.4.5 Radiation Power Density

Poynting Vector : The poynting vector is a quantity used to describe the power density associated with an electromagnetic wave and it is defined as:

$$\mathbf{W} = \mathbf{E} \times \mathbf{H} \qquad (2.9)$$

where

W = instantaneous Poynting vector (W/m^2), a power density.

E = instantaneous electric-field intensity (V/m).

H = instantaneous magnetic-field intensity (A/m). .(Balanis 2005).

The total radiation power crossing a closed surface is given by

$$P = \oiint \mathbf{W}.\mathbf{dA} \qquad (2.10)$$

where

P = total radiation power (W).

W = Poynting vector

dA = differential area

2.4.6 Radiation Intensity

Radiation intensity in a given direction is defined as the power radiated from an antenna per unit solid angle. The radiation intensity is a far-field parameter, it can be obtained by simply multiplying the radiation density by the square of the distance.

$$\mathbf{U} = r^2\mathbf{W} \tag{2.11}$$

The total power is obtained by integrating the radiation intensity over the entire solid angle of 4π. Thus

$$\mathrm{P} = \oiint \mathbf{U}.\mathbf{d\Omega} = \int_0^{\pi}\int_0^{2\pi} U \sin\theta d\theta d\varphi \tag{2.12}$$

where $d\Omega$ is the element of solid angle = sinθdθdφ. (Balanis 2005).

2.4.7 Directivity

Directivity is the ratio of the radiation intensity in a given direction from the antenna to the radiation intensity averaged over all directions. The average radiation intensity: total power radiated by the antenna divided by 4π. Stated more simply, the directivity of a nonisotropic source is equal to the ratio of its radiation intensity in a given direction over that of an isotropic source and it is given by

$$\mathbf{D} = \mathbf{D}(\theta,\varphi) = \frac{\mathbf{U}(\theta,\varphi)}{U_{\circ}} = \frac{4\pi\mathbf{U}(\theta,\varphi)}{P} \tag{2.13}$$

If the direction is not specified, the direction of maximum radiation intensity is implied.

$$\mathbf{D}_{max}= \frac{4\pi Umax}{P} \qquad (2.14)$$

where

- **D** = directivity (dimensionless)
- **U** =**U**(θ,φ) = radiation intensity (W/sr)
- $\mathbf{D_{max}}$ =maximum directivity
- $\mathbf{U_{max}}$ =maximum radiation intensity (W/sr)
- $\mathbf{U_0}$ = radiation intensity of isotropic source (W/sr)
- P = total radiated power (W) (Balanis 2005).

2.4.8 Antenna Efficiency

The total antenna efficiency e_0 is used to take into account losses at the input terminals and within the structure of the antenna. e_o is due to the combination of number of efficiencies:

$$e_o=e_r\, e_c\, e_d \qquad (2.15)$$

where

$\mathbf{e_o}$ = total efficiency.

$\mathbf{e_r}$ = reflection(mismatch)$=(1-|\Gamma|^2)$

$\mathbf{e_c}$ = conduction efficiency.

$\mathbf{e_d}$ =dielectric efficiency.

$$\Gamma=\frac{Zin-Zo}{Zin+Zo} \tag{2.16}$$

$$\text{VSWR}=\frac{1+|\Gamma|}{1-|\Gamma|} \tag{2.17}$$

where

Γ is the voltage reflection coefficient at the input terminals of the antenna, Z_{in} is the antenna input impedance, Z_0 is the characteristic impedance of the transmission line and VSWR is the voltage standing wave ratio.

It is usually more convenient to write e_o as:

$$e_o=e_r\, e_{cd}=e_{cd}(1-|\Gamma|^2) \tag{2.18}$$

where $e_{cd} = e_c\ e_d$ is the antenna radiation efficiency, which is used to relate the gain and directivity. (Balanis 2005).

2.4.9 Gain

Gain is defined as the ratio of the intensity, in a given direction, to the radiation intensity that would be obtained if the power accepted by the antenna were radiated isotropically. It is given by,

$$\text{Gain}=\frac{4\pi U(\theta,\varphi)}{Pin} \qquad (2.19)$$

We can write that the total radiated power (P_{rad}) is related to the total input power (P_{in}) by:

$$P_{rad}=e_{cd}\, P_{in} \qquad (2.20)$$

$$G(\theta,\varphi)=e_{cd}\, D(\theta,\varphi) \qquad (2.21)$$

The maximum value of the gain is related to the maximum directivity

$$G_o=e_{cd}\, D_o \qquad (2.22)$$

2.4.10 Polarization

Polarization is the curve traced by the end point of the arrow (vector) representing the instantaneous electric field. The field must be observed along the direction of propagation. Polarization is classified as linear, circular, or elliptical as shown in figure 2.11.

Linear polarization: If the electric field vector moves back and forward along a line it is assumed to be linearly polarized. A linearly polarized wave is considered as horizontally polarized if the electric field is parallel to the earth and vertically polarized if the electric field is perpendicular to the

earth. For a linearly-polarized antenna, the radiation pattern is taken both for a co-polarized and cross-polarized response.

Circular polarization: If the electric field vector remains constant in length but rotates around in a circular path then it is considered circularly polarized. For circular polarization, the field's components have same magnitude and the phase between two components is *90* degree.

Elliptical polarization: describes an antenna when its electric field vector at a far field point is such that traces elliptical curves constantly with time. Moreover, both the circular and elliptical polarizations are characterized for being right-hand (RH) or left-hand (LH) polarized, depending on the sense of the field. If the field is flowing in the clockwise direction, the field will be right hand polarized; otherwise it will be left hand polarized (Balanis 2005).

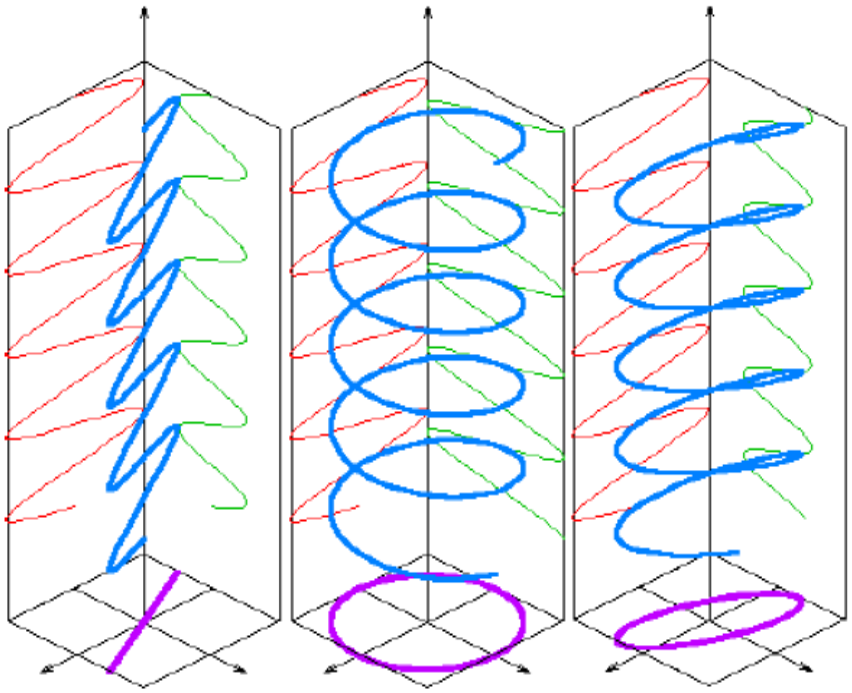

Figure(2.11): Three types of polarization (linear, circular and elliptical).(Ranga Rodrigo,2010)

2.5 Microstrip Antenna

Microstrip antenna is one of the most useful antennas at microwave frequencies (f > 1 GHz). It usually consists of a metal "patch" on top of a grounded dielectric substrate, the patch may be in a variety of shapes, but rectangular and circular are the most common as shown in figure 2.12.

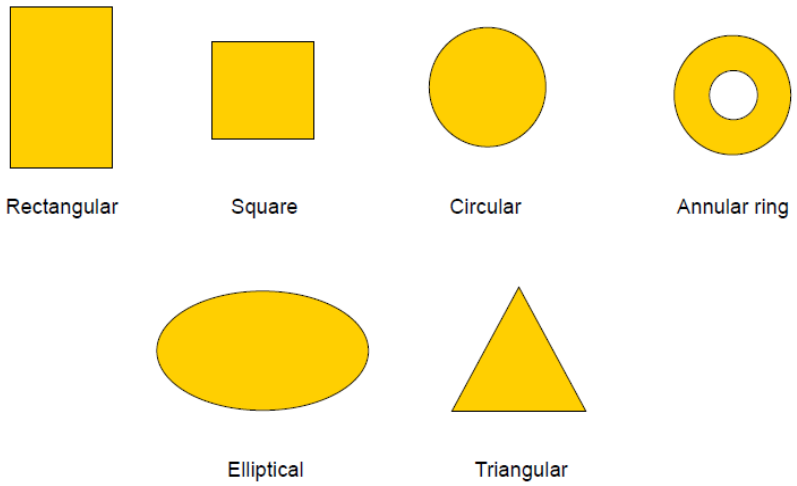

Figure(2.12): Common shapes of microstrip antenna

The common materials used for conducting surfaces are copper foil or copper foil plated with corrosion resistant metals like gold, tin and nickel.(Jackson , 2013). These metals are the main choice because of their low resistivity, resistant to oxidation, solderable.

In most cases, considerations in substrate characteristics involved the dielectric constant and loss tangent and their variation with temperature and frequency, dimensional stability with processing, homogeneity and isotropicity. In order to provide support and protection for the patch elements, the dielectric substrate must be strong and able to endure high temperature during soldering process and has high resistant towards chemicals that are used in fabrication process.

The surface of the substrate has to be smooth to reduce losses and adhere well to the metal used. Substrate thickness (h) and permittivity (ε_r) determine the electrical characteristics of the antenna. Thicker substrate will increase the bandwidth but it will cause the surface waves to propagate and

spurious coupling will happen. This problem however, can be reduced or avoided by using a suitably low permittivity substrate. (Jackson , 2013)

2.6 Feeding Techniques

The role of feeding is very important in case of efficient operation of antenna to improve the antenna input impedance matching**.**

2.6.1 Microstrip Line Feed

In this type of feed technique, a conducting strip is connected directly to the edge of the Microstrip patch as shown in figure 2.13. The conducting strip is smaller in width as compared to the patch and this kind of feed arrangement has the advantage that the feed can be etched on the same substrate to provide a planar structure. .(Gurdeep 2012).

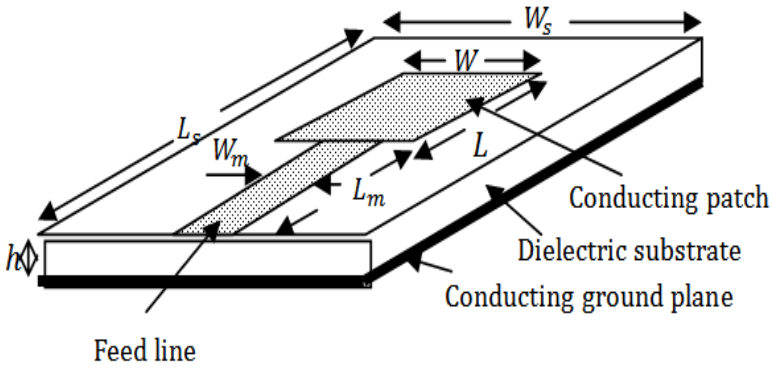

Figure (2.13): Microstrip line feed. (Ndujiuba, Oloyede 2015).

2.6.2 Inset Feed

In is a type of microstrip line feeding technique, in which the width of conducting strip is small as compared to the patch and has the advantage that the feed can provide a planar structure as shown in figure 2.14. (Pattnaik, Gianluca 1998) . The purpose of the inset cut in the patch is to match the impedance of the feed line to the patch input impedance without the need for

any additional matching element. This can be achieved by properly adjusting the inset cut position and dimensions. (Ndujiuba, Oloyede 2015).

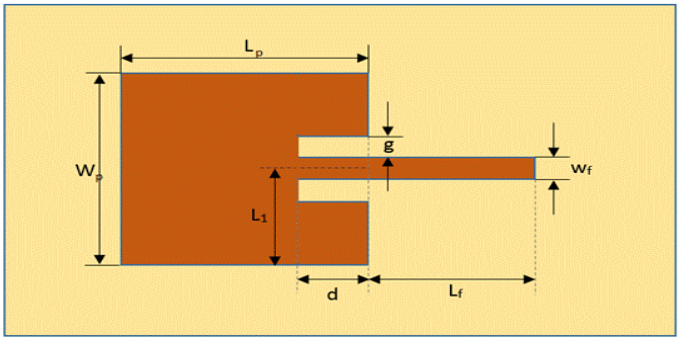

Figure(2.14): Inset feeding. (Ndujiuba, Oloyede 2015).

2.6.3 Coaxial Feed

The Coaxial probe feeding is a very common technique used for feeding microstrip patch antennas. The inner conductor of the coaxial cable extends through the dielectric and is soldered to the radiating metal patch, while the outer conductor is connected to the ground plane as shown in figure 2.15. The advantage of this feeding scheme is that the feed can be placed at any desired location on the patch in order to match cable impedance with the antenna input impedance.(Balanis 2009). The main aim to use probe feeding is it enhances the gain. (Ndujiuba, Oloyede 2015).

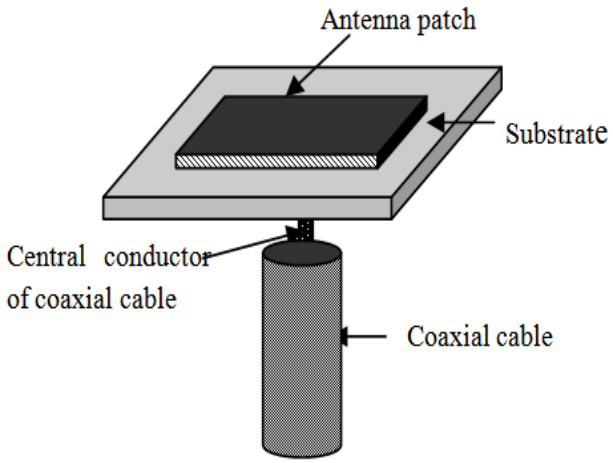

Figure(2.15): Coaxial feed. (Ndujiuba, Oloyede 2015).

2.6.4 Aperture Coupled Feed

In this type of feed technique, the radiating patch and the microstrip feed line are separated by the ground plane. Coupling between the patch and the feed line is made through a slot or an aperture in the ground plane as shown in figure 2.16.

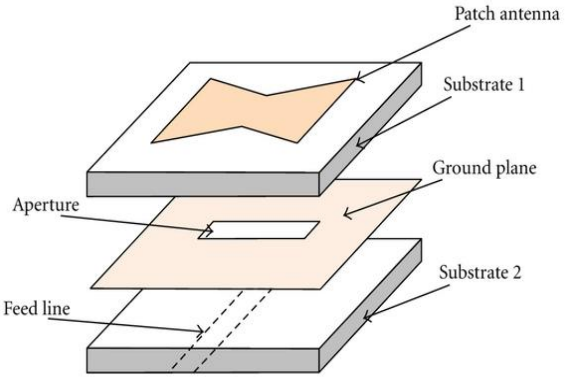

Figure (2.16): Aperture-coupled feed technique. (Ndujiuba, Oloyede 2015).

2.6.5 Proximity Coupled Feed

This type of feed technique is also called as the electromagnetic coupling scheme as shown in figure 2.17. Two dielectric substrates are used such that the feed line is between the two substrates and the radiating patch is on top of the upper substrate. The main advantage of this feed technique is that it eliminates spurious feed radiation and provides very high bandwidth (as high as 13%), due to overall increase in the thickness of the microstrip patch antenna.

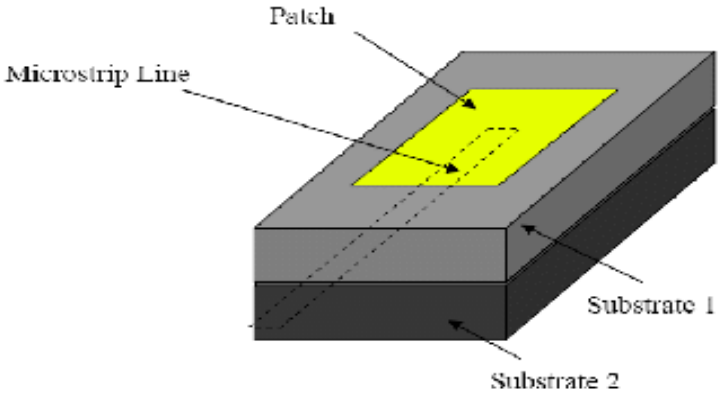

Figure(2.17): Proximity coupled feed. (Ndujiuba, Oloyede 2015).

2.6.6 Design Procedure

Consider figure 2.18 below, which shows a rectangular microstrip patch antenna of length L , width W resting on a substrate of height h . An effective dielectric constant ε_{eff} must be obtained in order to account for the fringing and the wave propagation in the line. The value of ε_{eff} is slightly less than ε_r because the fringing fields around the periphery of the patch are not confined in the dielectric substrate but are also spread in the air. The co-ordinate axis is selected such that the length is along the x direction, width is along the y direction and the height is along the z direction.(Girase, Tiwari, Sharma, Singh , 2014)

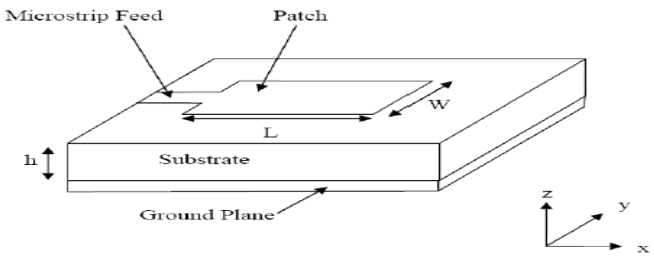

Figure(2.18): Microstrip patch antenna.(Girase, Tiwari, Sharma, Singh , 2014)

The effective dielectric constant is calculated by

$$\varepsilon_{eff} = \frac{\varepsilon_r+1}{2} + \frac{\varepsilon_r-1}{2}\left(\frac{1}{\sqrt{1+\frac{12h}{w}}}\right) \qquad (2.23)$$

where

ε_{eff} = Effective dielectric constant

ε_r = Dielectric constant of substrate

w = Width of the patch

h = Height of dielectric substrate

The microstrip patch antenna is represented by two slots, separated by a transmission line of length L and open circuited at both the ends. Along the width of the patch, the voltage is maximum and current is minimum due to the open ends. The fields at the edges can be resolved into normal and tangential components with respect to the ground plane**.**

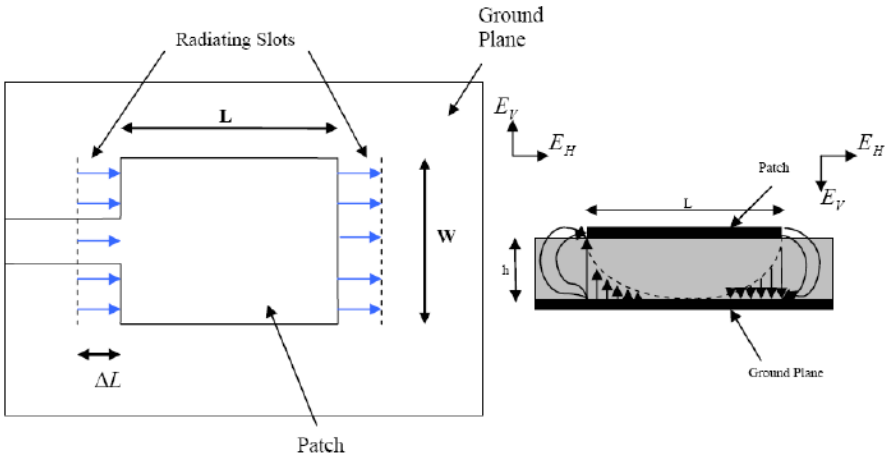

Figure(2.19): Top and side view of antenna.**(** Girase, Tiwari, Sharma, Singh , 2014)

It is seen from figure 2.19 that the normal components of the electric field at the two edges along the width are in opposite directions and thus out of phase since the patch is λ / 2 long and hence they cancel each other in the broadside direction. The tangential components (seen in figure 2.19), which are in phase, means that the resulting fields combine to give maximum radiated field normal to the surface of the structure. Hence the edges along the width can be represented as two radiating slots, which are λ / 2 apart and excited in phase and radiating in the half space above the ground plane. The fringing fields along the width can be modeled as radiating slots and electrically the patch of the microstrip antenna looks greater than its physical

dimensions. The dimensions of the patch along its length have now been extended on each end by a distance ΔL , which is given as :

$$\Delta L = \frac{0.412h(\varepsilon_{eff}+0.3)(\frac{w}{h}+0.264)}{(\varepsilon_{eff}-0.258)(\frac{w}{h}+0.8)} \quad (2.24)$$

The effective length $\mathbf{L_{eff}}$ of the patch now becomes:

$$L_{eff} = L + \Delta L \quad (2.25)$$

For a given resonance frequency f_o , the effective length is given by:

$$L_{eff} = \frac{c}{2f_o\sqrt{\varepsilon_{eff}}} \quad (2.26)$$

For efficient radiation, the width *W* is given by:

$$W = \frac{c}{2f_o\sqrt{\frac{\varepsilon_r+1}{2}}} \quad (2.27)$$

2.7 Microstrip Bow-tie Antenna

A bow-tie antenna is a dipole antenna with different shape which it's radiation patterns and other features are very similar to dipole antenna. Bow-tie antenna consist of two triangle sheet of metal with the feed line at it's vertex as shown in figure 2.20. It is used in many applications such as radar applications and mobile stations. The bow-tie antenna can be printed on substrate where each triangle is placed on the upper or lower of the substrate. The bow-tie antenna has many advantages such as wide band width, higher gain, simple design, light weight, low cost of fabrication.(Chakravarthy , Akram and Romana , 2013)

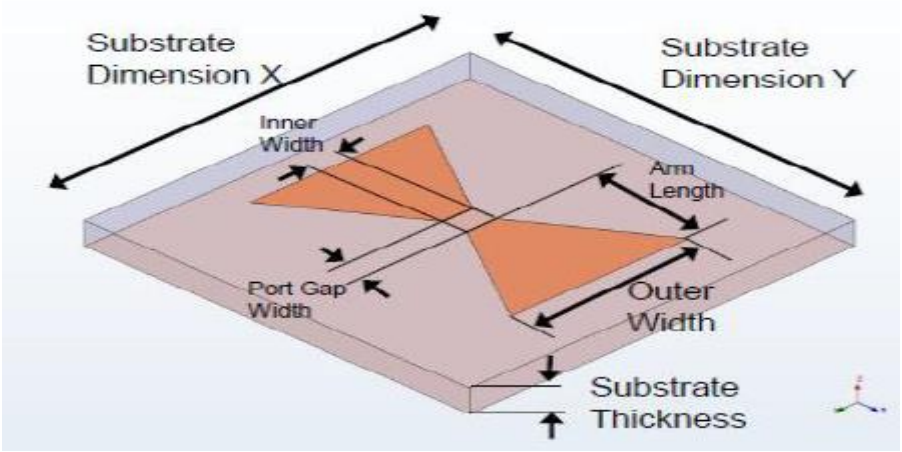

Figure(2.20): Bow-tie antenna

The radiating patch is considered as transmission line with two radiating patches connected at each ends. The fringing fields will be developed at the edges of patch which makes the length of patch higher than it's physical length by 2ΔL as shown in figure 2.21.(Chakravarthy , Akram and Romana , 2013)

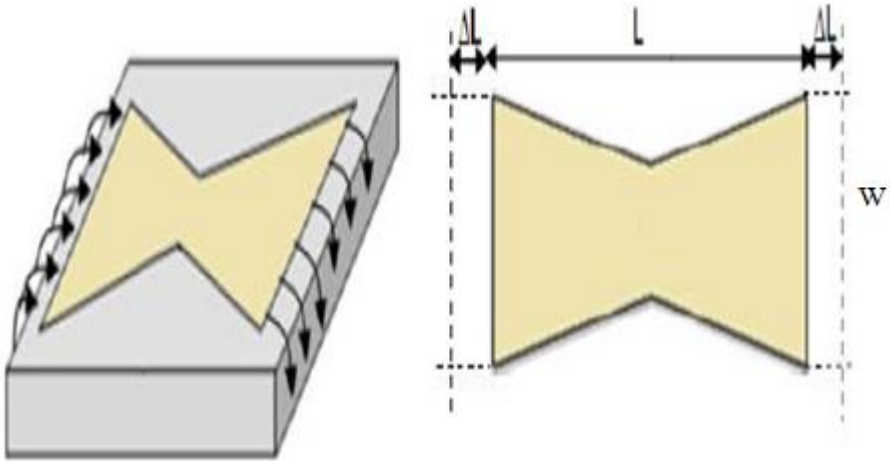

Figure(2.21): Fringing fields

Design of bow tie microstrip antenna is simply based on design of triangular microstrip antenna. The width W of each triangle of bow-tie antenna can be calculated by equation (2.27) . The distance between two triangles L can be calculated from equation (2.25) after ΔL was calculated from equation (2.24) and L_{eff} from equation (2.26) .

2.7.1 Bow Tie Literature Review

In (Abd El-Aziz , Abouelnage, Abdallah, Said and Abdo 2016), input impedance calculations by two methods are introduced, the curves for input impedance were developed according to the geometry of antenna. The design curves are used to design a bow-tie antenna type tag antenna, the results are obtained using CST software.

In (Harchandra and Singh 2014), different designs of bow-tie antenna are studied , the results showed sufficient isolation between the operating frequency bands and the improvement in gain and directivity. The results showed better improvement in the return loss and radiation pattern.

In (Chakravarthy, Akram and Romana 2013), the bow-tie antenna is designed at 2.6 GHz for wide band applications. The basic antenna

parameters like radiation pattern, gain , band width are presented, the antenna was designed by HFSS software.

In (Sayidmarie and Fadhel 2013), design of bow-tie antenna for UWB applications was presented. The principle has been applied to triangle monopole antenna with bending feed line, the antenna has high frequency band compared to traditional bow-tie antenna. The simulation results are obtained by CST and HFSS software.

In (Pan, Brown, Subramanyam, Penno, Jiang, Zhang, Patterson, Kuhl, Leedy and Cerny 2012), a novel printed antenna with a frequency reconfigurable feed network is presented. The antenna consists of a bow-tie structure patch radiating element in the inner space of an annulus that is on a non-grounded substrate with a ferroelectric (FE) Barium Strontium Titanate (BST) thin film. The bow-tie patch is fed by a coplanar waveguide (CPW) transmission line that also includes a CPW-based BST shunt varactor. Reconfiguration of the compact 8mm × 8mm system has been demonstrated by shifting the antenna system's operating frequency 500MHz in the 7–9GHz band by applying a DC voltage bias.

In (Johari and Singh 2012), comparative analysis of simple bow-tie antenna and a bow-tie slot antenna using simulated results of far field parameters and the radiation characteristics. A bow-tie slot antenna shows good performance for Ku band application , the return loss <-18 dB. The operating frequency is 12 GHz.

In (Bhosale and Deshmukh 2012), design of bow-tie antenna which operated for WLAN-2.4 GHz application. The bow tie can operate in multiband with moderate gain (3.5-7 dBi) and high efficiency (60%-80%). It

is a practical angle dependent frequency independent antenna because of its ultra-broad band, thin profile configurations, reliability and conformability.

In (Abu Foul and Ouda 2012), a new antenna design for gain and bandwidth enhancement of the slotted bowtie microstrip antenna using the principle of partial substrate removal. This new design is a lightweight and compact one that is suitable for broadband communications due to its high gain and wide bandwidth. The slotted bowtie shape achieves the required wide bandwidth without increasing the microstrip size. This antenna was designed to achieve a bandwidth of more than 5 GHz. Furthermore, the gain of the bowtie antenna was enhanced by more than 2 dB due to the loss reduction in surface waves by using partial substrate removal.

In (Roslee, Subari and Shahdan 2011), design a bow-tie antenna for ground penetrating radar (GPR) applications. The low frequency range (below 2 GHz) is used because the test equipment used. A bow-tie antenna is used because it has good directivity compared to other antennas.

In (Mahmoud 2010), the proposed algorithm is used to design a bow-tie antenna for 2.45 GHz Radio Frequency Identification (RFID) readers. The antenna is analyzed completely using Method of Moments (MoM). The simulated antenna and the optimization algorithm programs were implemented using MATLAB to verify the validity of numerical simulations.

However , all previous structures in literature do not use the bow-tie antenna with pattern re-configurability, but only with frequency re-configurability. This thesis introduces a novel design of reconfigurable bow-tie antenna combined with microstrip filter with varactors. This proposed antenna can be operated for pattern and frequency reconfigurable. The proposed structure can be operated in frequency range (1.70-2.77) GHz.

Chapter 3

Filter Theory

Chapter3

Filter theory

This chapter will discuss introduction to filters , filter types and microstrip filter design procedure.

3.1 Introduction

Radio frequency (RF) and microwave filters represent a class of electronic filter, designed to operate on signals in the megahertz to gigahertz frequency ranges (medium frequency to extremely high frequency). This frequency range is the range used by most broadcast radio, television, wireless communication (cellphones, Wi-Fi, etc.), and thus most RF and microwave devices will include some kind of filtering on the signals transmitted or received as shown in figure 3.1. Such filters are commonly used as building blocks for duplexers and diplexers to combine or separate multiple frequency bands . (Hong and Lancaster 2001).

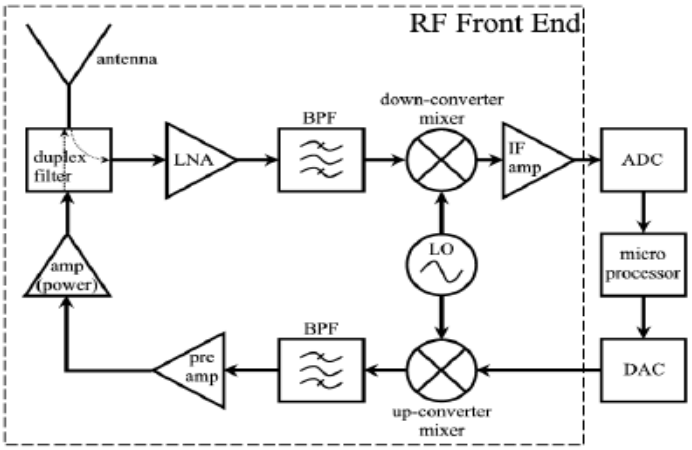

Figure(3.1): Transceiver system

Microwave filters consist of a number of resonators between two ports, this number can identify the filter's order. These resonators can be coupled electrically or magnetically or both. Microwave resonators are tunable circuits used in filters and frequency meters. Their operation is very similar

to that of lumped element resonators (such as parallel and series RLC circuits) of circuit theory(Hong and Lancaster 2001).

3.2 Types of Filter

Generally, there are four most common types of filter according to frequency selection ; Low pass, High-pass, Bandpass and Bandstop as shown in figure 3.2.

1) Low-Pass filter

A filter that block high frequencies and allows low frequencies to pass through the output.

2) High-Pass filter

A filter that allows high frequencies and block low frequencies.

3) Bandpass filter

A filter that passes the frequencies between the specified ranges and rejects those unwanted frequencies.

4) Bandstop filter

A filter that blocks the frequencies between specified range and allows the others.

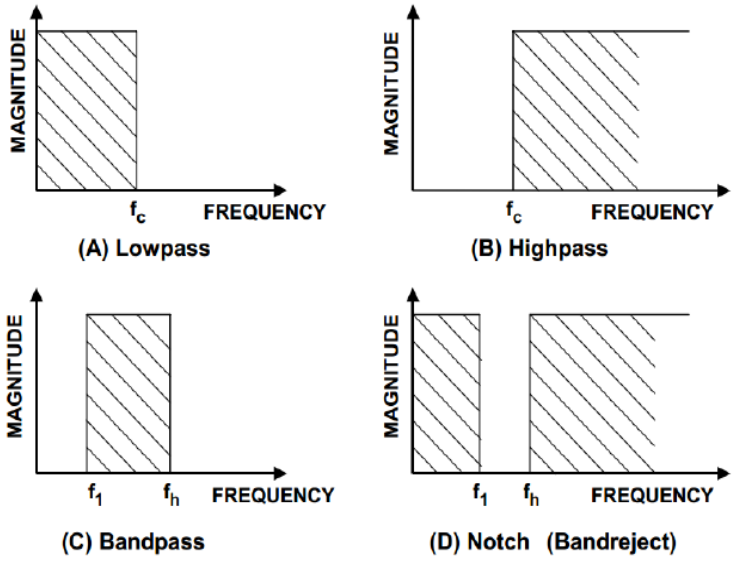

Figure(3.2): Types of filters according to frequency selection(Hong and Lancaster 2001).

According to filter response as shown in figure 3.3 , it can be classified as:

1) Chebyshev filter, has the best approximation to the ideal response of any filter for a specified order and ripple.

2) Butterworth filter, has a maximally flat frequency response.

3) Elliptic filter, has the steepest cutoff of any filter for a specified order and ripple.

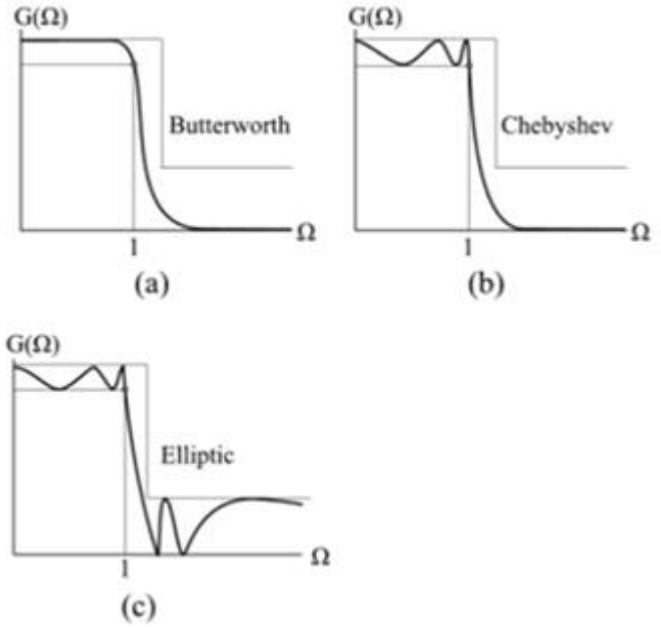

Figure(3.3): Types of filters according to frequency response(Hong and Lancaster 2001).

According to transmission media, filter can be characterized into two: Lumped elements and distributed elements.

When the behavior of a resistor, capacitor, or inductor can be fully described by a simple linear equation, microwave engineers refer it to as a lumped element where operation is restricted to lower frequencies where they are physically much smaller than a quarter-wavelength.

At microwave frequencies, other factors must also be considered. To accurately calculate the behavior of the same 50-ohm resistor, you need to consider its length, width, and thickness of metal and its proximity to the ground plane. This is when we must consider it as a distributed element. The

transmission media at microwave frequencies include the following: coaxial transmission lines, microstrip lines, strip lines and waveguides(Hong and Lancaster 2001).

Most transmission media that use two conductors, where one is considered ground include coaxial, microstrip and stripline. The transmission line that does not use a pair of conductors is waveguide(Hong and Lancaster 2001).

Finally filters are classified according to fractional bandwidth or percentage bandwidth that gives a normalized measure of how much frequency variation a system or component can handle. If we know the center frequency and the bandwidth, the percentage bandwidth is :

- Narrow band Filters: below 5%
- Moderate band Width: between 5% to 25%
- Wide band Filters: greater than 25%

3.3 Filter Characteristics

In designing a filter, there are some important parameters that must be taken into consideration as shown in figure 3.4.

1) Bandwidth

Bandwidth is commonly defined as a difference between the upper and the lower cutoff frequency (f_1 and f_2) of the circuit.

2) Selectivity

The ability to select wanted and unwanted frequency for filtering process. It is also a measure of steepness or sharpness of the cutoff slope.

3) Stopband Rejection

The ratio of the amplitude of unwanted frequency components before filter insertion to the amplitude existing after filter insertion. It is measured of the extent to which it rejects unwanted energy.

4) Return Loss

The ratio of reflected signal to incident signal where it is measured in dB. In the pass band, a smaller return loss is desirable. In S-parameter, return loss is represented by S_{11}.

5) Insertion Loss

When a component or group of components are inserted between a generator and its load, some of the signal from the generator is absorbed in those components due to their inherent resistive losses. Thus, not as much of the transmitted signal is transferred to the load as when the load is connected directly to the generator. The attenuation that results is called insertion loss. In S-parameter, the insertion loss is represented by S_{21}.

6) Ripple

A measure of the flatness of the pass band of a resonant circuit and it is expressed in decibels. Physically, it is measured in the response characteristic as the difference between the maximum attenuation in the pass band and the minimum attenuation in the pass band.

7) Resonance frequency

The exact frequency at which the filter response is resonated(Hong and Lancaster 2001).

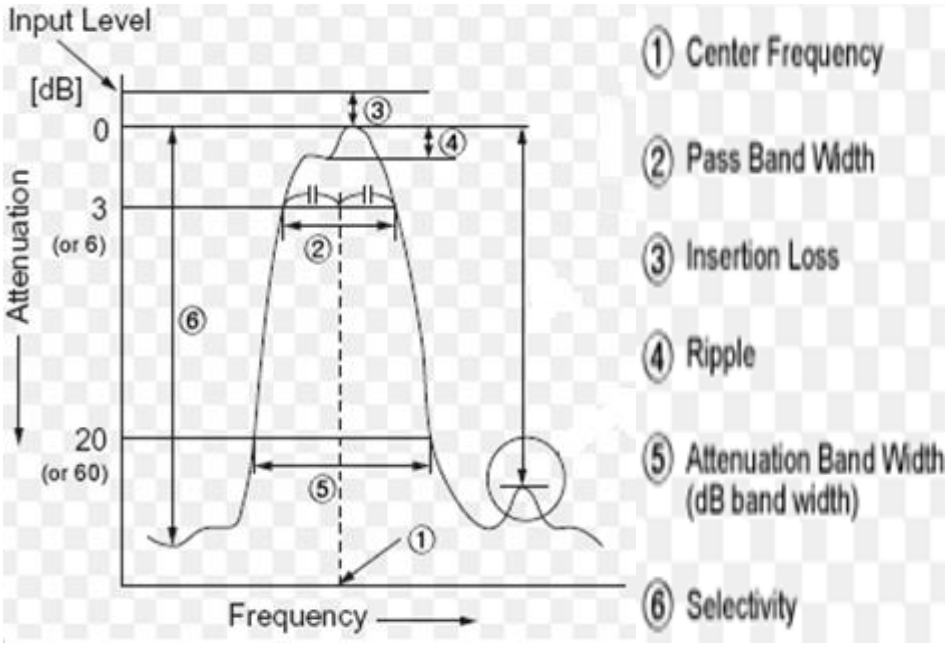

Figure(3.4): Filter characteristics.

3.4 Lowpass Prototype Filters

A lowpass prototype filter is in general defined as the lowpass filter whose element values are normalized to make the source resistance or conductance equal to one, denoted by g_0=1, and the cutoff angular frequency to be unity, denoted by Ω_c=1 (rad/s). There are two possible forms of an N -pole lowpass prototype for realizing an all-pole filter response, including Butterworth, Chebyshev, and Gaussian responses. Lowpass prototype filters are demonstrated in figure 3.5. They both are dual from each other and give the same response, so either form may be used (Hong and Lancaster 2001).

It should be noted that in figure 3.5 , g_i for $i = 1$ to N represent either the inductance of a series inductor or the capacitance of a shunt capacitor; therefore, and N is the number of reactive elements. If g_1 is the shunt capacitance or the series inductance, then g_0 is defined as the source resistance or the source conductance(Hong and Lancaster 2001).

Similarly, if g_n is the shunt capacitance or the series inductance, g_{n+1} becomes the load resistance or the load conductance. Unless otherwise specified these g-values are supposed to be the inductance in henries, capacitance in farads, resistance in ohms, and conductance in mhos (Hong and Lancaster 2001).

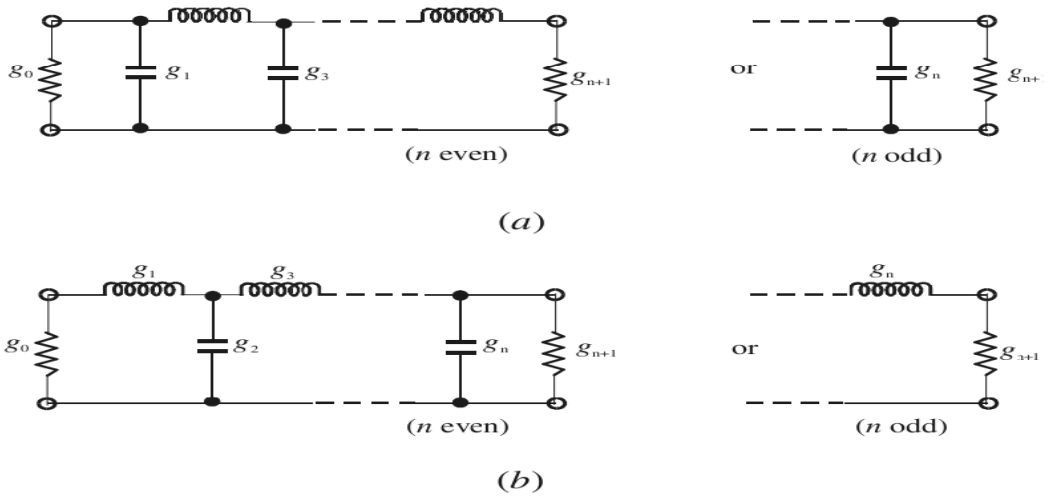

Figure(3.5): Lowpass prototype filters for all-pole filters with (a) a ladder network structure and(b) its dual(Hong and Lancaster 2001).

This type of lowpass filter can serve as a prototype for designing many practical filters with frequency and element transformations. For Chebyshev lowpass prototype filter with a passband ripple L_{Ar} dB and the cutoff frequency $\Omega_c = 1$, the element values may be computed using the following formulas:

$$g_o = 1 \tag{3.1}$$

$$g_1 = \frac{2}{\gamma}\sin\left(\frac{\pi}{2N}\right) \tag{3.2}$$

$$g_i=(1/g_{i-1})\frac{4\sin\left[\frac{(2i-1)\pi}{2N}\right]\sin\left[\frac{(2i-3)\pi}{2N}\right]}{\gamma^2+\sin^2\left[\frac{(i-1)\pi}{N}\right]} \quad \text{for i=2,3,…,N} \qquad (3.3)$$

$$g_{N+1}=\begin{cases}1 & for\ N\ odd\\ \coth^2\left(\frac{\beta}{4}\right) & for\ N\ even\end{cases} \qquad (3.4)$$

where

$$\beta=ln\left[\coth\left(\frac{L_{Ar}}{17.37}\right)\right] \qquad (3.5)$$

$$\gamma=\sinh\left(\frac{\beta}{2N}\right) \qquad (3.6)$$

Some typical element values for such filters are tabulated in Table 3.1 for various passband ripples L_{Ar}, and for the filter degree of N = 1 to 9 (Hong and Lancaster 2001). For a given passband ripple L_{Ar} dB, minimum stopband attenuation L_{As} dB at $\Omega=\Omega_s$, the degree of a Chebyshev lowpass prototype, which will meet this specification, can be found by:

$$N\geq\frac{\cosh^{-1}\sqrt{\frac{10^{0.1L_{As}}-1}{10^{0.1L_{Ar}}-1}}}{\cosh^{-1}\Omega_s} \qquad (3.7)$$

TABLE (3.1): Element values for Chebyshev lowpass prototype filters (g_0= 1.0, Ωc= 1) (Hong and Lancaster 2001).

For passband ripple L_{Ar} = 0.01 dB

n	g_1	g_2	g_3	g_4	g_5	g_6	g_7	g_8	g_9	g_{10}
1	0.0960	1.0								
2	0.4489	0.4078	1.1008							
3	0.6292	0.9703	0.6292	1.0						
4	0.7129	1.2004	1.3213	0.6476	1.1008					
5	0.7563	1.3049	1.5773	1.3049	0.7563	1.0				
6	0.7814	1.3600	1.6897	1.5350	1.4970	0.7098	1.1008			
7	0.7970	1.3924	1.7481	1.6331	1.7481	1.3924	0.7970	1.0		
8	0.8073	1.4131	1.7825	1.6833	1.8529	1.6193	1.5555	0.7334	1.1008	
9	0.8145	1.4271	1.8044	1.7125	1.9058	1.7125	1.8044	1.4271	0.8145	1.0

For passband ripple L_{Ar} = 0.04321 dB

n	g_1	g_2	g_3	g_4	g_5	g_6	g_7	g_8	g_9	g_{10}
1	0.2000	1.0								
2	0.6648	0.5445	1.2210							
3	0.8516	1.1032	0.8516	1.0						
4	0.9314	1.2920	1.5775	0.7628	1.2210					
5	0.9714	1.3721	1.8014	1.3721	0.9714	1.0				
6	0.9940	1.4131	1.8933	1.5506	1.7253	0.8141	1.2210			
7	1.0080	1.4368	1.9398	1.6220	1.9398	1.4368	1.0080	1.0		
8	1.0171	1.4518	1.9667	1.6574	2.0237	1.6107	1.7726	0.8330	1.2210	
9	1.0235	1.4619	1.9837	1.6778	2.0649	1.6778	1.9837	1.4619	1.0235	1.0

For passband ripple L_{Ar} = 0.1 dB

n	g_1	g_2	g_3	g_4	g_5	g_6	g_7	g_8	g_9	g_{10}
1	0.3052	1.0								
2	0.8431	0.6220	1.3554							
3	1.0316	1.1474	1.0316	1.0						
4	1.1088	1.3062	1.7704	0.8181	1.3554					
5	1.1468	1.3712	1.9750	1.3712	1.1468	1.0				
6	1.1681	1.4040	2.0562	1.5171	1.9029	0.8618	1.3554			
7	1.1812	1.4228	2.0967	1.5734	2.0967	1.4228	1.1812	1.0		
8	1.1898	1.4346	2.1199	1.6010	2.1700	1.5641	1.9445	0.8778	1.3554	
9	1.1957	1.4426	2.1346	1.6167	2.2054	1.6167	2.1346	1.4426	1.1957	1.0

Sometimes, the minimum return loss L_R in the passband is specified instead of the passband ripple L_{Ar}. If the minimum passband return loss is L_R dB ($L_R<0$), the corresponding passband ripple is(Hong and Lancaster 2001):

$$L_{Ar} = -10\log(1 - 10^{0.1L_R}) \text{ dB} \qquad (3.8)$$

$$L_R = 10\log(1 - 10^{-0.1L_{Ar}}) \quad \text{dB} \qquad (3.9)$$

3.5 Coupled Resonator Filters

A microwave resonators are a tunable circuits that are used in microwave devices, filters and frequency meters. Resonators can be made of closed sections of transmission lines or waveguides (cavity) such as microstrip resonators. Cavity resonators are defined in English dictionary as " cavity or a hollow chamber with dimensions chosen to permit internal resonant oscillation of acoustical waves or electromagnetic waves of specific frequencies. A microstrip resonators are defined as" structure that is able to contain at least one oscillating electromagnetic field. These definitions let that the resonator has the effect to identify the filter's frequencies (Hong and Lancaster 2001).

3.5.1 Resonator Types

Resonators can be classified to three major types: Transmission line resonators, cavity resonators, dielectric resonators, microstrip resonators.

3.5.1.1 Transmission Line Resonators

Transmission line usually consists of two parallel conductors as shown in figure 3.6. it can be coaxial cable, parallel plate wave guide, two wire transmission line, microstrip line and coplanar wave guide .

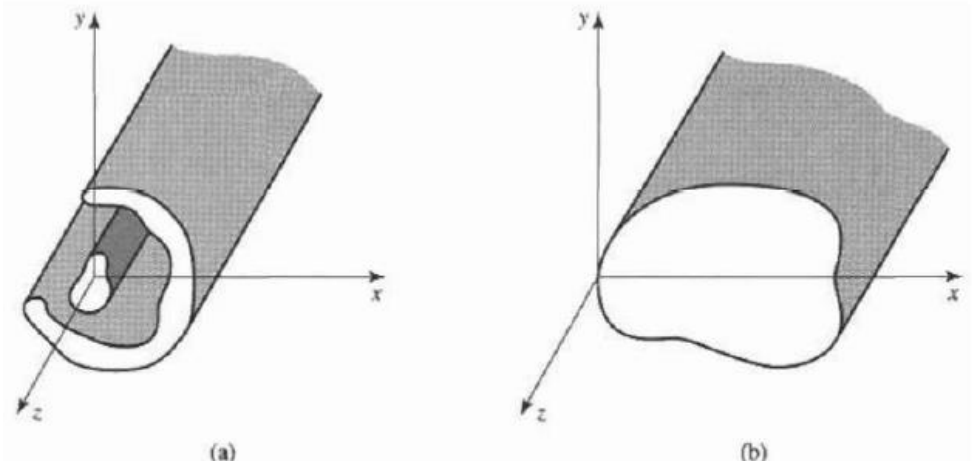

Figure(3.6): (a) General two-conductor transmission line (b) Closed waveguide

3.5.1.2 Cavity Resonators

Resonators can be constructed from closed sections of waveguide as in figure 3.7. Waveguide resonators are usually short circuited at both ends because of radiation loss from open ended waveguide. These shorted ends (closed ends) are forming a closed box or cavity, and electric and magnetic energy is stored within the cavity. Coupling to the resonator can be done by a small probe or a small aperture or loop. Power can be dissipated in the metallic walls of the cavity as well as in the dielectric filling the cavity .

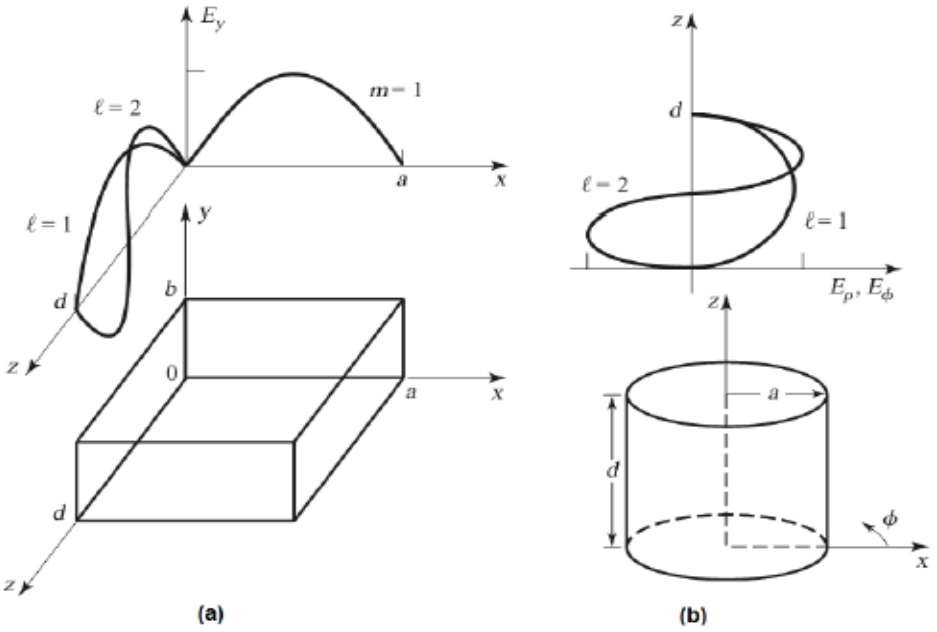

Figure(3.7): (a) A rectangular resonant cavity,(b) A cylindrical resonant cavity (Hong and Lancaster 2001).

3.5.1.3 Dielectric Resonators

The microwave resonators can be constructed from a small disc or cube of low-loss high dielectric constant material. Dielectric resonators are similar in principle to the rectangular or cylindrical waveguide cavities. The high dielectric constant of the resonator ensure that most of the fields are contained within the dielectric, but unlike metallic cavities, there is some leakage or field fringing from the sides and ends of the dielectric resonator.

3.5.1.4 Microstrip Resonators

A microstrip resonator is any structure that is able to contain at least one oscillating electromagnetic field. This definition means that there are many forms of microstrip resonators. Figure 3.8 shows some typical configurations of microstrip resonators.

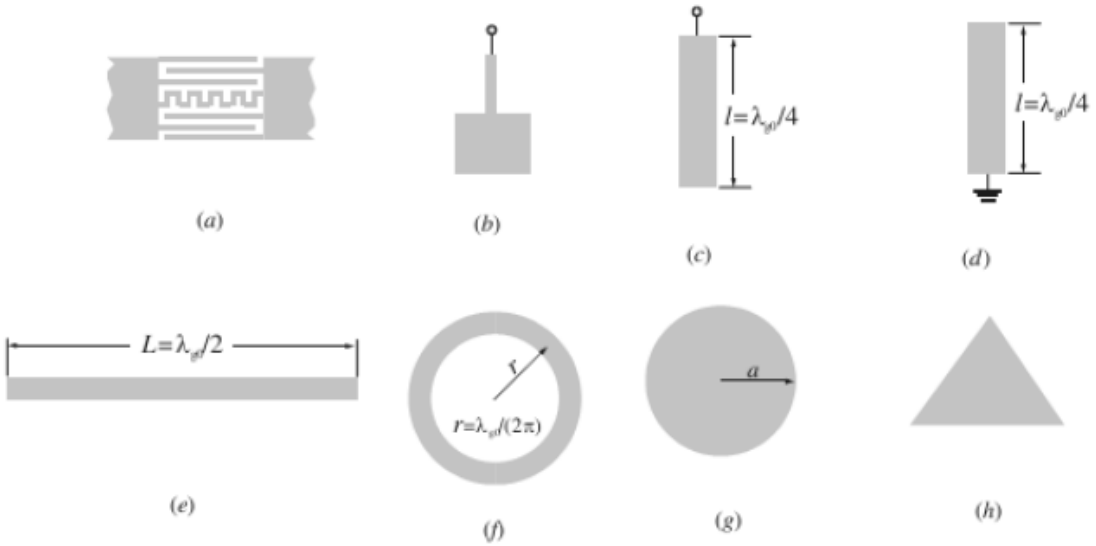

Figure(3.8):(a) lumped-element resonator; (b) quasilumped-element resonator; (c) $\lambda g_0/4$ line resonator (shunt series resonance); (d) $\lambda g_0/4$ line resonator (shunt parallel resonance); (e) $\lambda g_0/2$ line resonator; (f) ring resonator; (g) circular patch resonator; (h) triangular patch resonator

The microstrip open loop resonator can be obtained by folding a straight open resonator as shown in figure 3.9.

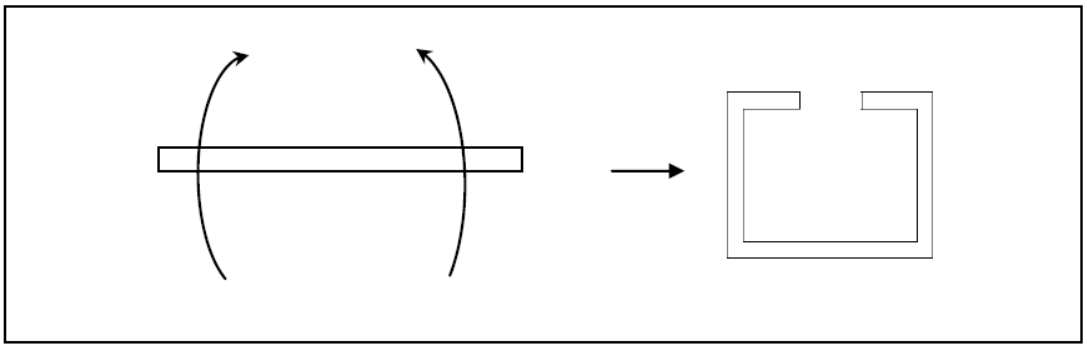

Figure(3.9): Open loop resonator

The main interaction mechanism between resonators for filter application is due to proximity coupling. This coupling can be characterized by a coupling coefficient that depends upon the ration of coupled energy to stored energy as follows:

$$\mathbf{k} = \frac{\int \boldsymbol{\varepsilon} \mathbf{E}_a \mathbf{E}_b d\boldsymbol{v}}{\sqrt{\int \boldsymbol{\varepsilon} \boldsymbol{E}_a{}^2 d\boldsymbol{v} \int \boldsymbol{\varepsilon} \boldsymbol{E}_b{}^2 d\boldsymbol{v}}} + \frac{\int \boldsymbol{\mu} \mathbf{H}_a \mathbf{H}_b d\boldsymbol{v}}{\sqrt{\int \boldsymbol{\mu} \boldsymbol{H}_a{}^2 d\boldsymbol{v} \int \boldsymbol{\mu} \boldsymbol{H}_b{}^2 d\boldsymbol{v}}} \qquad (3.10)$$

Where $\mathbf{E}_a$ and $\mathbf{H}_a$ are, respectively the electric and magnetic fields produced by the first resonator, and $\mathbf{E}_b$, $\mathbf{H}_b$ are the corresponding fields of the second resonator. The first term on the right hand side of equation 3.10 represents the coupling due to the interaction between the electric fields of the resonators, or more simply the electric coupling. Similarly, the second term represents the magnetic coupling between the resonators. Depending on which term dominates the sum the coupling is said to be electric, magnetic, or mixed.

Four canonical arrangements are shown in the figure 3.10. When the resonators are operating near their first resonant frequency, the pair of resonators depicted in figure 3.10a interact mainly through their magnetic fields, this is because the magnetic field is maximum near the center of the resonator opposite to its open ends. The configuration of figure 3.10b produces, in turn, an electric coupling since the electric field is maximum near the open ends. The coupling produced by the two configurations of figure 3.10c and 3.10d are collectively referred as mixed coupling because neither the electric fields nor the magnetic fields dominate the interaction between the resonators(Hong and Lancaster 2001).

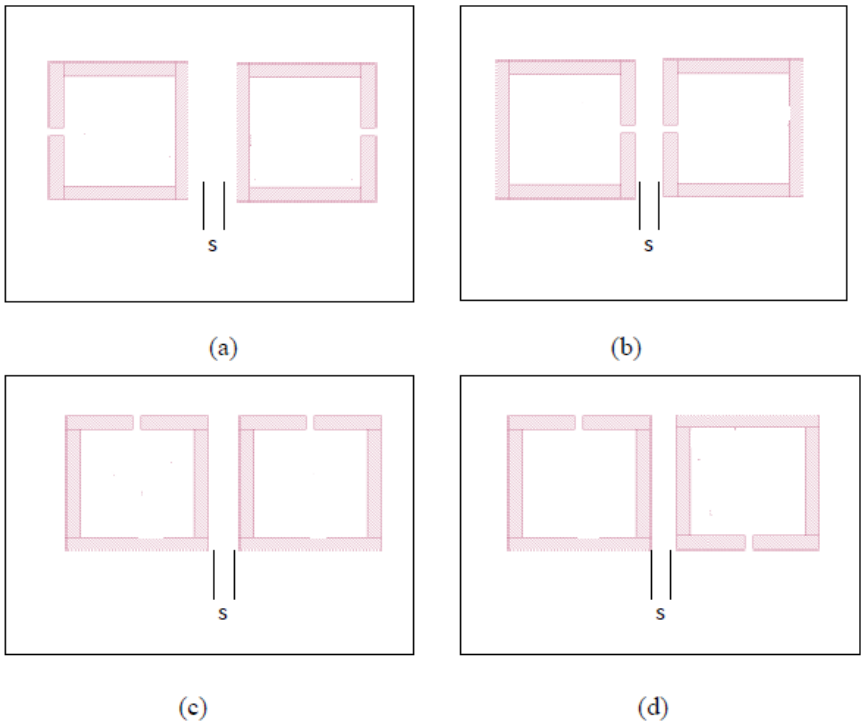

Figure(3.10): (a) magnetic coupling; (b) electric coupling; (c) and (d) mixed coupling(Hong and Lancaster 2001).

The definition of k given in equation (3.11) is not practical for calculation purposes since it requires the knowledge of the electromagnetic fields everywhere. A useful alternative expression for k can be obtained from a well known fact in physics, when two resonators are coupled to each other they resonate together at two frequencies f_1 and f_2, that are in general different from their original resonant frequency f_o. A formula giving the exact relationship between these quantities is given by:

$$\pm K = \frac{f_2^2 - f_1^2}{f_2^2 + f_1^2} \qquad (3.11)$$

Coupled microstrip filters have two typical input/output (I/O) coupling structures. The first type is tapped line structure and the second is coupled line structure(Hong and Lancaster 2001). For the tapped line structure, usually a 50 ohm feed line is directly tapped onto the I/O resonator and the coupling or the external quality factor is controlled by the tapping position *t*, as indicated in figure 3.11a. The coupling of coupled line structure can be found from the coupling gap *g* and the line width *w* as indicated in figure 3.11b. (Hong and Lancaster 2001).

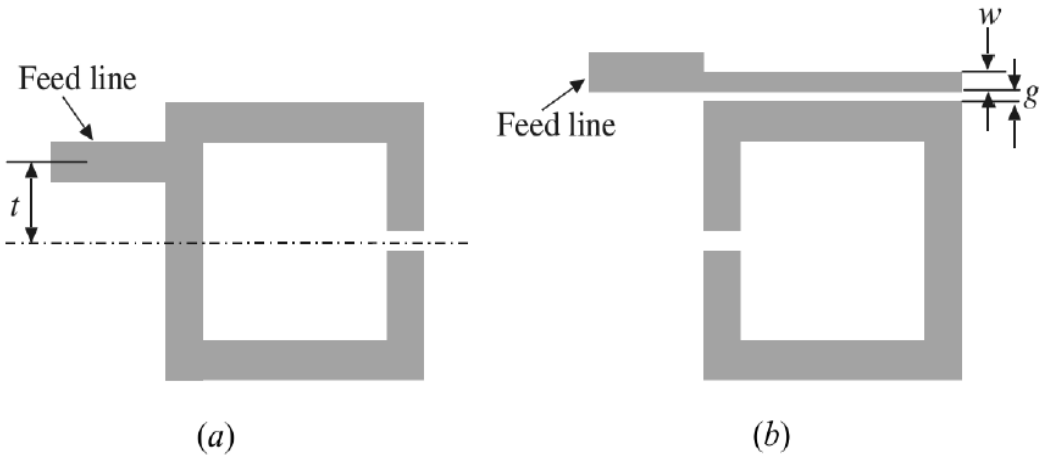

Figure(3.11): (a)Tapped-line coupling.(b) Coupled-line coupling (Hong and Lancaster 2001).

3.6 Loaded and Unloaded Quality Factor

Quality factor *Q* is the characteristic of the resonant circuit itself with no loading effects. It is a measurement of the loss of a resonant circuits. If the circuit is effected by a load from external circuitry then the external circuitry effect is defined as external quality factor Q_e. So quality factor *Q* is defined as unloaded quality factor . The loaded quality factor Q_L takes the account for characteristic of the resonant circuit and these loading effects because in practice a resonant circuit is invariably coupled to other circuitry, so Q_L is lower than *Q*.

External quality factor can be calculated directly from the low pass prototype filter as the following:

$$Q_e = \frac{g_0 g_1}{FBW} \tag{3.12}$$

$$Q_e = \frac{g_n g_{n+1}}{FBW} \tag{3.13}$$

$$K = \frac{FBW}{\sqrt{g_n g_{n+1}}} \tag{3.14}$$

where *FBW* is a shortcut for a fractional bandwidth that is equal to $FBW=BW/f_0$ where f_0 is the center frequency of any single resonator and *BW* is the bandwidth of the filter. The g-values are presented in previous section.

3.7 Frequency and Element Transformation

Since in the lowpass prototype filters, that have a normalized source resistance/conductance g_0= 1 and a cutoff frequency Ω_c=1. It is important to get frequency characteristics and element values for practical filters based on the lowpass prototype. One may apply frequency and element transformations or frequency mapping (Hong and Lancaster 2001).

In addition to the frequency mapping, impedance scaling is also required to accomplish the element transformation. The impedance scaling will remove the g_0=1 normalization and adjust the filter to work for any value of the source impedance denoted by Z_0. For our formulation, it is convenient to define an impedance scaling factor γ_0 as

$$\gamma_o = \begin{cases} \frac{Z_o}{g_o} & for\ g_o\ being\ the\ resistance \\ \frac{g_o}{Y_0} & for\ g_o\ being\ the\ conductance \end{cases} \tag{3.15}$$

where $Y_0 = 1/Z_0$ is the source admittance.

3.7.1 Bandpass Transformation

Assume that a lowpass prototype response is to be transformed to a bandpass response having a passband $\omega_2 - \omega_1$, where ω_1 and ω_2 indicate the passband-edge angular frequency(Hong and Lancaster 2001).

The required frequency transformation is

$$\Omega = \frac{\Omega_c}{FBW}\left(\frac{\omega}{\omega_o} - \frac{\omega_o}{\omega}\right) \qquad (3.16)$$

With

$$FBW = \frac{\omega_2 - \omega_1}{\omega_o} \qquad (3.17)$$

$$\omega_o = \sqrt{\omega_1 \omega_2} \qquad (3.18)$$

where ω_0 denotes the center angular frequency and *FBW* is defined as the fractional bandwidth. The elements for the *LC* resonators transformed to the bandpass filter , where serial inductance (g) is transformed to L_s and C_s while shunt capacitance (g) is transformed to C_p and L_p.

$$L_s = \left(\frac{\Omega_c}{FBW\omega_o}\right)\gamma_o g \qquad (3.19)$$

$$C_s = \left(\frac{FBW}{\omega_o \Omega_c}\right)\frac{1}{\gamma_o g} \qquad (3.20)$$

$$C_p = \left(\frac{\Omega_c}{FBW\omega_o}\right)\frac{g}{\gamma_o} \qquad (3.21)$$

$$L_p = \left(\frac{FBW}{\omega_o \Omega_c}\right)\frac{\gamma_o}{g} \qquad (3.22)$$

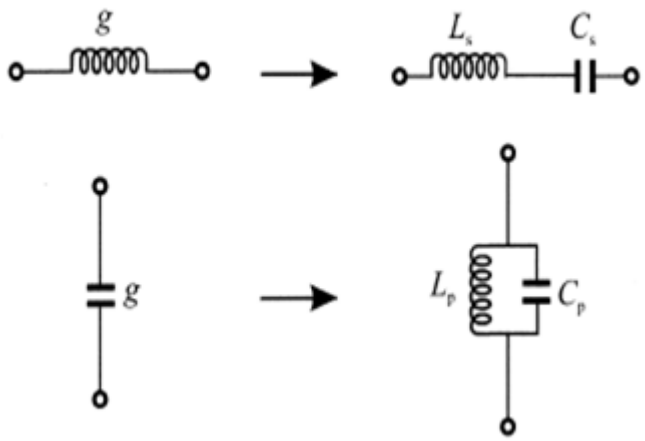

Figure (3.12): Lowpass prototype to bandpass transformation(Hong and Lancaster 2001).

3.8 Design Procedures of Microstrip Filter

Before designing microstrip filter , there are some steps to be considered

1- Preparing basic calculations needed for the design, frequency range , center frequency , band width.

2- Choose the shape and structure for the resonators and the final structure of the filter, which is chosen as 3rd order microstrip band pass filter.

3- Choose the simulation program that is chosen as CST. Using software program for example (TX line) to obtain effective dielectric constant ε_e and the width of the microstrip and get the initial length of the resonator ($\lambda_g / 2$).

4- Obtain the prototype g-values from the table of ripple for example L_{Ar}= 0.1 dB according to the order of filter.

5- Find the dimensions of a single resonator that achieve the proposed center frequency.

6- For single resonator as shown in figure (3.13), calculate external quality factor (Q_e) by using equation (3.13). Figure (3.14) is shown the external quality factor. The external quality factor can be get from equation

$$Q_e = {}^{f_0}/_{BW_{3dB}} \qquad (3.23)$$

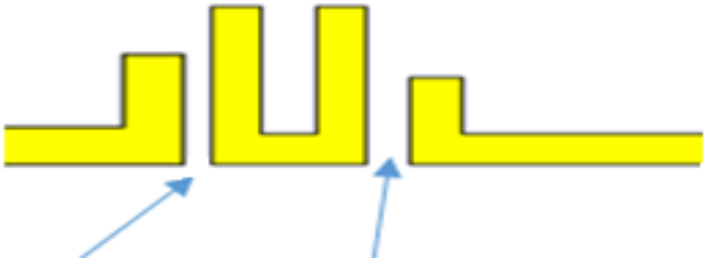

Figure(3.13): Determine external quality factor

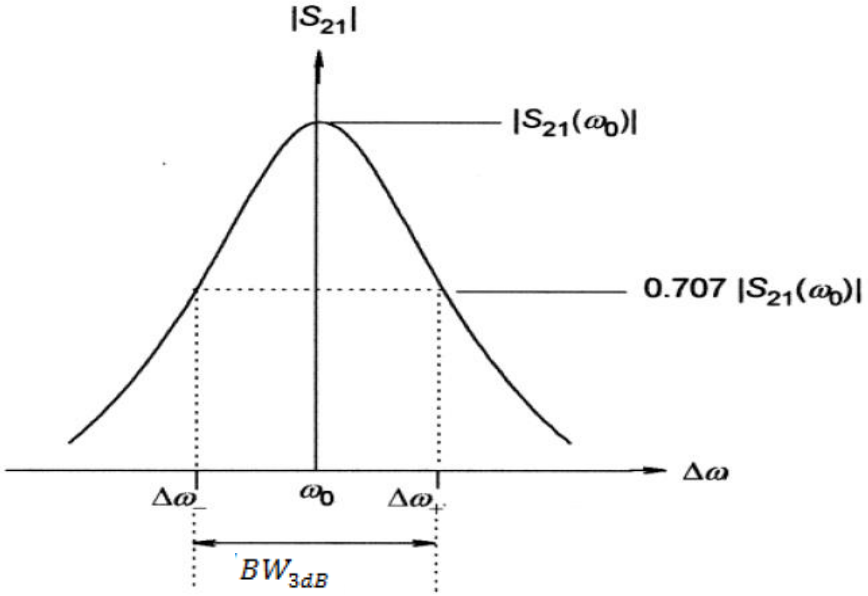

Figure(3.14): External quality factor

7- The required inter resonator coupling from equation (3.14) will be generally as in figure 3.15. It can be deduced by studying two resonators and

make the resonators weakly coupled to the ports as in figure 3.16. The coupling coefficient can be calculated from equation (3.11)

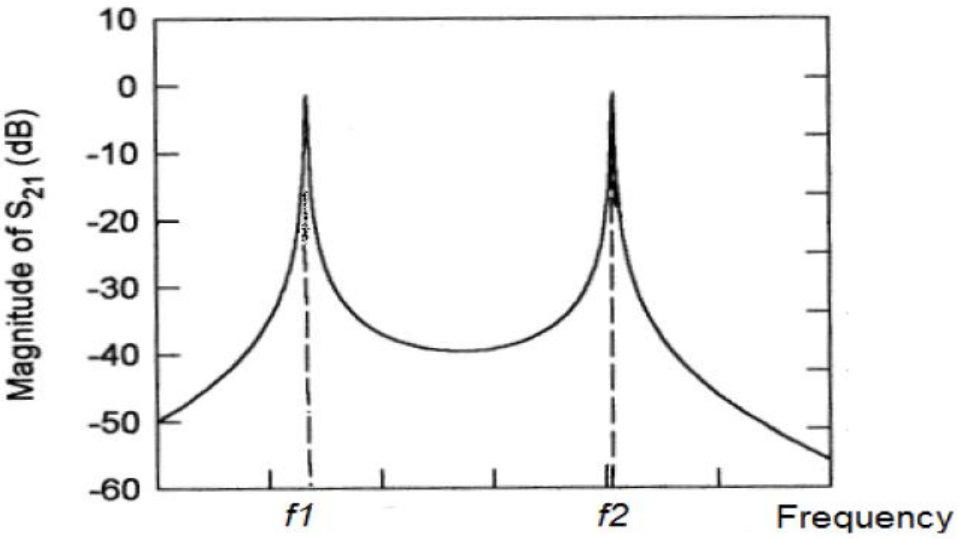

Figure(3.15): General coupling between two resonators (Hong and Lancaster 2001).

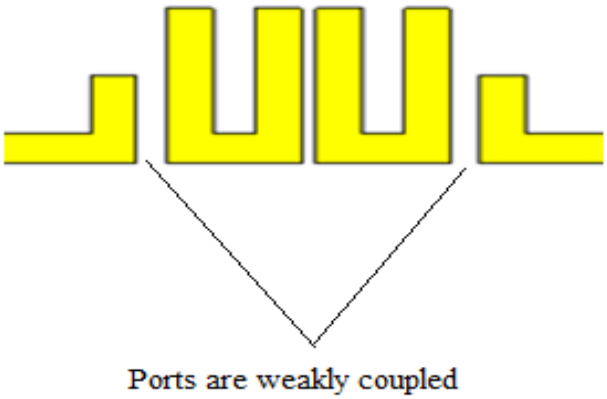

Figure(3.16): The resonators are coupled

8- Construct the initial design of the filter for the required external quality factor in step 6 and required coupling coefficients in step 7, then run the simulation as shown in figure 3.17.

Figure(3.17): The initial filter layout

Chapter 4

Design of Pattern and Frequency Reconfigurable Microstrip Filtering Antenna

Chapter 4

Design of pattern and frequency reconfigurable microstrip filtering antenna

4.1 Introduction

This chapter presents the design of bow-tie antenna. The operating frequency range is from 1.80 GHz to 2.77 GHz . The designed antenna is pattern and frequency reconfigurable.

To achieve pattern reconfigurable, Microstrip segments will be added to the bow-tie antenna and PIN diodes are used in the design that can be switched ON to connect these microstrip segments to the original bow-tie structure. In this work three designs of bow-tie antenna will be presented, the first design is the original design without any microstrip segments, but with increasing one of triangles of bow-tie antenna. The second antenna is designed by adding the microstrip segments on the top of substrate and those segment can be connected to the ground via substrate using PIN diodes. The third design has microstrip segments on the bottom of substrate from ground side and they can be connected to the ground through PIN switches.

Microstrip filter is designed with varactors to achieve frequency reconfigurable. The filter will be added to feed line of antenna. Both the antenna and the filter will be combined together to achieve both pattern and frequency reconfigurable. This proposed antenna achieves a reconfigurable radiation pattern and reconfigurable frequency filtering that operates within (1.80 to 2.77) GHz .

4.2 Design of Bow-tie Antenna

Figure (4.1) Shows the structure of the proposed antenna with its design parameters. The final values of the design dimensions are presented in table (4.1). As shown in figure (4.1) the bow tie antenna consists of two triangles separated by distance (L) connected to the feed line on the top of substrate with the ground on the bottom of substrate. This antenna is operating at frequency range (1.80-2.77) GHz.

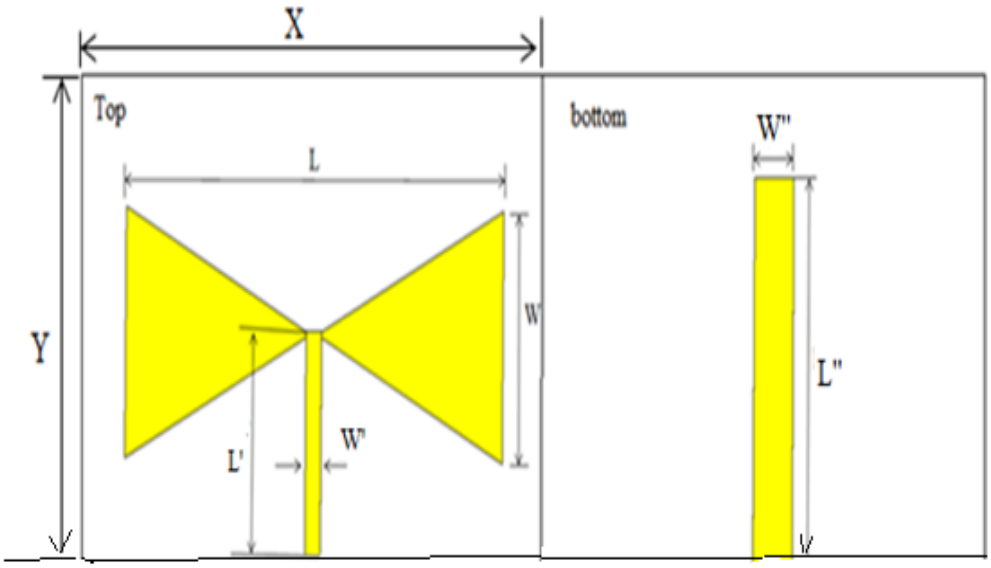

Figure(4.1): Structure of proposed bow-tie antenna

The antenna is designed on FR4 (lossy) substrate with dielectric constant 4.3 , thickness of 1.6 mm and loss tangent of 0.02. The final dimensions of the proposed antenna are listed in table 4.1.

Table(4.1): Dimensions of the proposed bow-tie antenna **.**

Dimensions	**(mm)**
Substrate thickness	1.6
Substrate width (X)	42
Substrate length(Y)	50
Feed line width(W')	3.085
Feed line length(L')	25.3

Ground plane width(W")	3.8
Ground plane length(L")	43.8
Distance between Bow-Tie triangles (L)	35.8
Width of triangle (W)	26.89

The simulations were performed using the CST Microwave Studio package which utilizes the finite integration technique for computation. CST provides Complete Technology for High Frequency EM Field Simulation, simulation of return loss, radiation pattern, E-Field ,H-Field, far field and S-parameters.

Figure (4.2) shows the simulation results for the return loss ($S_{1,1}$).

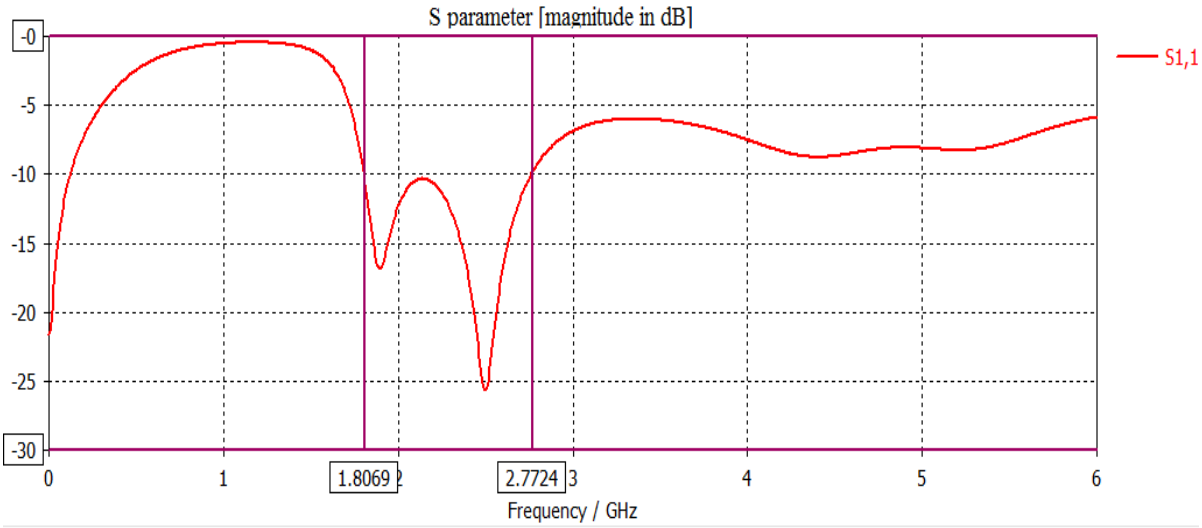

Figure(4.2): Simulated return loss curve

The figure above shows the band width of antenna at -10 dB which operates at frequency range (1.80-2.77) GHz.

4.3 Design of Modified Bow-tie Antenna

Figure (4.3) Shows the structure of the proposed modified bow tie antenna with its design parameters. The final values of the design parameters are presented in table (4.2). In this design, the left triangle of the proposed antenna is increased in size until it becomes bigger than other. This proposed modified antenna is different from the conventional bow-tie antenna , it has directional pattern in the elevation plane as will be shown.

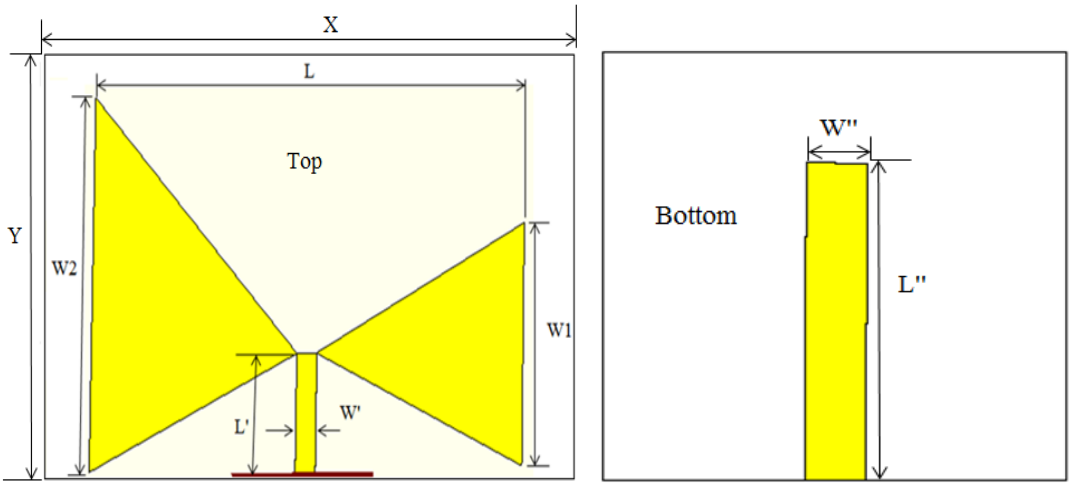

Figure(4.3): Structure of modified bow-tie with increasing size of left triangle

Table(4.2): Dimensions of the proposed modified bow-tie antenna with increasing size of left triangle.

Dimensions	**(mm)**
Substrate thickness	1.6
Substrate width (X)	47
Substrate length(Y)	60
Feed line width(W')	3.085
Feed line length(L')	22.6
Ground plane width(W")	6
Ground plane length(L")	43.1

Distance between Bow-Tie triangles (L)	41
Width of the right triangle (W1)	40
Width of the left triangle (W2)	55

The simulation results in Figure (4.4) show that the -10dB band width of the antenna is (1.87-2.76) GHz.

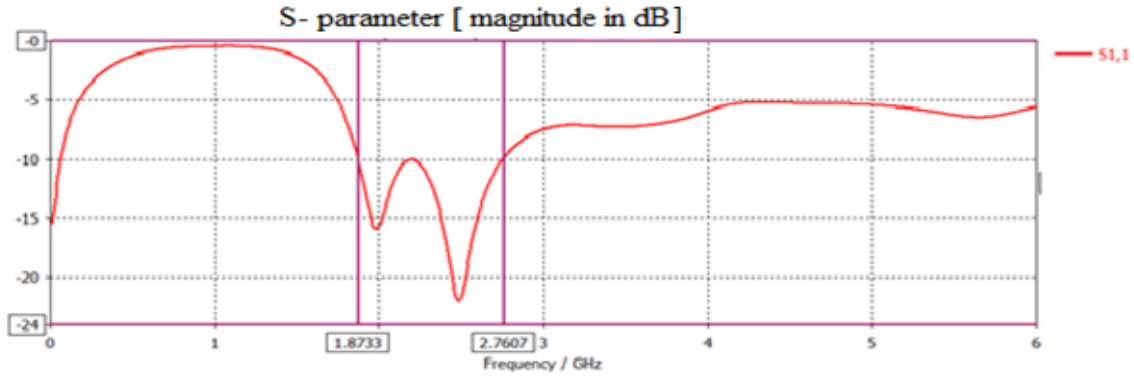

Figure(4.4): Simulated return loss (S_{11}) with (W2=55mm)

The radiation pattern of modified antenna is changed to directional since the left triangle is increased in size. Figure (4.5) shows the radiation pattern of the proposed antenna at different frequencies and the gain at those frequencies.

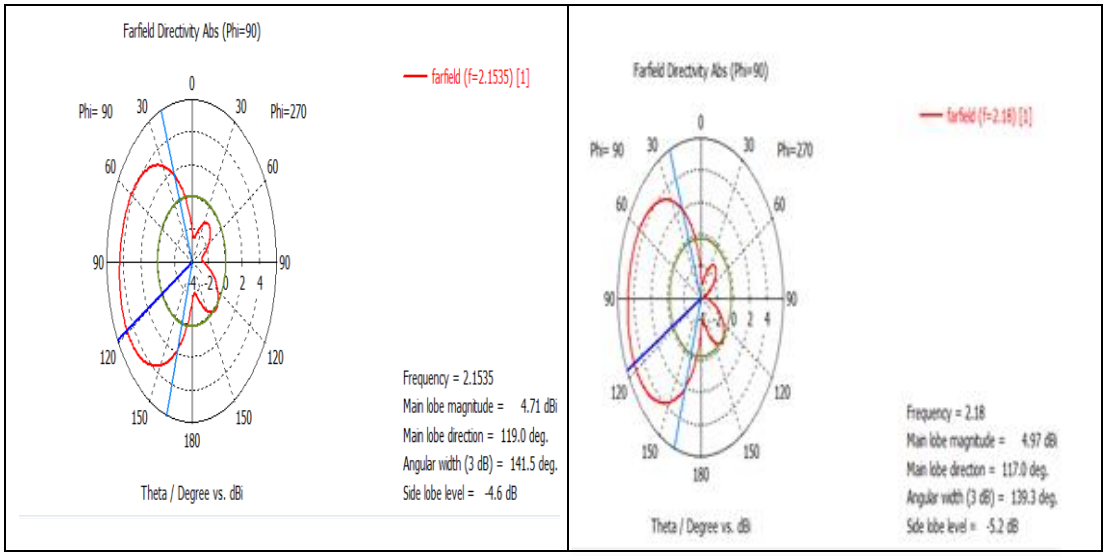

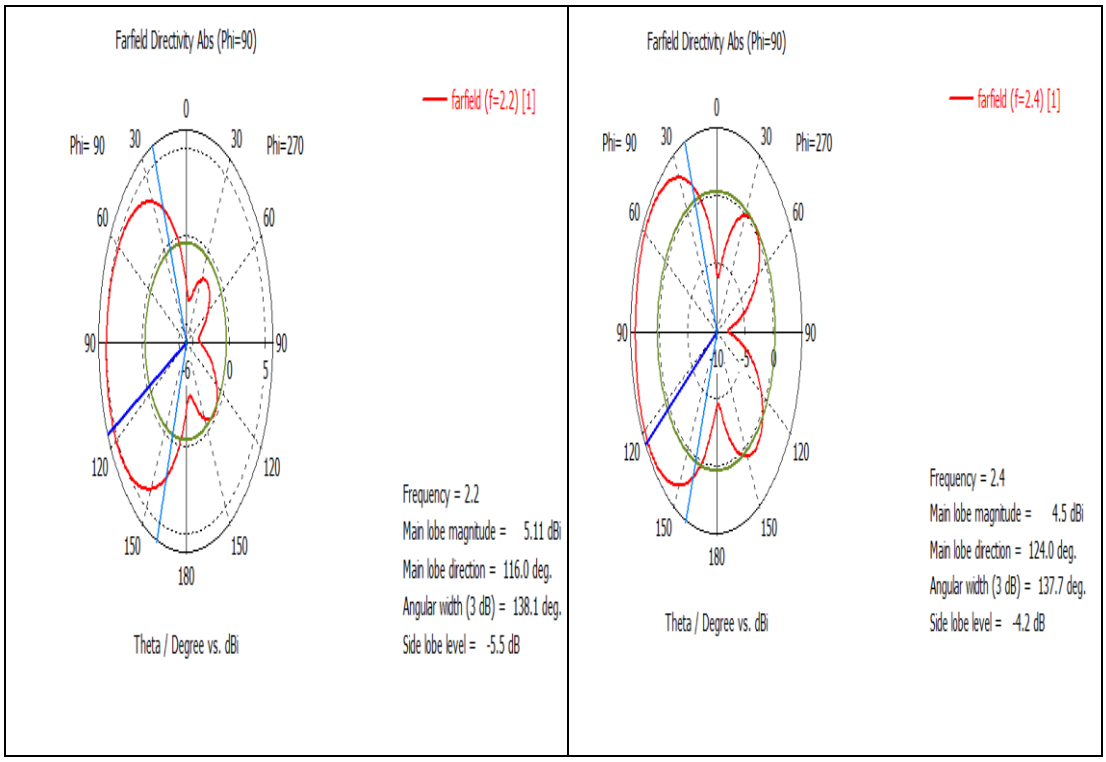

Figure (4.5): Simulated radiation patterns and the gains at different frequencies of the modified antenna(W2=55mm).

Now, the width of left triangle (W2)=45 mm.

The simulation results in Figure (4.6) show that the -10dB band width of the antenna is (1.86-2.70) GHz.

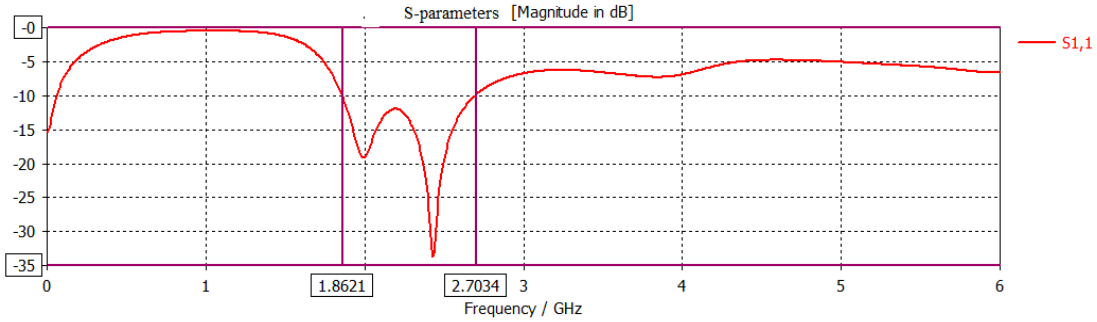

Figure(4.6): Simulated return loss (S_{11}) with (W2=45mm)

Figure (4.7) shows the radiation pattern of the proposed antenna at different frequencies and the gain at those frequencies.

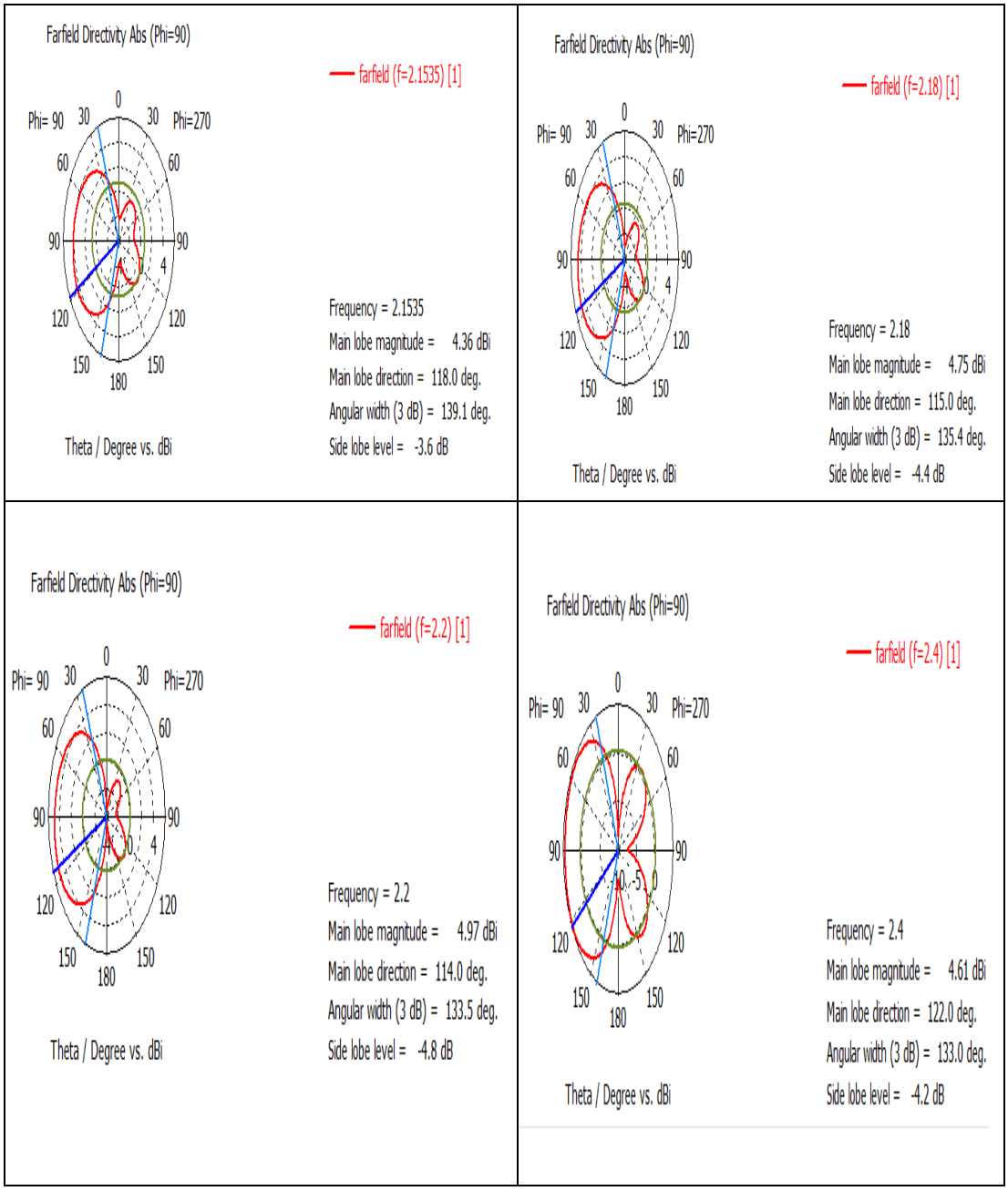

Figure (4.7): Simulated radiation patterns and the gains at different frequencies of the modified antenna(W2=45mm).

The width of left triangle (W2)=35 mm.

The simulation results in Figure (4.8) show that the -10dB band width of the antenna is (1.86-2.627) GHz.

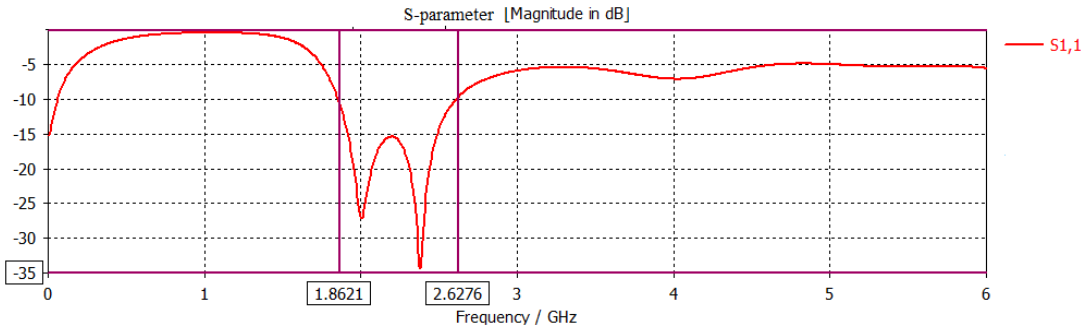

Figure(4.8): Simulated return loss (S_{11}) with (W2=35 mm)

Figure (4.9) shows the radiation pattern of the proposed antenna at different frequencies and the gain at those frequencies.

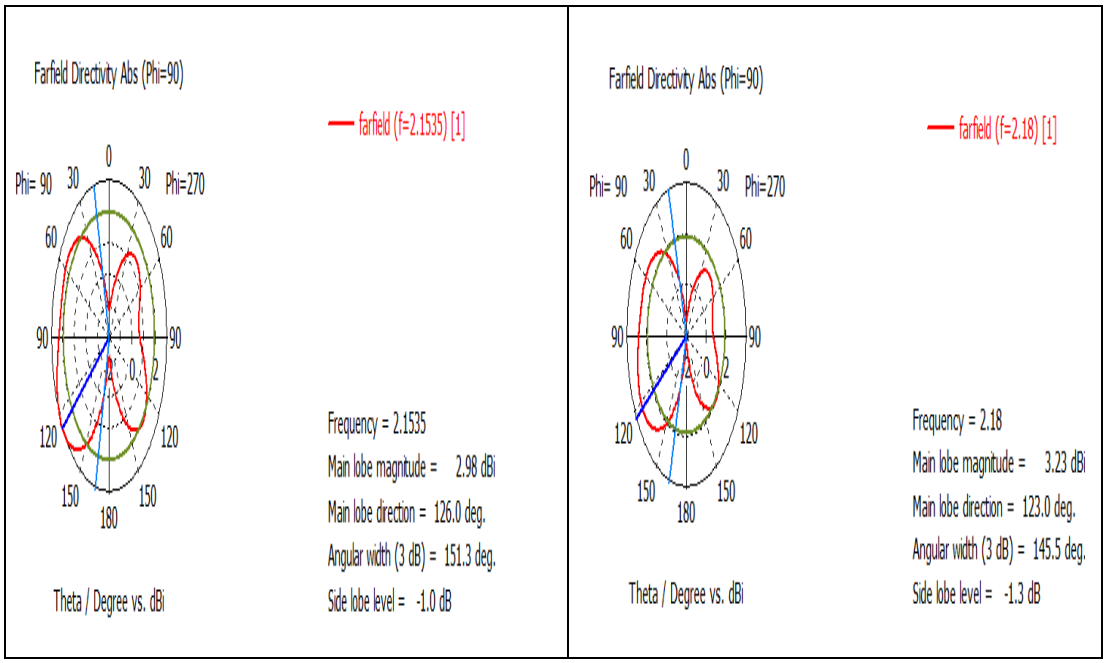

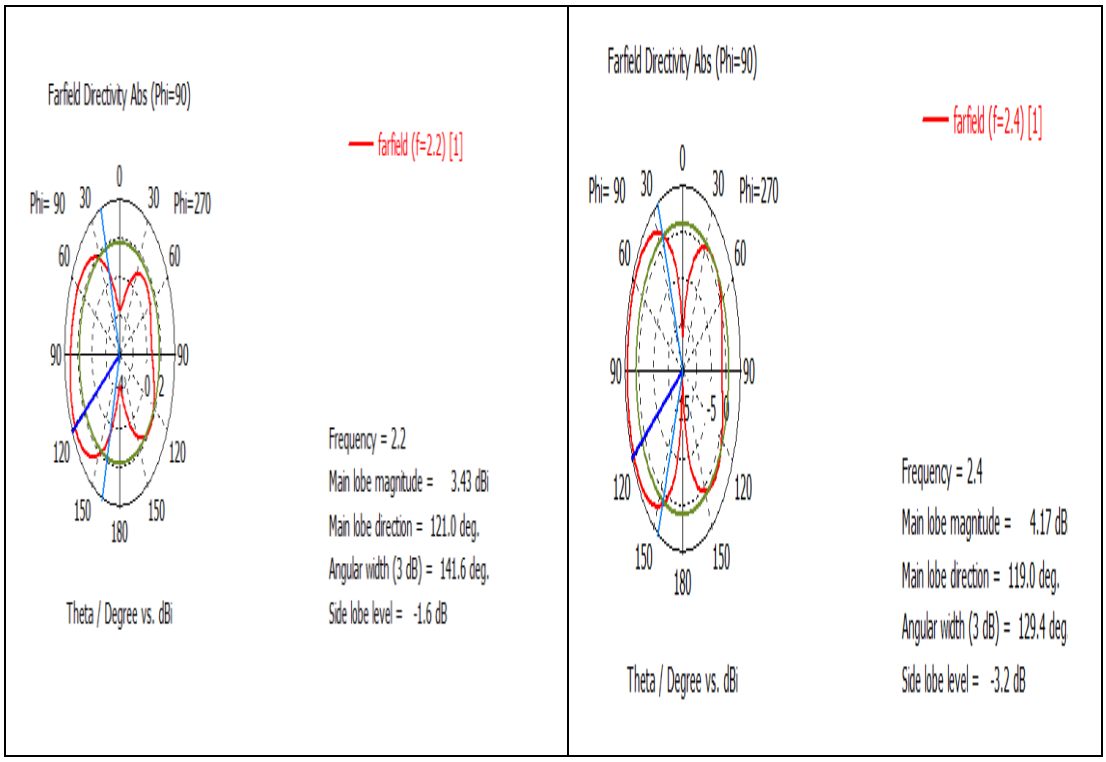

Figure (4.9): Simulated radiation patterns and the gains at different frequencies of the modified antenna(W2=35mm).

With decreasing the width of the left triangle, the gains at different frequencies are decreased. The radiation patterns are reconfigured to the left side and they are approached to the dipole antenna radiation pattern.

Similar simulation has been performed with the right triangle of proposed antenna increased until becoming bigger than the other triangle as shown in Figure (4.10). The final dimensions of the proposed antenna are listed in table 4.3.

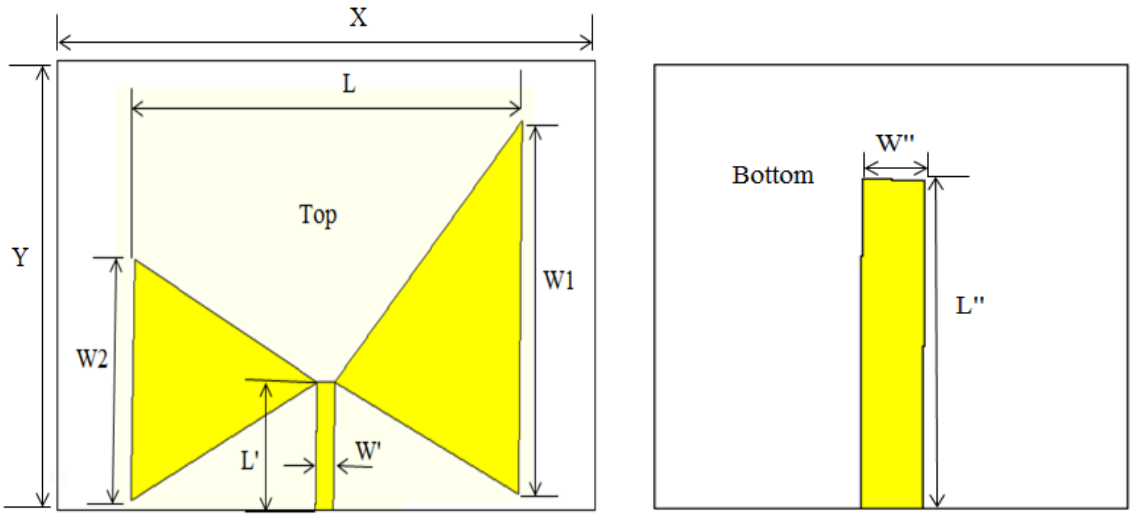

Figure(4.10): Structure bow-tie antenna with increasing at right triangle

Table(4.3): Dimensions of the modified bow-tie antenna with increasing of right triangle.

Dimensions	**(mm)**
Substrate thickness	1.6
Substrate width (X)	47
Substrate length(Y)	60
Feed line width(W')	3.085
Feed line length(L')	22.6
Ground plane width(W'')	6
Ground plane length(L'')	43.1
Distance between Bow-Tie triangles (L)	41
Width of the first triangle (W1)	55
Width of the second triangle (W2)	40

Figure (4.11) shows the return loss S_{11} and the band width of proposed modified bow-tie antenna is (1.87-2.76) GHz.

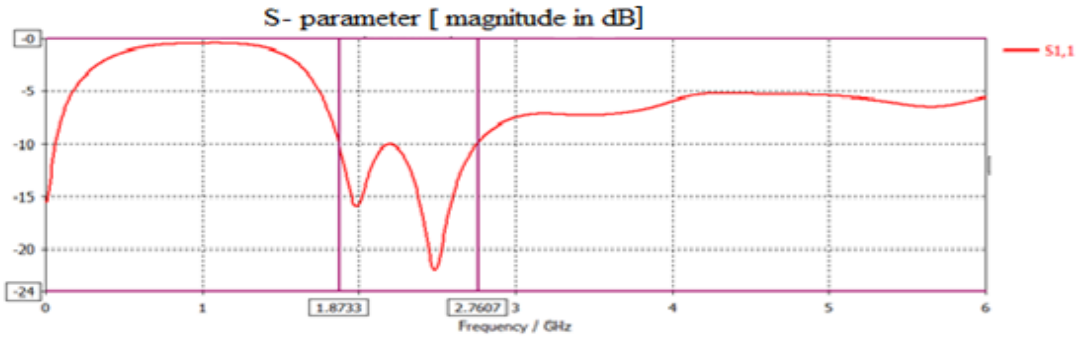

Figure(4.11): Return loss of modified antenna with increased size of right triangle(W1=55mm)

The radiation pattern of the modified antenna with large right triangle is directional and it is in opposite direction to that of the antenna with large left triangle. Figure (4.12) shows the radiation pattern of the proposed antenna at different frequencies and the gain at those frequencies.

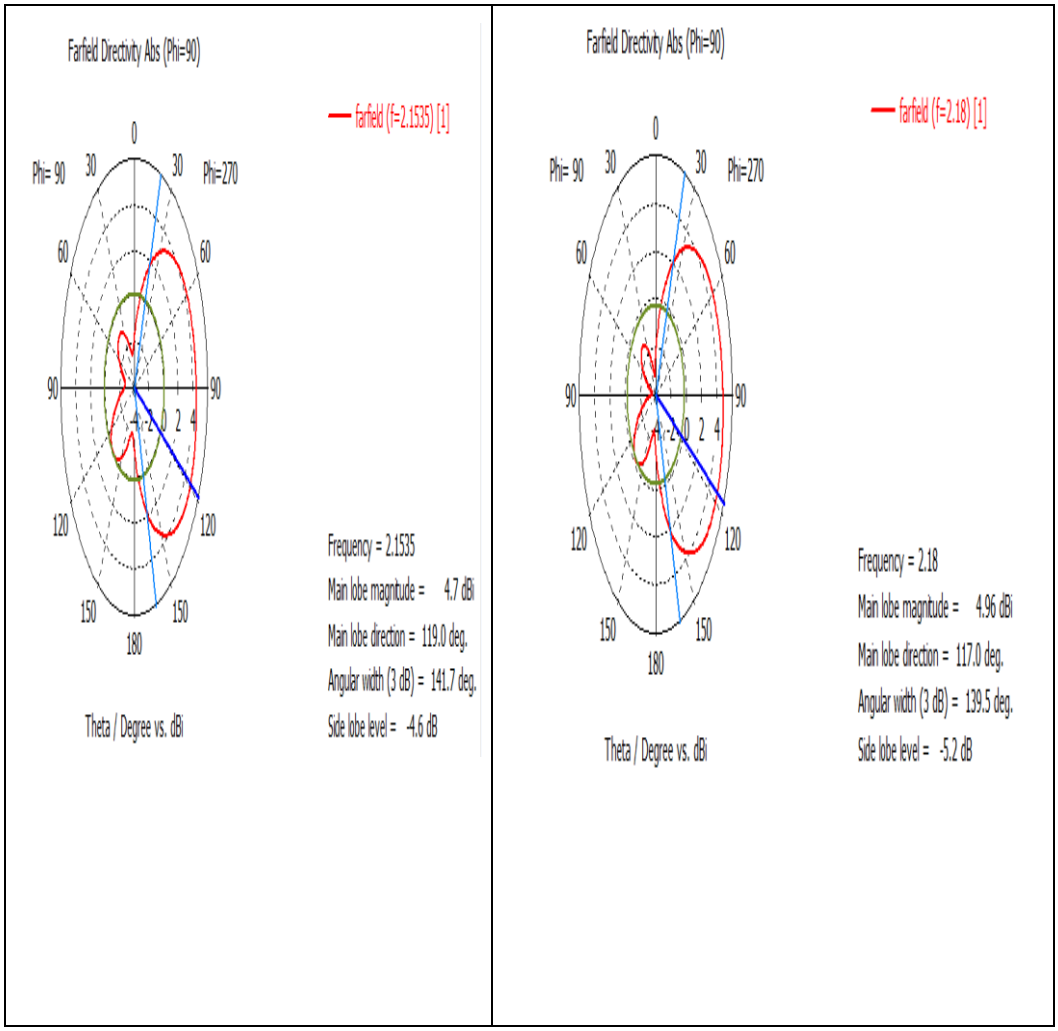

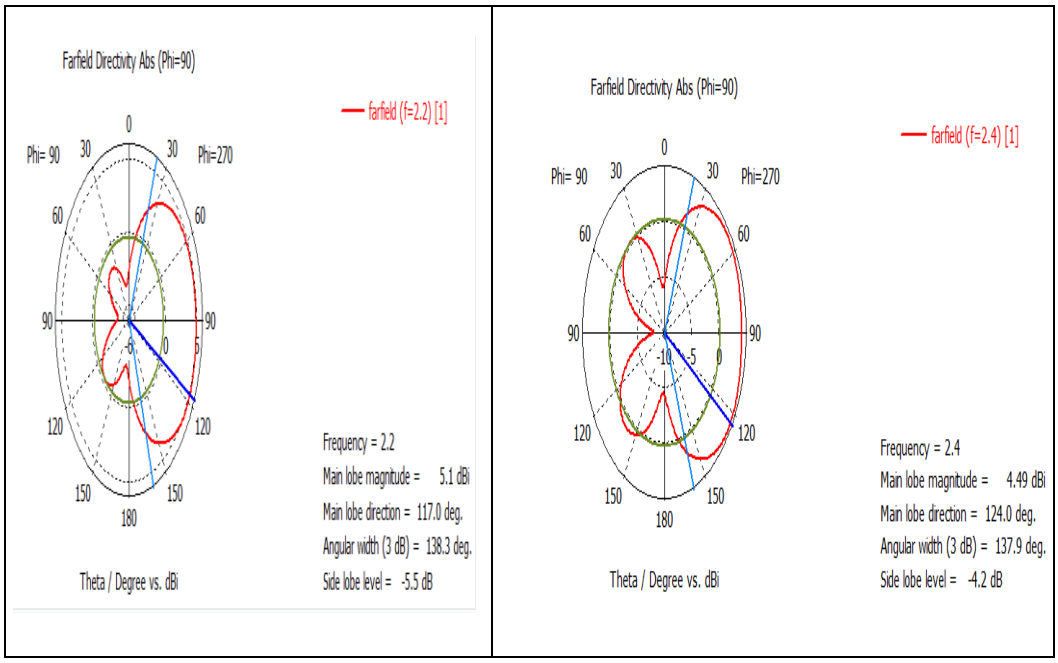

Figure(4.12): Simulated radiation patterns and the gains at different frequencies for modified antenna with large right triangle(W1=55mm).

Now, the width of right triangle (W1)=45 mm.

The simulation results in Figure (4.13) show that the -10dB band width of the antenna is (1.86-2.70) GHz.

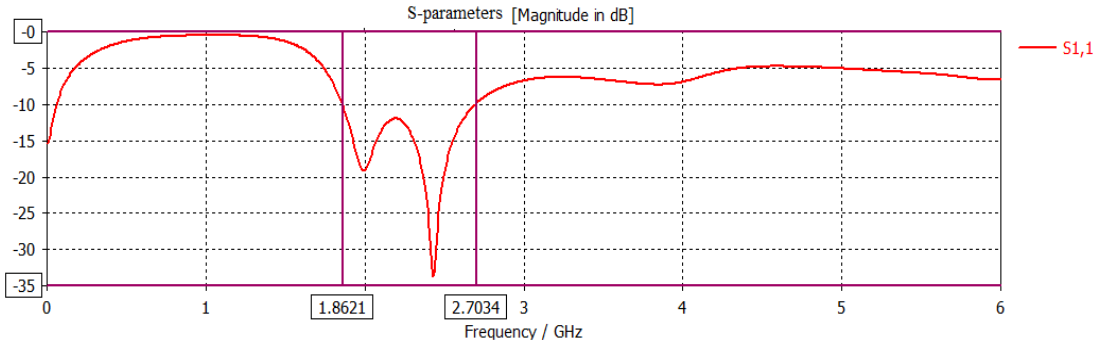

Figure (4.13): Return loss of modified antenna with increased size of right triangle(W1=45mm)

Figure (4.14) shows the radiation pattern of the proposed antenna at different frequencies and the gain at those frequencies.

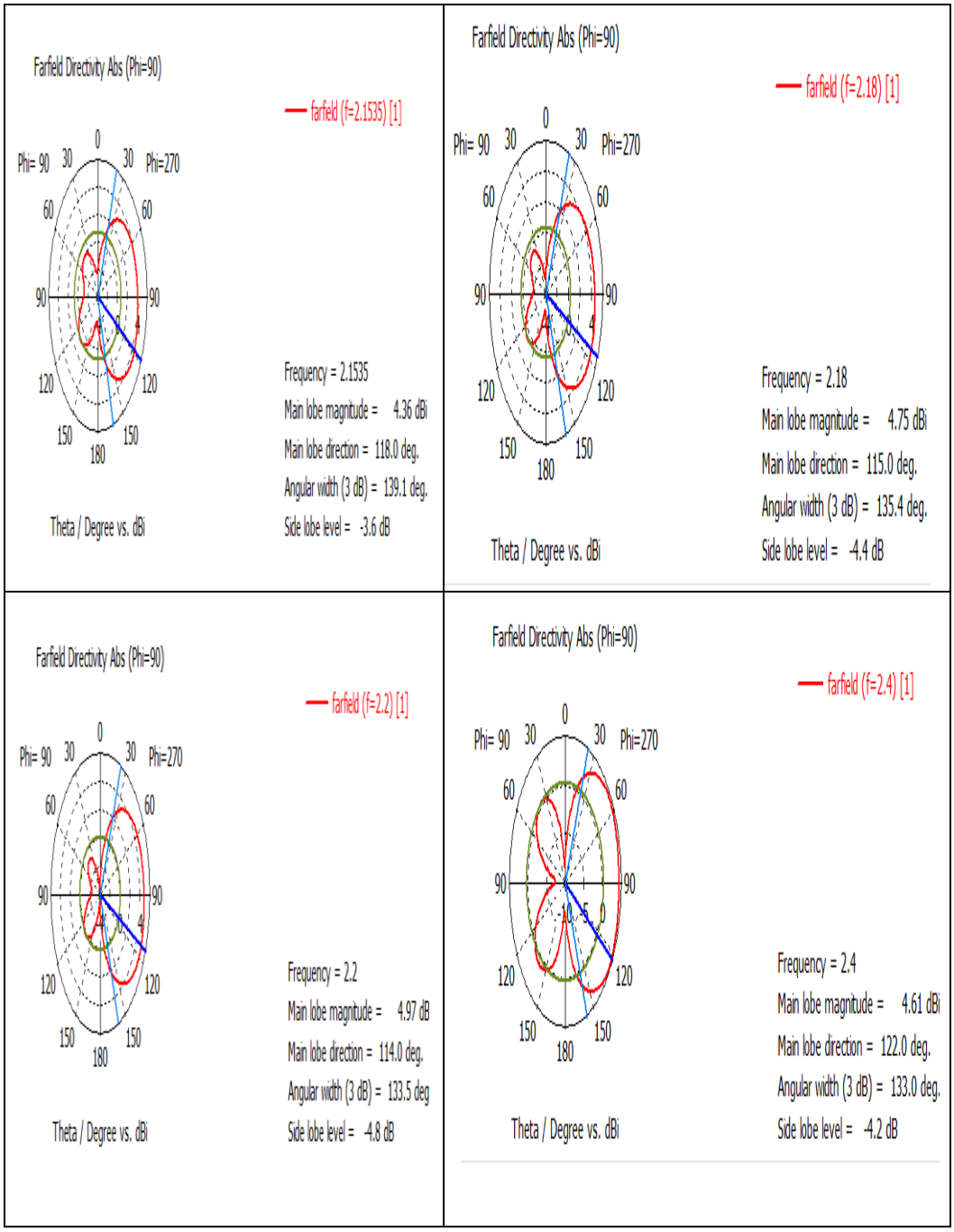

Figure(4.14): Simulated radiation patterns and the gains at different frequencies for modified antenna with large right triangle(W1=45mm).

The width of right triangle (W1)=35 mm.

The simulation results in Figure (4.15) show that the -10dB band width of the antenna is (1.86-2.62) GHz.

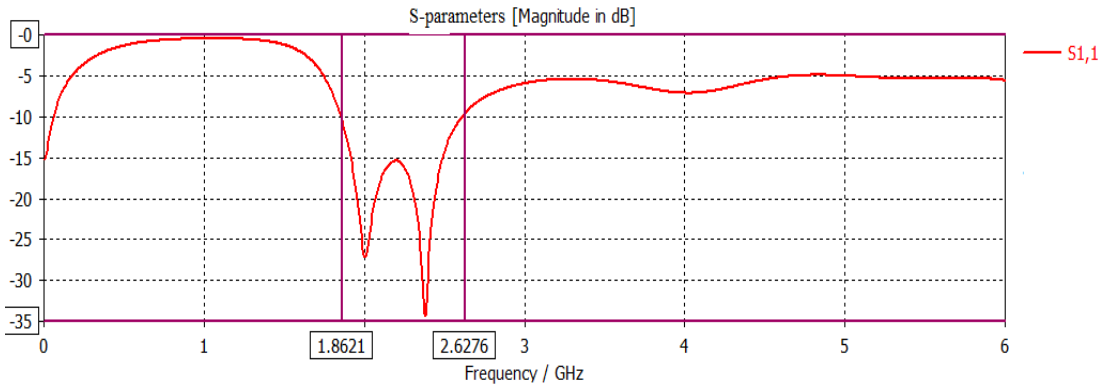

Figure (4.15): Return loss of modified antenna with increased size of right triangle(W1=35mm)

Figure (4.16) shows the radiation pattern of the proposed antenna at different frequencies and the gain at those frequencies.

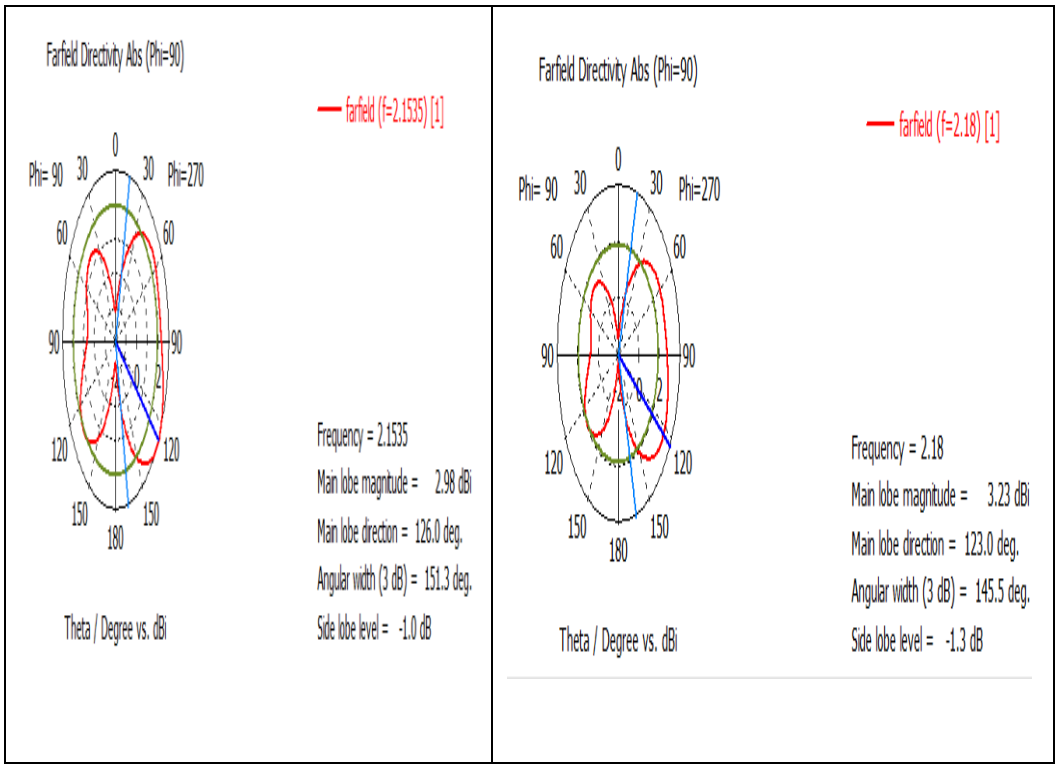

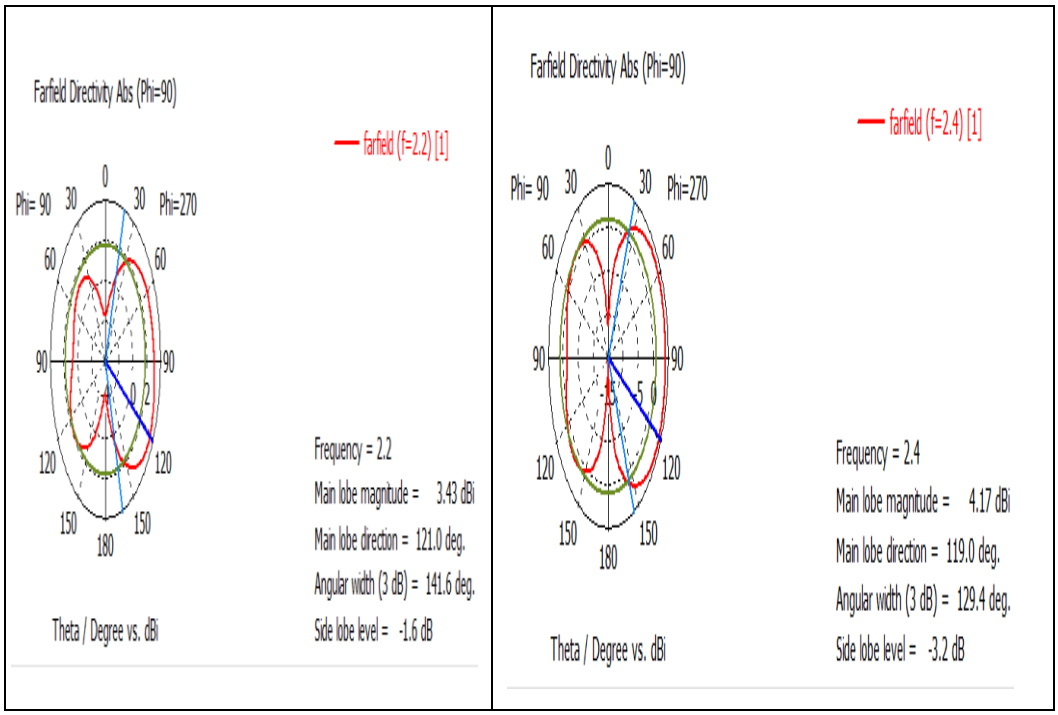

Figure(4.16): Simulated radiation patterns and the gains at different frequencies for modified antenna with large right triangle(W1=35mm).

With decreasing the width of the right triangle, the gains at different frequencies are decreased. The radiation patterns are reconfigured to the right side and they are approached to the dipole antenna radiation pattern.

4.4 Design of Pattern Reconfigurable Bow-tie Antenna

In this section reconfigurable pattern bow tie antenna will be designed by two methods, The first antenna is designed by adding the microstrip segments on the top of substrate and those segment can be connected to the ground via substrate using PIN diodes. The second design has microstrip segments on the bottom of substrate from ground side and they can be connected to the ground through PIN switches.

4.4.1 Design Pattern Reconfigurable Bow-tie Antenna with Microstrip Segments on Top

Figure (4.17) shows the same structure of bow tie antenna as in section (4.2) with adding microstrip segments on the top of substrate and those segments can be connected to the ground through vias and switches. The antenna is operated at three states of different radiation patterns . The final values of the design sizes are presented in table (4.4).

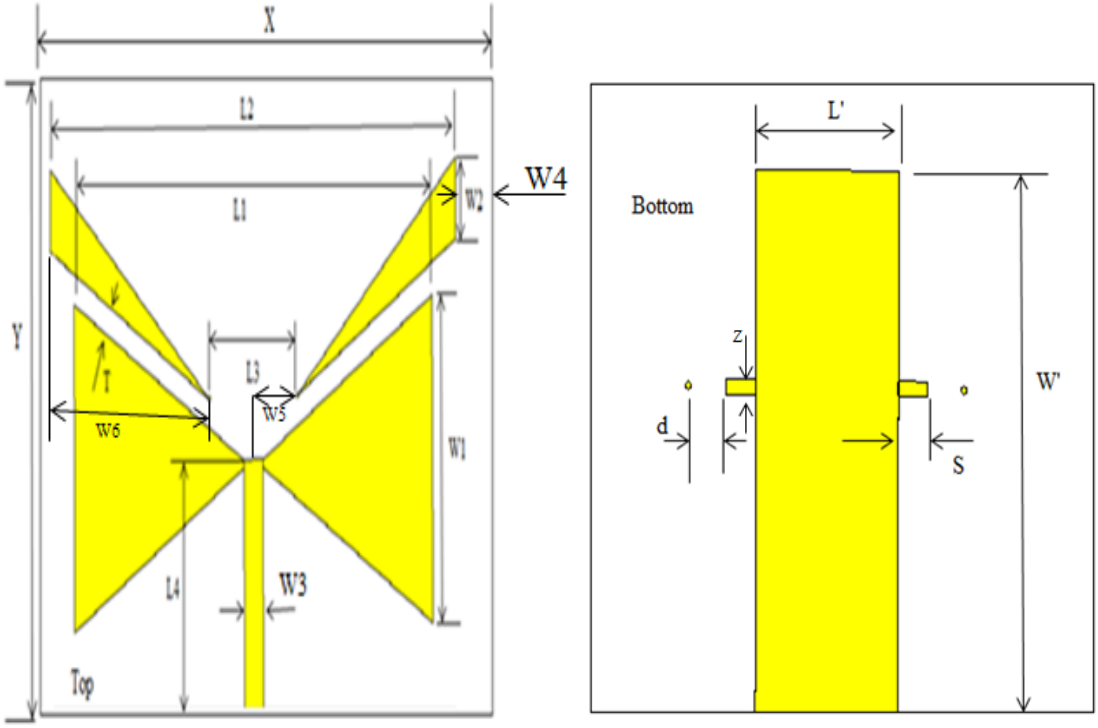

Figure(4.17): Bow-tie antenna with microstrip segments on the top.

Table(4.4): Dimensions of the proposed pattern reconfigurable bow-tie antenna with adding microstrip segments on the top.

Dimensions	**(mm)**
Substrate thickness	1.6
Substrate width (X)	90
Substrate length(Y)	60
Feed line width(W3)	3.085

Feed line length(L4)	25.3
Ground plane width(W')	3.8
Ground plane length(L')	43.8
Distance between Bow-Tie triangles (L1)	35.8
Width of triangle (W1)	26.89
Width of adding segment (W2)	6.7
The distance between the triangle segment and the substrate(W4)	9
The distance between the center of the feed line and the triangle segment(W5)	10.50
The length of the triangle segment(W6)	35
Distance between two adding segments (L2)	85.6
Distance between two holes (L3)	18.5
Distance between the adding segment and Bow-Tie antenna (T)	2.8
Distance between the hole and the ground plane segment (d)	2.2
Length of the ground plane segment (S)	2
Width of the ground plane segment (Z)	0.8

Two PIN diode switches are placed on the bottom surface and their purpose is to connect the segments on top to the ground through vias. Figure (4.18) shows the bottom of the proposed antenna and the locations of the switches. Three working states are considered here to give reconfigurable antenna pattern: State (0): Switch1 is OFF and switch2 is OFF. State (1): Switch1 is ON and switch2 is OFF and State (2): Switch1 is OFF and switch2 is ON. The final values of the design sizes of PIN diodes are presented in table (4.5).

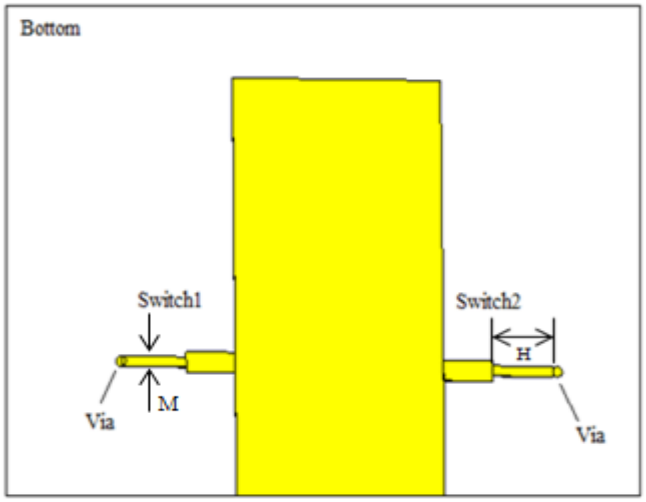

Figure(4.18): Bottom of proposed antenna with microstrip segments on top

Table(4.5): Dimensions of the PIN diodes

Dimensions	**(mm)**
The length of PIN diode(H)	2.2
The width of PIN diode(M)	0.4
PIN diode thickness	0.02

Figure (4.19) shows the return loss (S_{11}) for the antenna at state(0) , the -10 dB band width of the proposed antenna is (1.82-2.56) GHz.

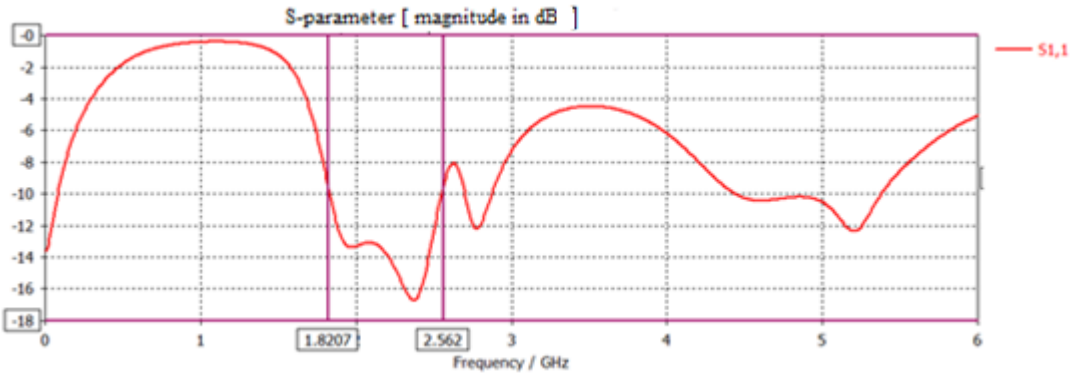

Figure(4.19): Simulated return loss (S_{11}) of state (0) for the antenna with microstrip segments on top

The radiation patterns are shown in the figure (4.20) of the proposed antenna at different frequencies .

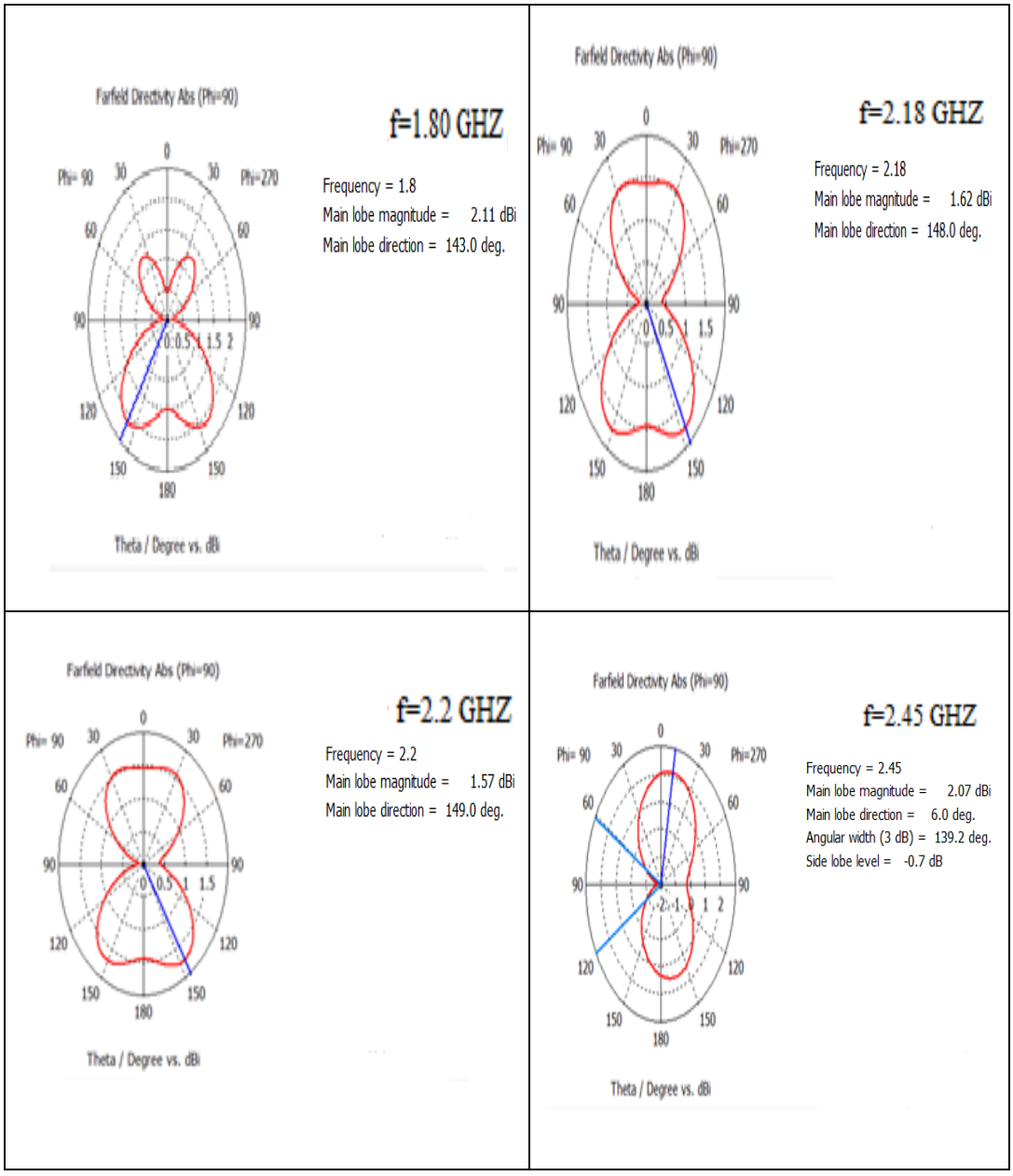

Figure(4.20): Simulated radiation patterns of state (0) for the antenna with microstrip segments on top.

The radiation patterns for state(0) are reconfigured like dipole antenna radiation pattern.

The simulated return loss (S_{11}) for state (1) is shown in the figure (4.21) , the -10 dB band width of the proposed antenna is (1.70-2.54) GHz.

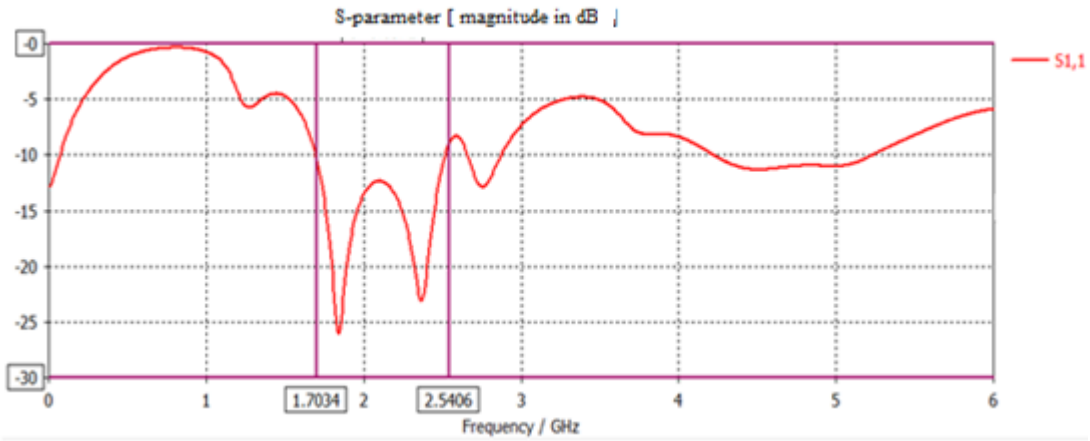

Figure(4.21): Simulated return loss (S_{11}) of state (1) for the antenna with microstrip segments on top

For state (1), the radiation patterns are directional as presented in figure (4.22) at different frequencies.

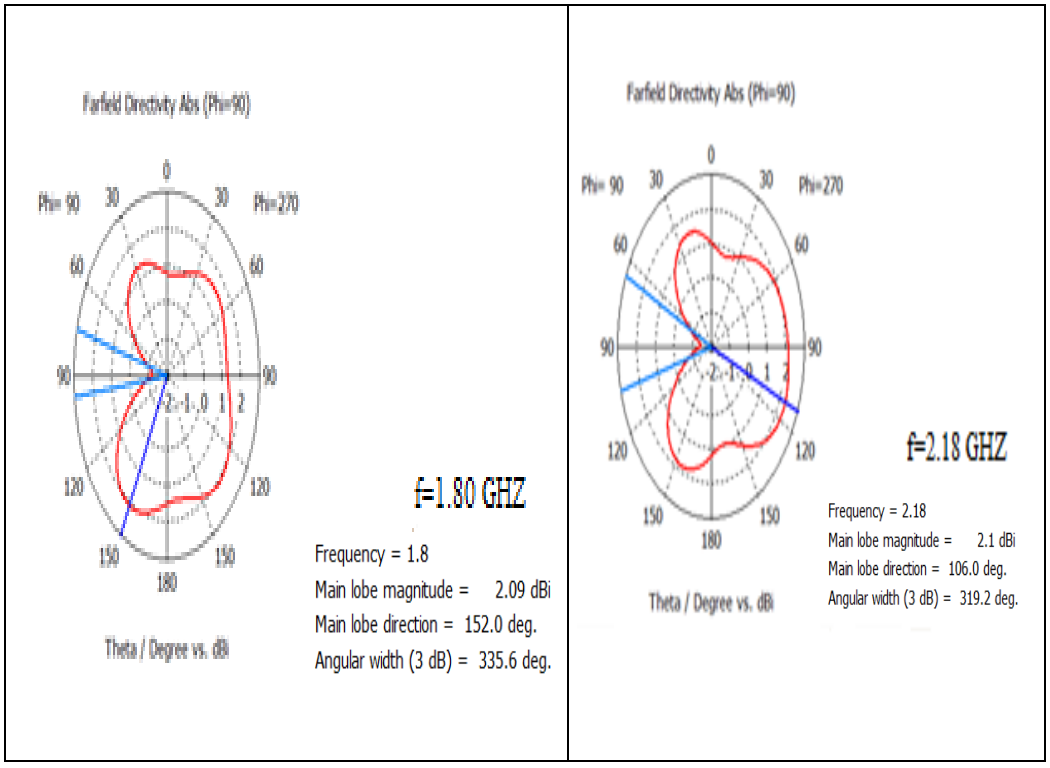

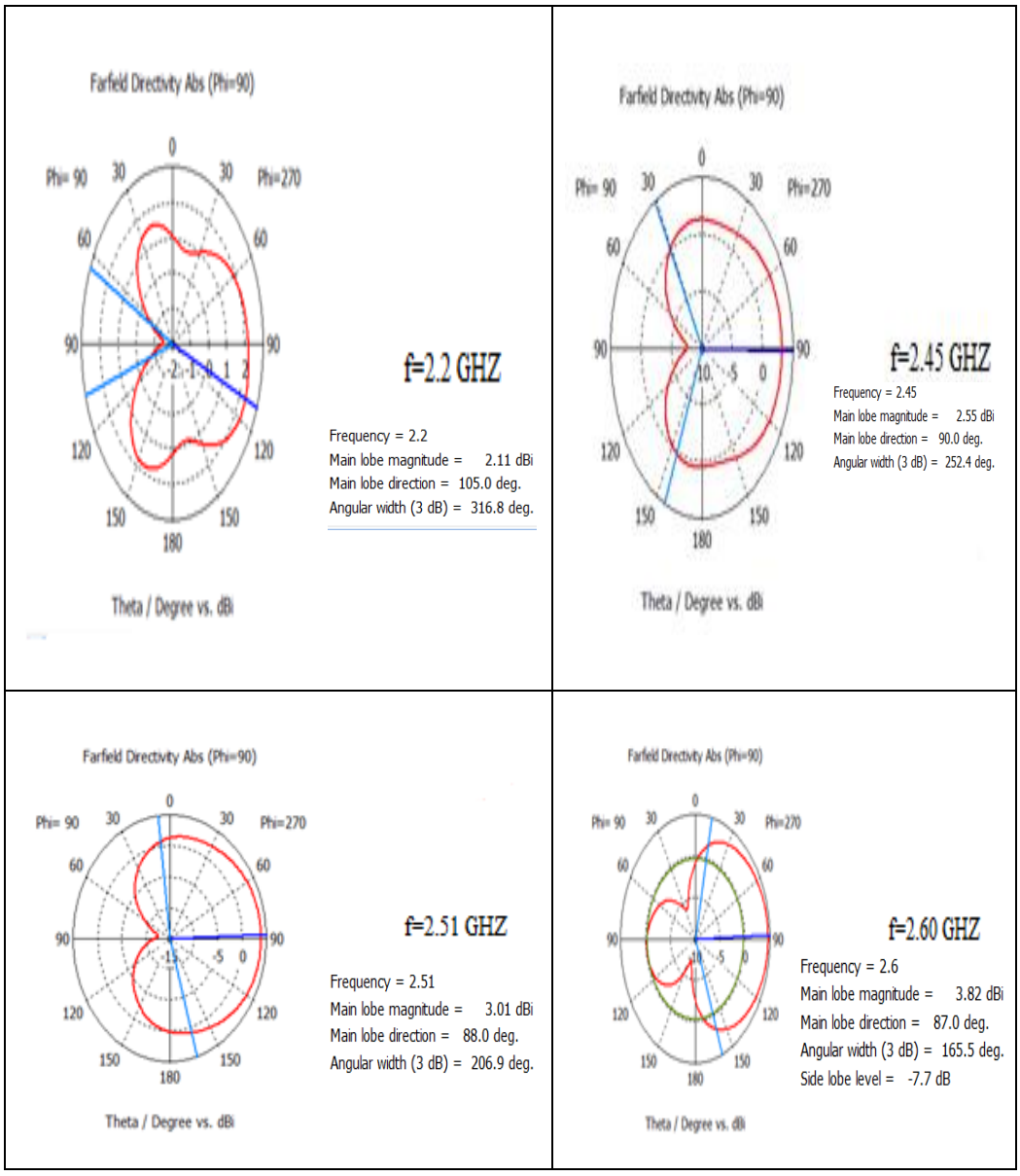

Figure (4.22): Simulated radiation patterns of state(1) for the antenna with microstrip segments on top.

The radiation patterns for state(1) are reconfigured to the right side because the right triangle segment on the top is connected to the ground via substrate through switch1.

Figure (4.23) shows the return loss (S_{11}) of state (2) , the -10 dB band width of the proposed antenna is (1.70-2.56) GHz.

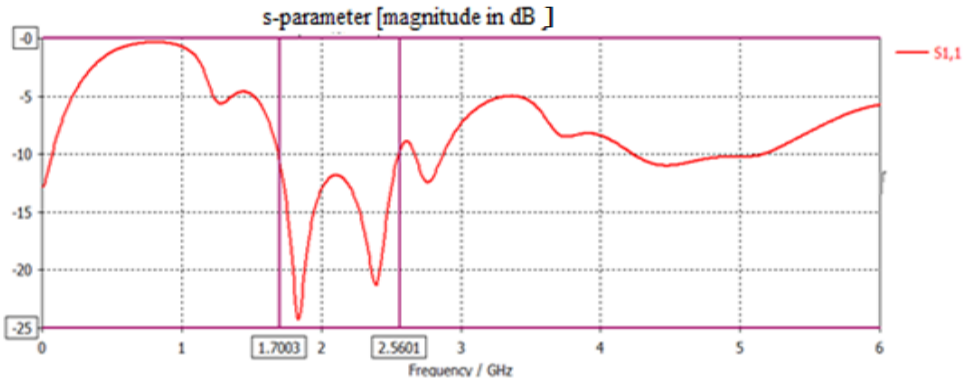

Figure(4.23): Simulated return loss S_{11} of state (2) for the antenna with microstrip segments on top.

For state(2), the radiation patterns are directional as shown in figure (4.24) at different frequencies.

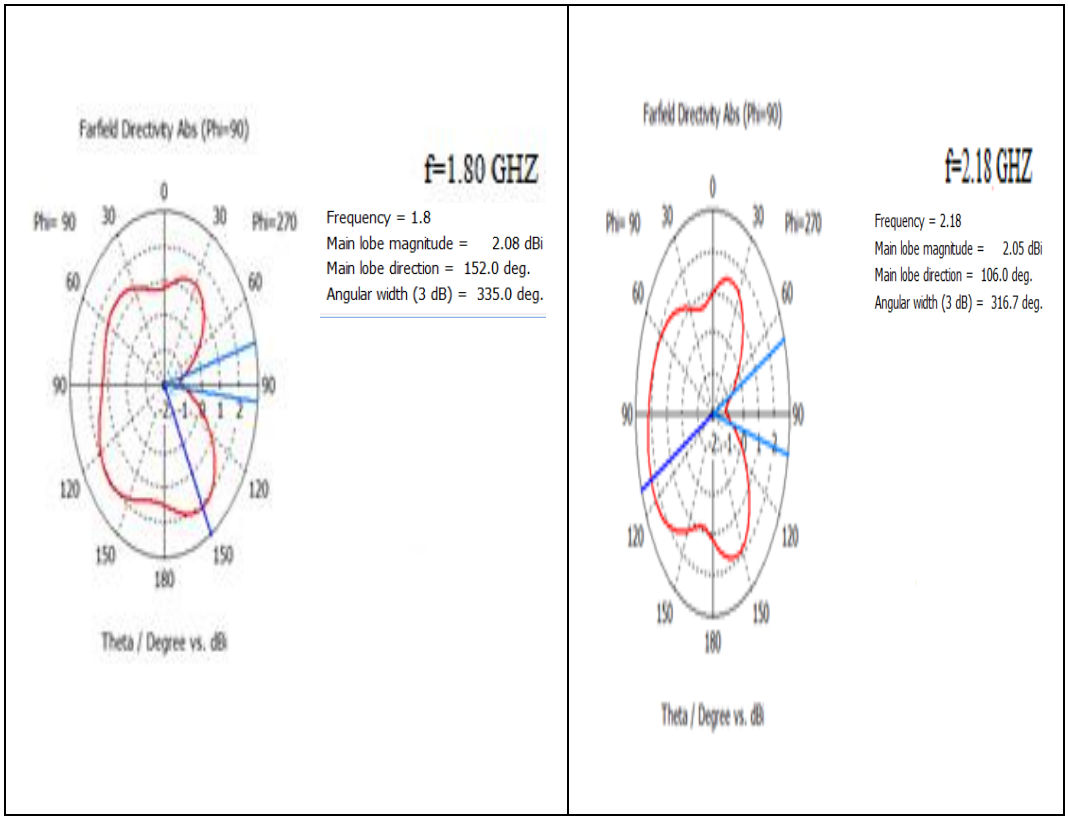

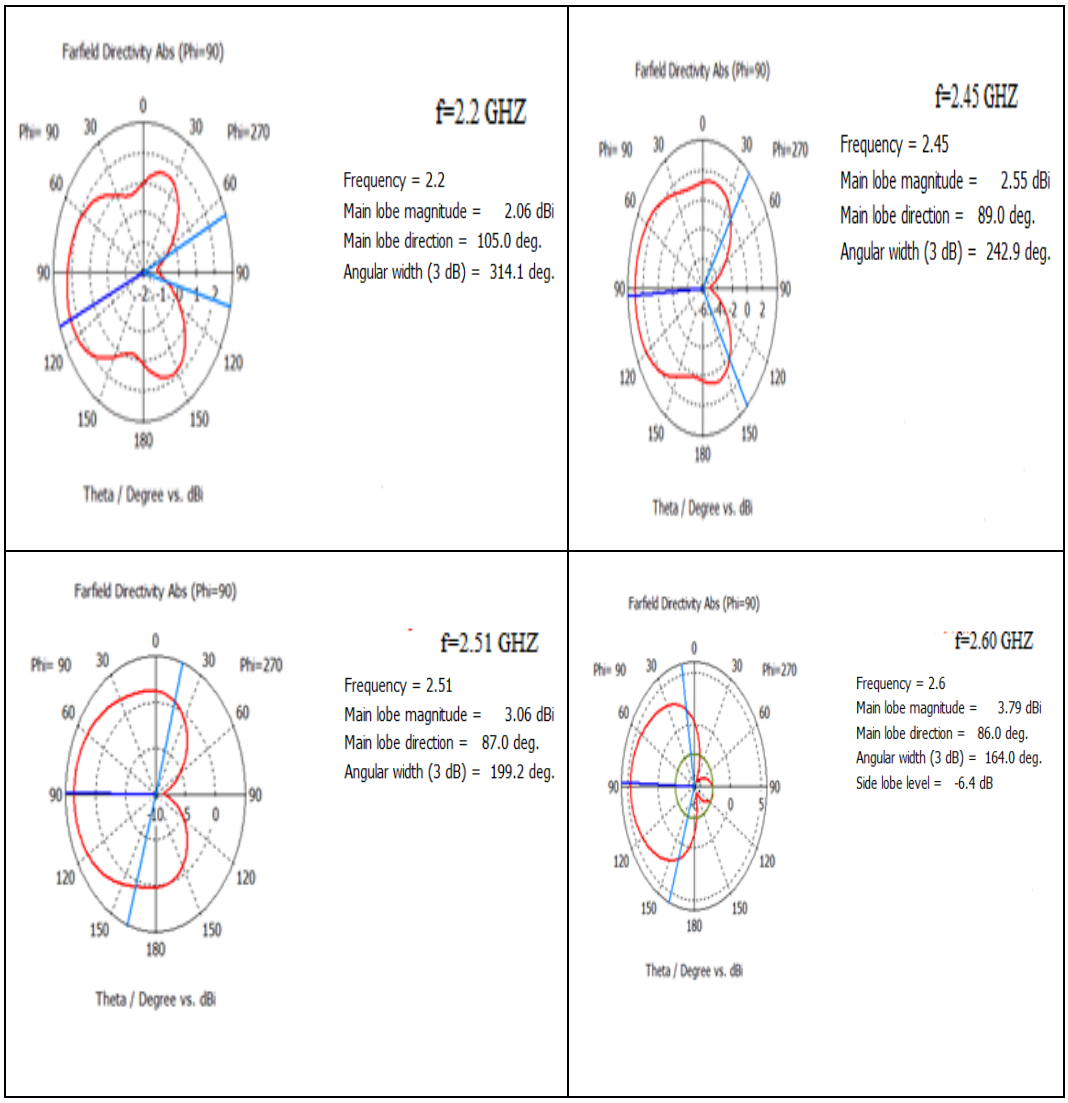

Figure(4.24): Simulated radiation patterns of state (2) for the antenna with microstrip segments on top.

The radiation patterns for state(2) are reconfigured to the left side because the left triangle segment on the top is connected to the ground via substrate through switch2.

4.4.2 Design Pattern Reconfigurable Bow-tie Antenna with Microstrip Segments on the Bottom

Figure (4.25) shows the same structure of bow-tie antenna as in section (4.2) with adding microstrip segments on the bottom of substrate and those segments can be connected to the ground through switches. The antenna is operated at three working states and the final values of the design parameters are presented in table (4.6).

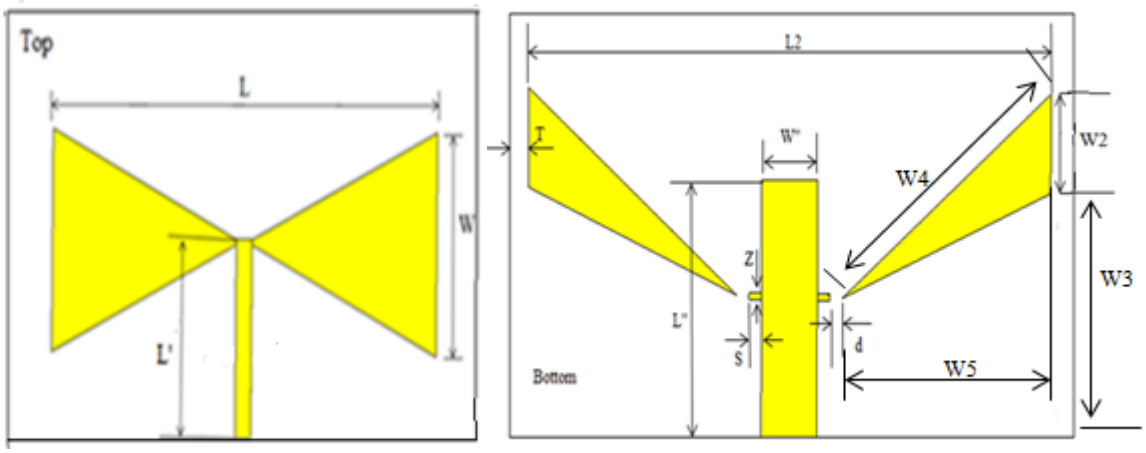

Figure(4.25): Proposed bow-tie antenna with microstrip segment on the bottom

Table(4.6): Dimensions of the proposed pattern reconfigurable bow-tie antenna with microstrip segments on the bottom.

Dimensions	**(mm)**
Substrate thickness	1.6
Feed line length(L')	25.3
Ground plane width(W")	3.8
Ground plane length(L")	43.8
Distance between Bow-Tie triangles (L)	35.8
Width of triangle (W)	26.89
Width of adding segments (W2)	11.7

The distance between the triangle segment and the substrate(W3)	41
The length of the triangle string(W4)	41.5
The length of the triangle side(W5)	35
Distance between adding segments (L2)	84.1
Distance between adding segments and the substrate (T)	1.5
Length of ground plane segment (S)	2
Distance between the ground plane segment and the adding segment (d)	2
Width of the ground plane segment (Z)	0.8

Two PIN diode switches are placed on the bottom surface to connect the triangular segments on the bottom to the ground. Figure (4.26) shows the bottom of the proposed antenna and the locations of the switches. Three working states give reconfigurable antenna pattern: State (0): Switch1 is OFF and switch2 is OFF. State (1): Switch1 is ON and switch2 is OFF, and State (2): Switch1 is OFF and switch2 is ON. The final values of the design sizes of PIN diodes are presented in table (4.7).

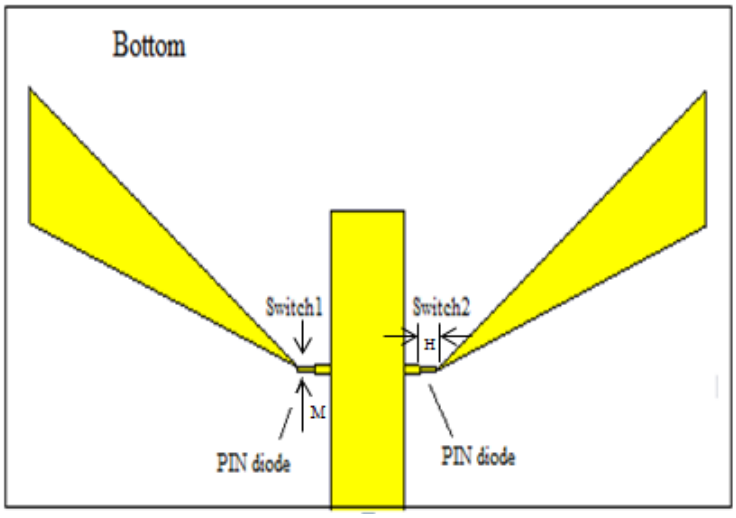

Figure(4.26): Bottom of the proposed antenna with microstrip segments

Table(4.7): PIN dimensions

Dimensions	**(mm)**
The length of PIN diode(H)	2
The width of PIN diode(M)	0.4
PIN diode thickness	0.02

Figure (4.27) shows the return loss (S_{11}) for state (0), the band width of the proposed antenna is (1.81-2.81) GHz.

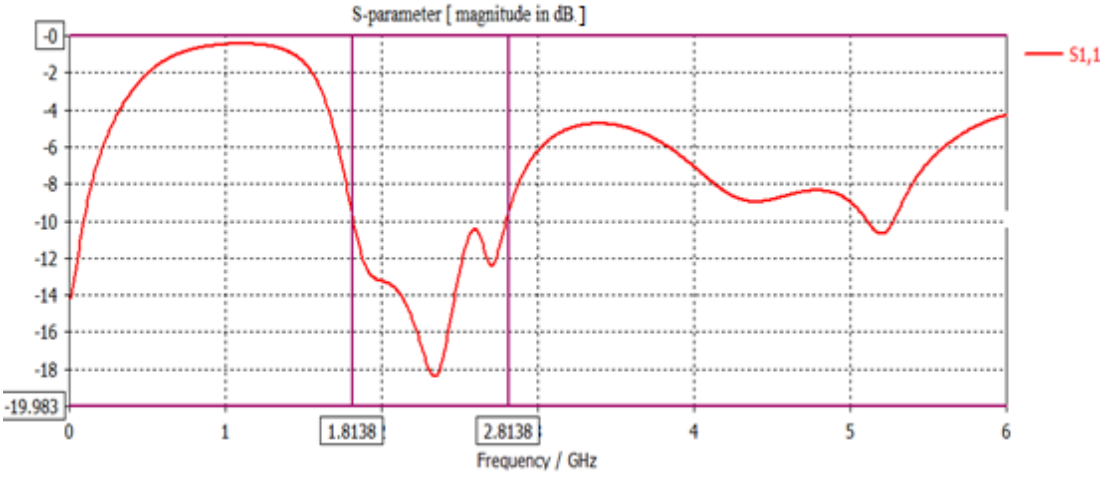

Figure(4.27): Simulated return loss S_{11} of state (0) for the antenna with microstrip segments on the bottom

The radiation patterns are shown in the figure (4.28) at different frequencies.

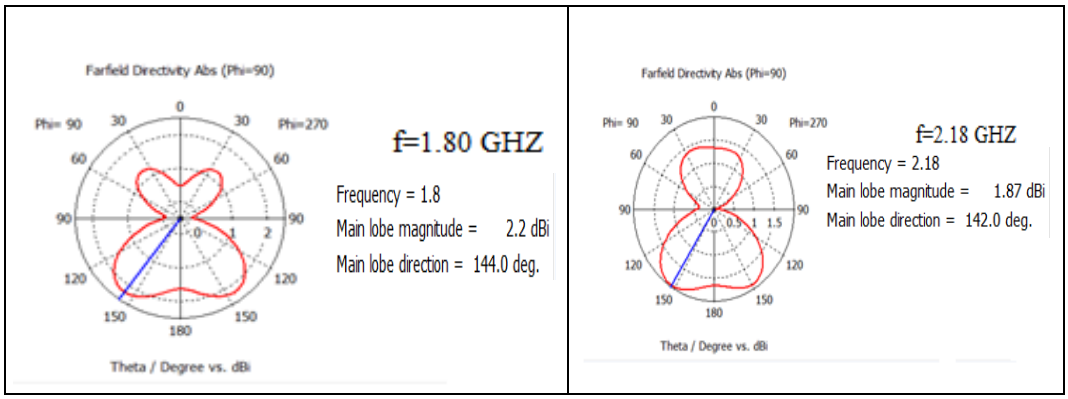

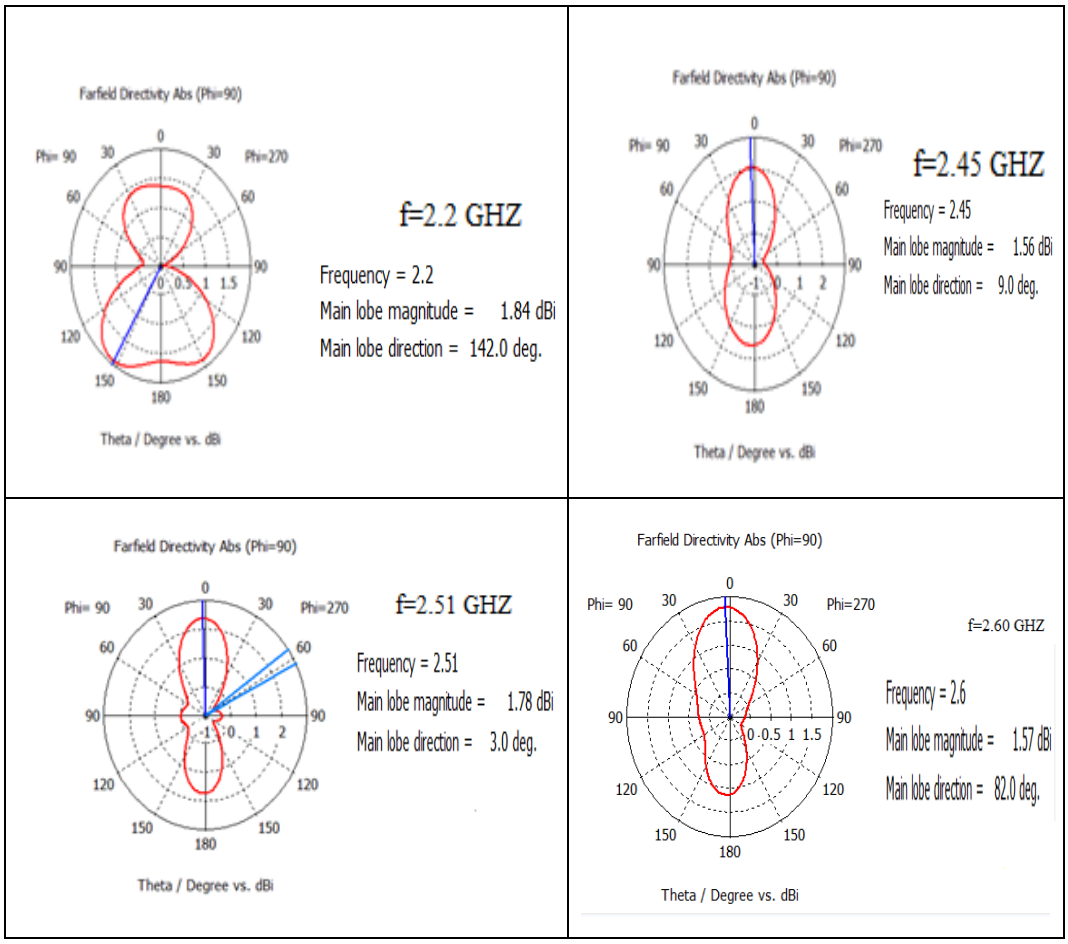

Figure(4.28): Simulated radiation patterns of state (0) for the antenna with microstrip segments at the bottom.

The radiation patterns for state(0) are reconfigured like dipole antenna radiation pattern.

Figure (4.29) shows the return loss (S_{11}) for state (1) , the band width of the proposed antenna is (1.65-2.80) GHz.

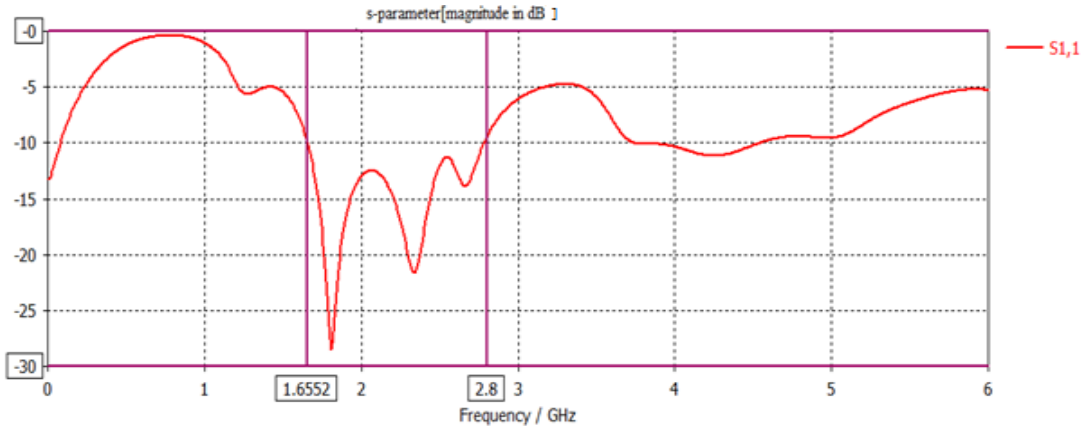

Figure(4.29): Simulated return loss S_{11} of state(1) for the antenna with microstrip segments at the bottom.

The radiation patterns are shown in the figure (4.30) for the proposed antenna at different frequencies.

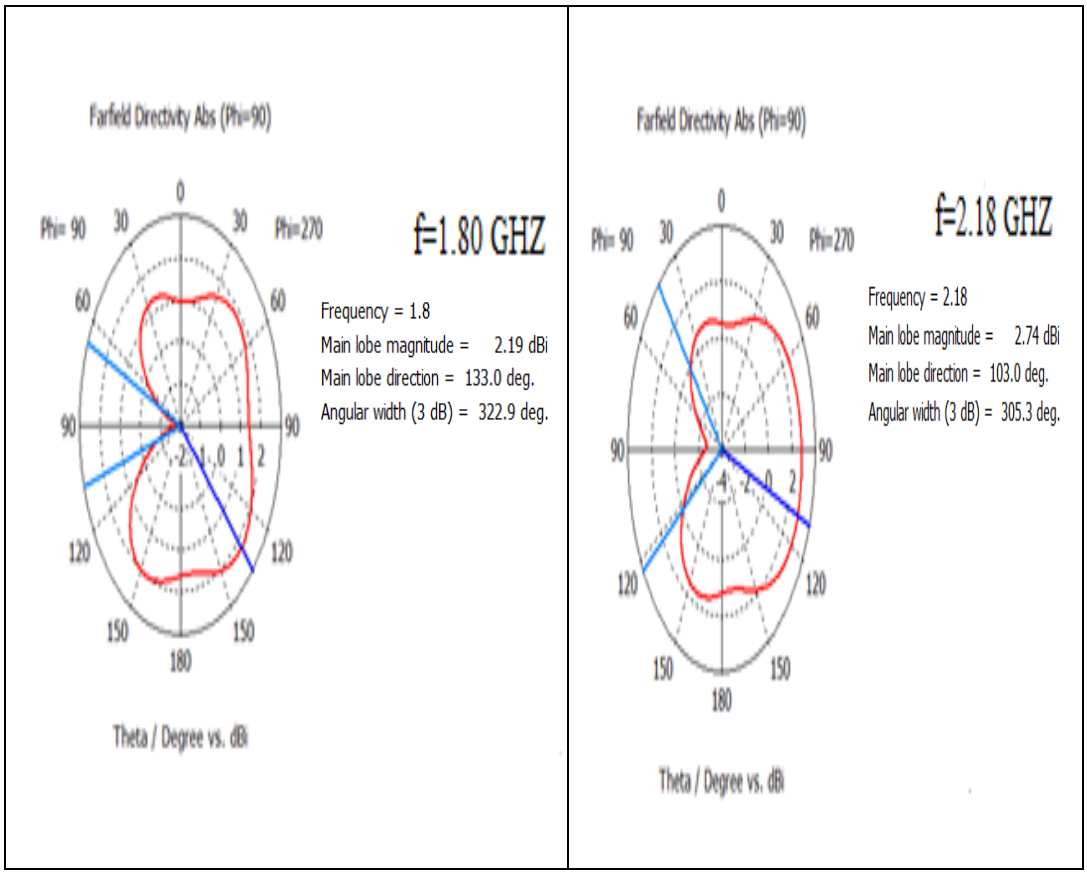

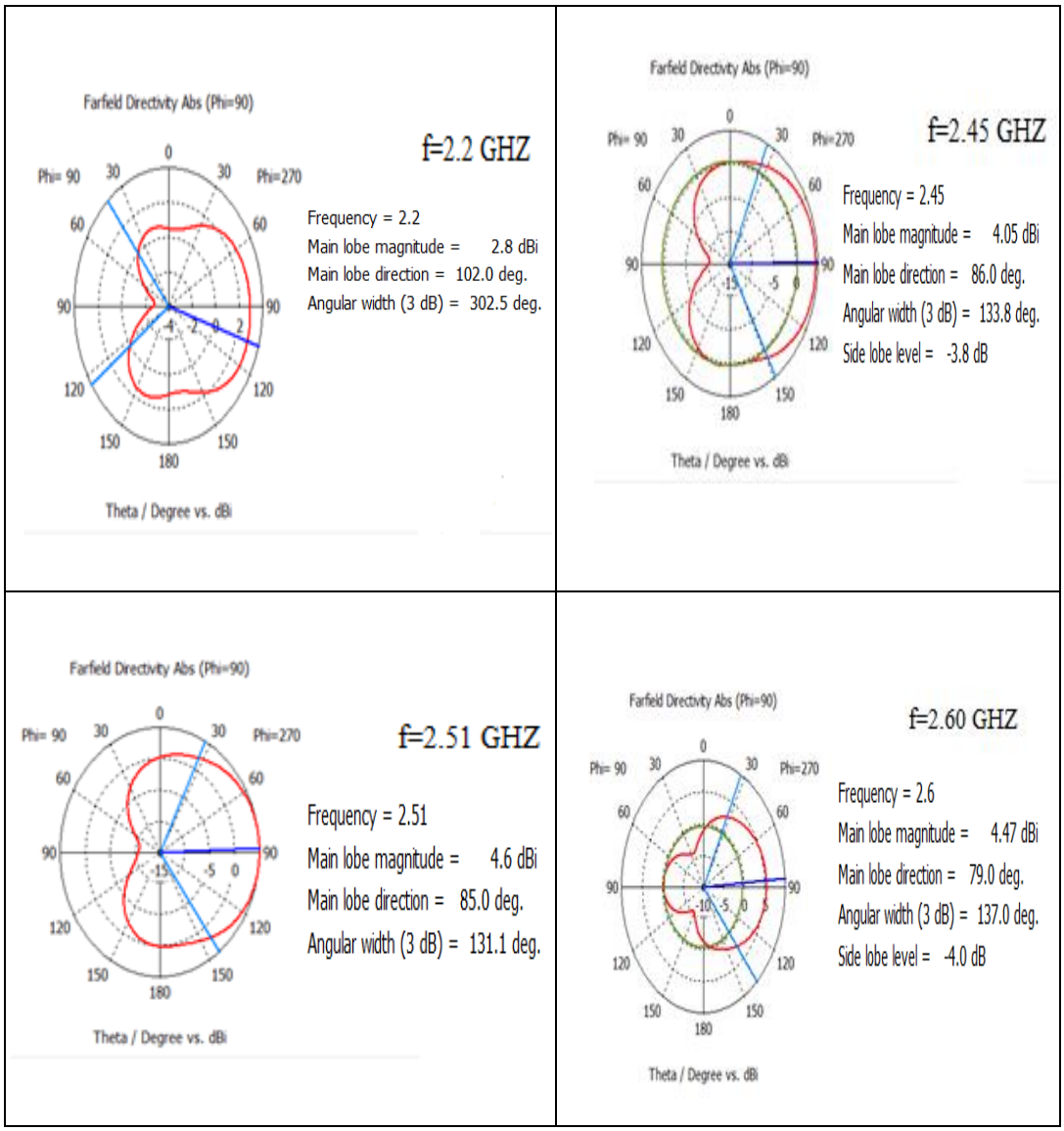

.

Figure(4.30): Simulated radiation patterns of state(1) for the antenna with microstrip segments at the bottom.

The radiation patterns for state(1) are reconfigured to the right side because the right triangle segment on the bottom is connected to the ground through switch1.

Figure (4.31) shows the return loss (S_{11}) for state (2) , the band width of the proposed antenna is (1.66-2.80) GHz.

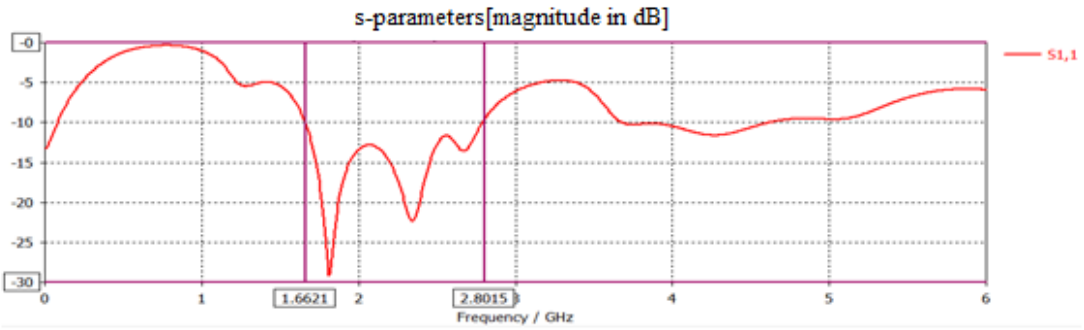

Figure(4.31): Simulated return loss S_{11} of state(2) for the antenna with microstrip segments at the bottom.

The radiation patterns are shown in the figure (4.32) of the proposed antenna at different frequencies.

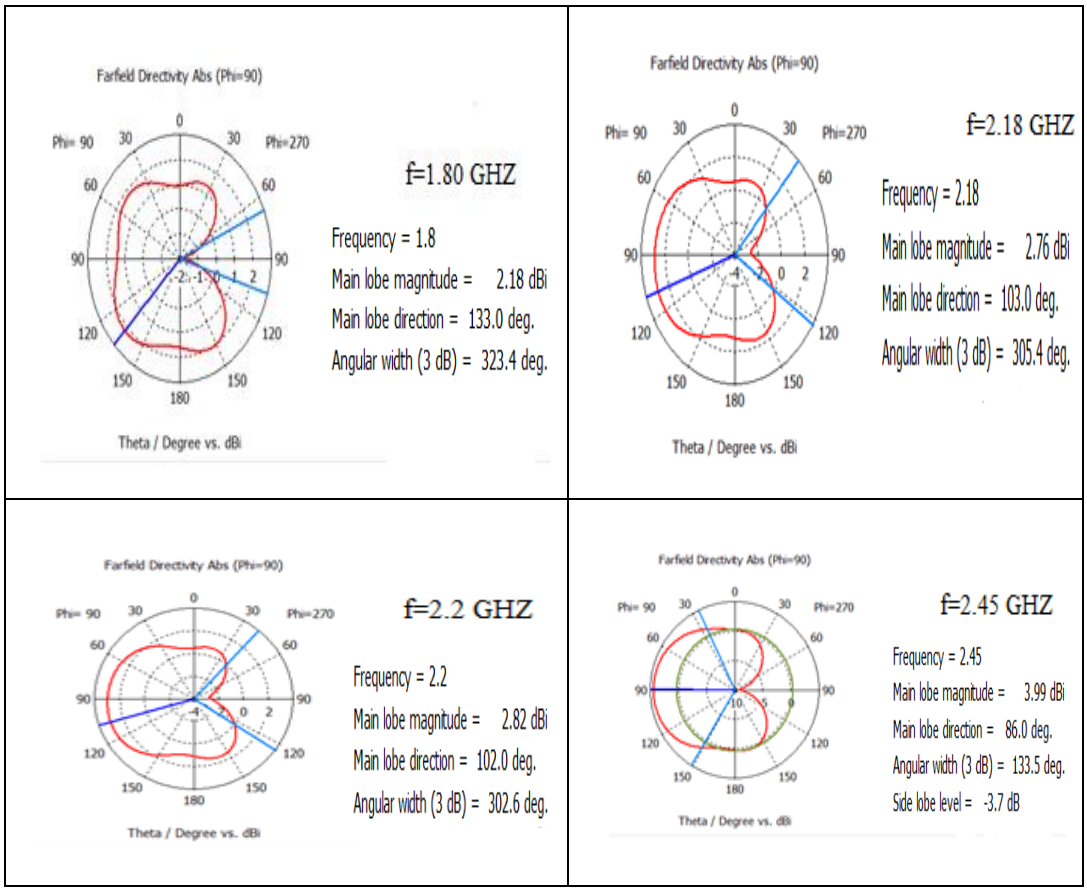

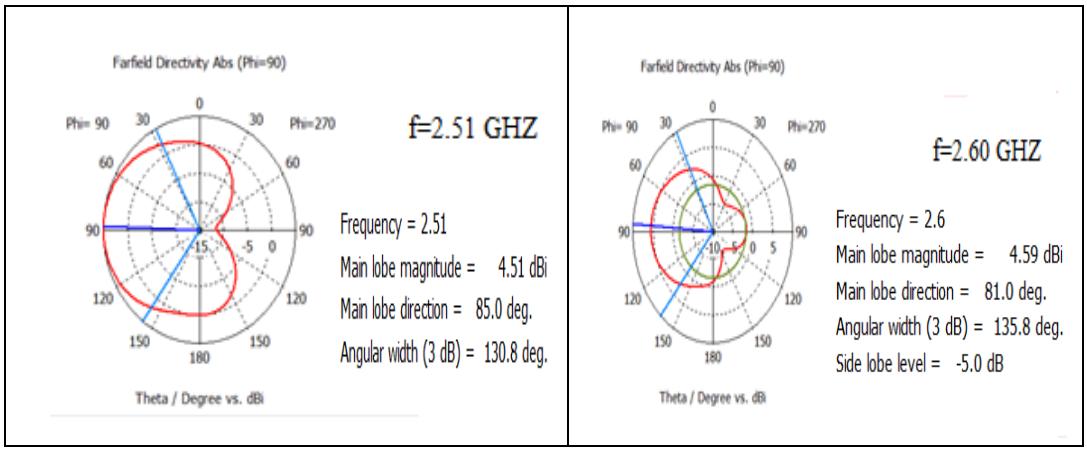

Figure(4.32): Simulated radiation patterns of state (2) for the antenna with microstrip segments at the bottom.

The radiation patterns for state(2) are reconfigured to the left side because the left triangle segment on the bottom is connected to the ground through switch2.

4.5 Design of the 3rd order Microstrip Bandpass Filter

This section will discuss the design of a 3rd order bandpass filter with open loop resonators and its specifications, equations, calculations and simulations.

4.5.1 Filter Design Specifications

The first step to design any filter is to identify the proposed filter specifications. The proposed filter is tunable and it operates in the frequency range (1.70-2.77)GHz band. Varactors will be used to shift center frequency through that band. The filter is initially designed with center frequency of 2.2GHz and a bandwidth of 120GHz. Later, it is tuned via varactors embedded within the resonators to other center frequencies.

Next step in filter design procedure is to find the element values of the corresponding low pass prototype filter for filter order of 3 which means that the number of resonators is n=3.

The filter's pass band ripple is assumed 0.04321dB, and from Table 3.1 the g-element values will be g_0=g_4=1, g_1=g_3=0.8516, g_2=1.1032. From Equation 3.17 the fractional bandwidth is FBW=120 MHz/2.20 GHz=5.45 %. External quality factors can be calculated from Equations 3.12 that will be Q_e =15.153. Coupling coefficients can be calculated from Equation 3.14 that will be K_{12}=K_{23}=0.0562.

So the filter calculations are shown in table (4.8).

Table (4.8): Proposed filter calculations

n	FWB	Q_e	K_{12}	K_{23}
3	5.45 %	15.153	0.0562	0.0562

4.5.2 The Single Resonator Design

The next step is to choose the shape of the resonator that is open loop resonator. Initially, design the resonator at center frequency 2.20GHz with adding three varactors within each resonator as shown in Figure (4.33). The value for these varactors are initially set to 1.16pF for the center frequency to be 2.2GHz. The final values of the design parameters of the resonator are presented in table (4.9).

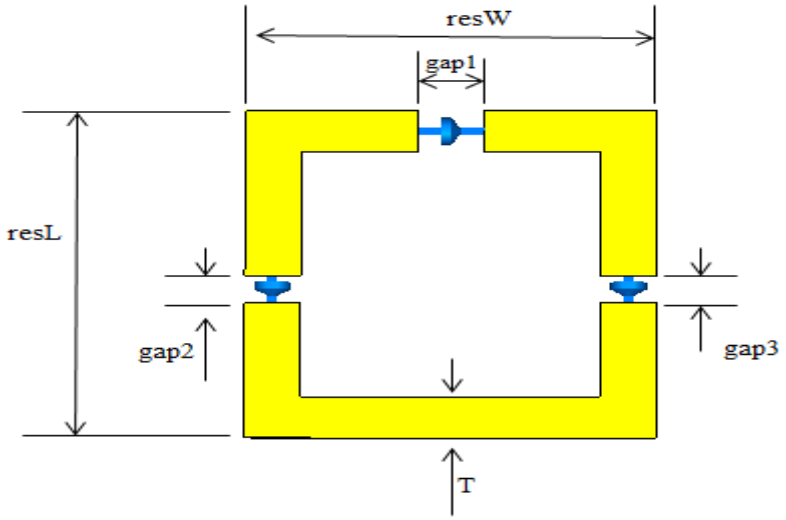

Figure (4.33): Single resonator with varactors

The dimensions for varactors are shown in the figure (4.34).

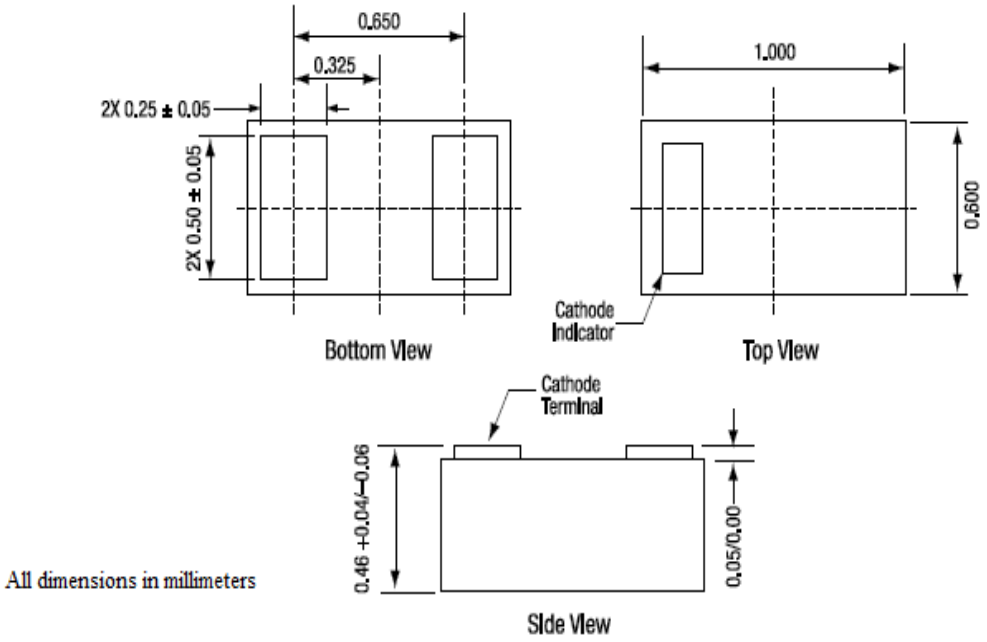

Figure(4.34): Varactor dimensions

Table (4.9): Dimensions of the proposed resonator.

Dimensions	(mm)
Substrate thickness	1.6
Width of resonator (resW)	11
Length of resonator (resL)	11.9
Width of gap1 (gap1)	1.78
Width of gap2 (gap2)	1
Width of gap3 (gap3)	1
Thickness of resonator (T)	1.50

Next step in filter design is determining the separation distance (feedX) between the port and first resonator that achieves the required external quality factor of Q_e= 15.153. See Figure (4.35). The results are shown in table (4.10) for different values of distance (d).

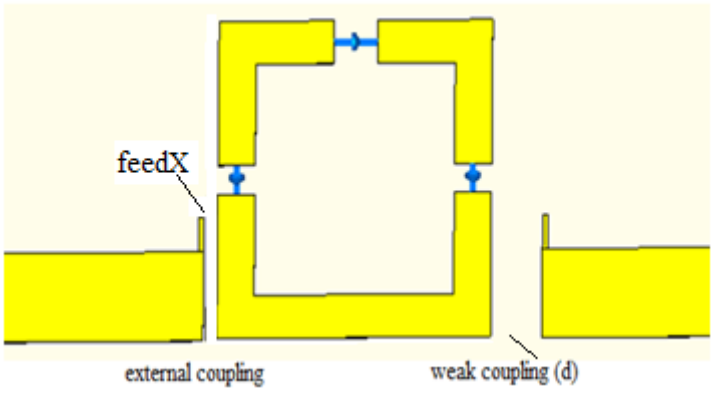

Figure(4.35): Structure of single resonator with port 2 is weakly coupled and port 1 is coupled

Table (4.10): External quality factor for coupled feeder with different spacing for Figure 4.35.

d in mm	*feedX* in mm	f_0 in GHz	BW_{3dB} in GHz	*Qe*
0.1	0.1	2.2	0.23	9.5
0.2	0.2	2.2	0.22	10
0.5	0.3	2.2	0.19	11.57
0.6	0.3	2.3	0.12	19.16
0.78	0.32	2.2	0.1372	15.66

At d=0.78 mm. The external quality factor Q_e=15.66 and this is approximately equal to calculated Q_e . Figure (4.36) shows how Q_e is obtained for the graph of S_{21}.

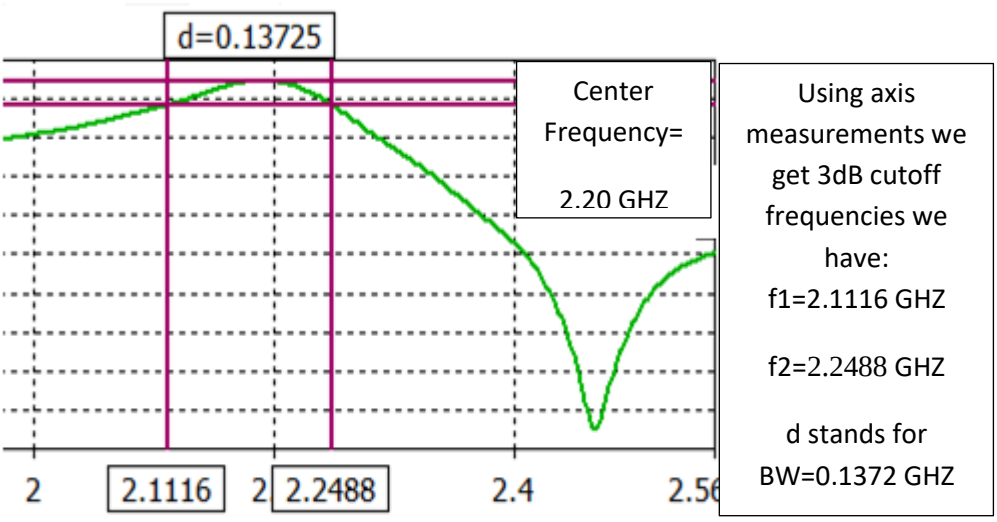

Figure(4.36): Simulated S_{21} of the first resonator

4.5.3 Coupled Resonator Design

After designing the single resonator and its feeder , the next step is to find the inter resonator coupling between two resonators to build the initial design of the filter. In this step it is needed to make both ports weakly coupled to calculate the coupling between two resonators by equation 3.14.

In this case parameter of interest is *S* which is the distance between the resonators. The two ports are weakly coupled as shown in Figure (4.37). Table (4.11) presents the coupling coefficients for different values of separation distance "S".

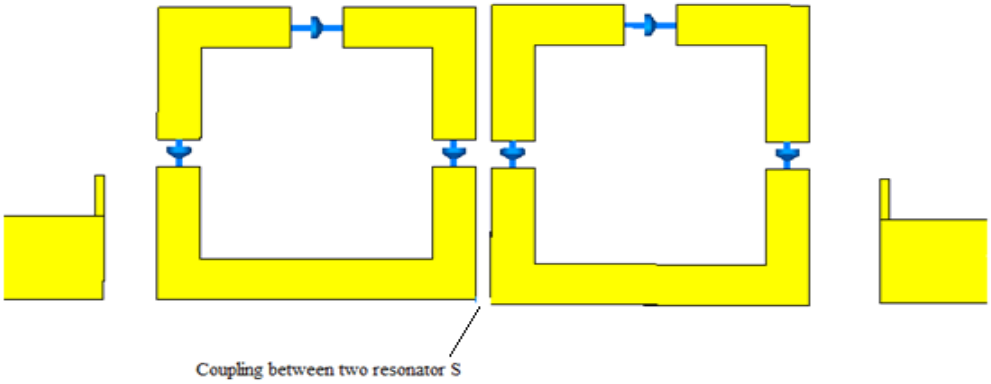

Figure(4.37): Structure of two resonators design with ports are weakly coupled and the resonators are coupled

Table (4.11): Coupling Coefficient for different values of "S" for two resonators design.

S (mm)	f_1 (GHZ)	f_2 (GHZ)	K
0.25	2.211	2.31	0.045
0.28	2.26	2.32	0.02727
0.30	2.25	2.324	0.0336
0.35	2.264	2.336	0.0327
0.34	2.166	2.288	0.0554
0.34	2.168	2.296	0.0581

0.32	2.18	2.24	0.0272
0.33	2.19	2.225	0.0159
0.24	2.18	2.22	0.01818
0.33	2.20	2.26	0.02727
0.31	2.17	2.22	0.0227
0.32	2.1116	2.2488	0.02834
0.33	2.175	2.26	0.0386
0.34	2.21	2.31	0.4545

The chosen value of the parameter "S" is S=0.34 mm , where the coupling coefficient at this value is k=0.0554 approximately equal to the required.

4.5.4 Final Third Order Filter Design

After completing steps in previous subsections, it is needed to build the initial design by integrating the three resonators together to form the filter structure as shown in Figure (4.38).

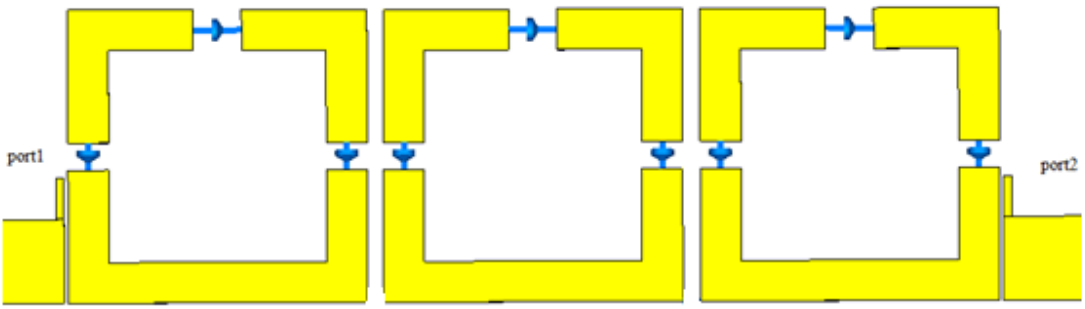

Figure(4.38): Initial structure of 3rd order filter

For initial response of the final structure of filter , the resulted return loss S_{11} and S_{21} are illustrated in the figure (4.39) at varactors value = 0.71 PF.

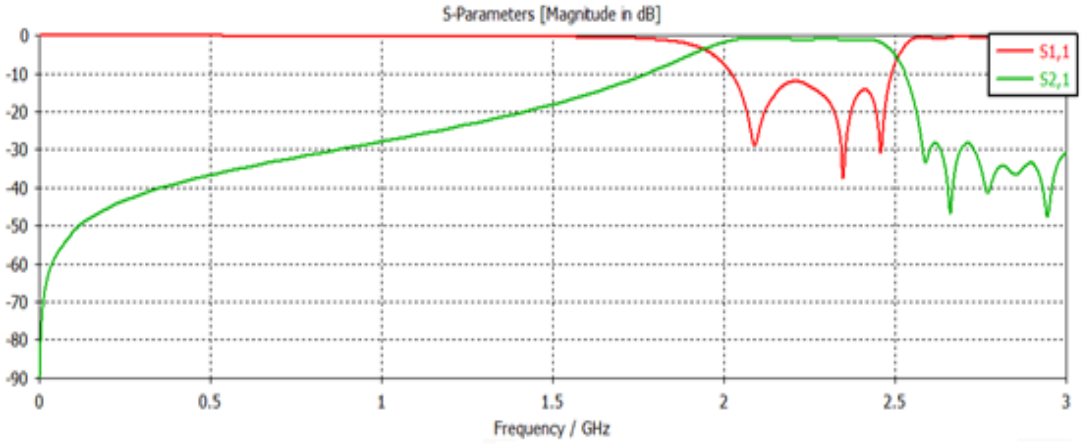

Figure(4.39): Simulated return loss S_{11} & S_{21} of initial structure

To reach the final filter specifications, some optimizations processes are done on the initial structure. Adding varactors between the resonators which are called (coupling varactors) to adjust the coupling between the resonators and to maintain the required bandwidth almost fixed for tuned different center frequencies. Figure (4.40) shows the final structure of 3rd order filter.

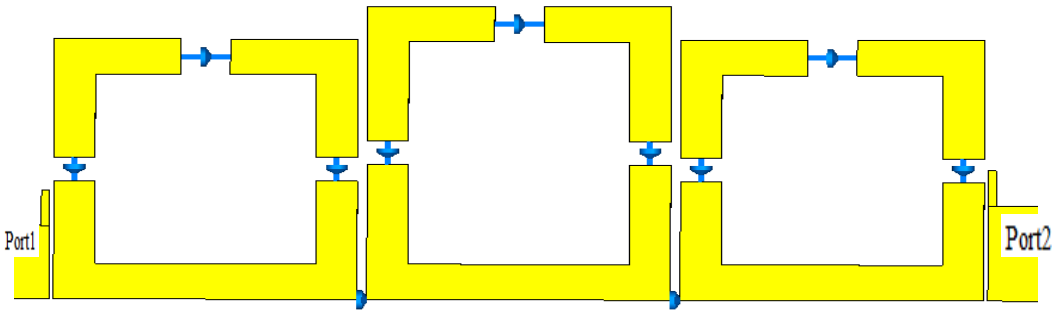

Figure(4.40): Final structure of 3rd order filter

The simulated return loss S_{11} & S_{21} for the final structure of 3rd order filter at center frequency 2.2 GHz are shown in the figure (4.41).

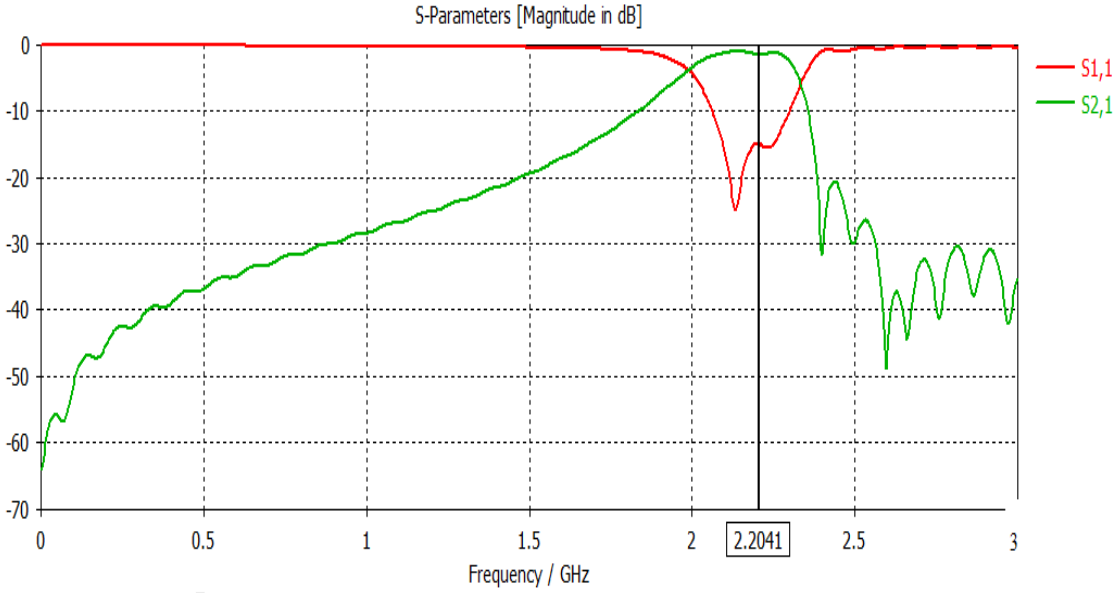

Figure(4.41): Simulated return loss S_{11} & S_{21} for the final structure at center frequency 2.20 GHz

Table (4.12) presents 4 states at different values of varactors and coupling varactors for the final structure 3rd order filter. Figure (4.42) shows the simulated return loss S_{21} at that states .

Table (4.12): 4 states at different values of varactors and coupling varactors.

State	Varactor (PF)	Coupling varactor (PF)	Center frequency (GHz)	Bandwidth (GHz)
1	0.33	0.23	2.7521	0.487
2	0.55	0.23	2.44	0.21
3	0.76	0.55	2.1918	0.24
4	1.34	2.10	1.70	0.23

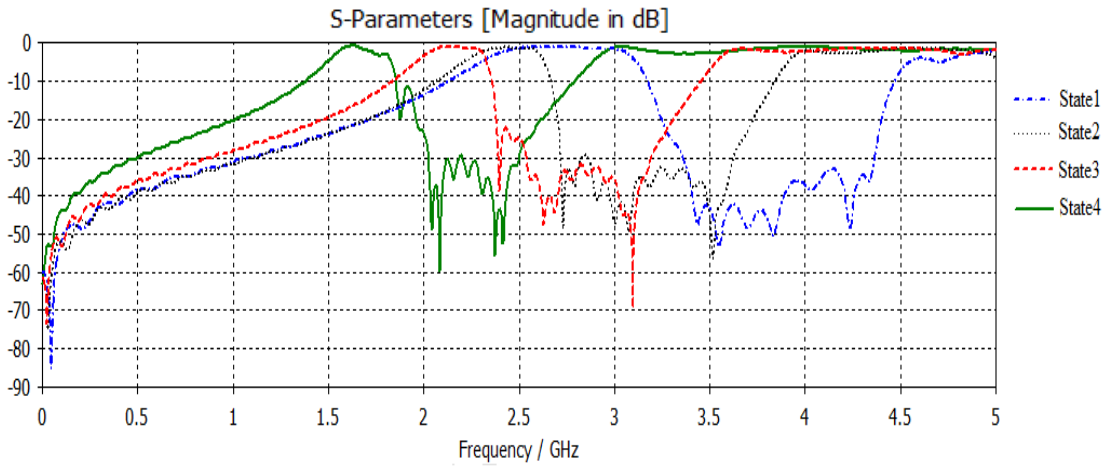

Figure(4.42): Simulated return loss S_{21}

4.6 Design Pattern and Frequency Reconfigurable Bow tie Antenna

The result from combining the pattern reconfigurable bow-tie antenna which was presented in section (4.4.2) with adding microstrip segments on the bottom and the microstrip 3rd order filter which was designed in section (4.5) is the proposed pattern and frequency reconfigurable bow-tie antenna

as shown in the figure (4.43). The matching operation between the antenna and the filter is done through the matching line.

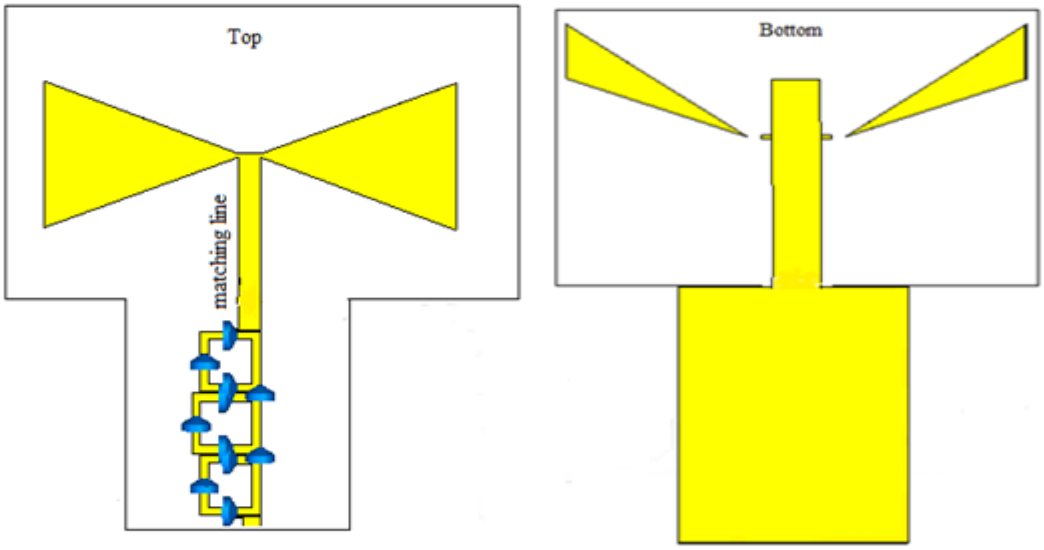

Figure(4.43): The proposed pattern and frequency reconfigurable bow-tie antenna

For state (0) , switch1 is OFF and switch2 is OFF at the bottom of substrate as shown in figure (4.44).

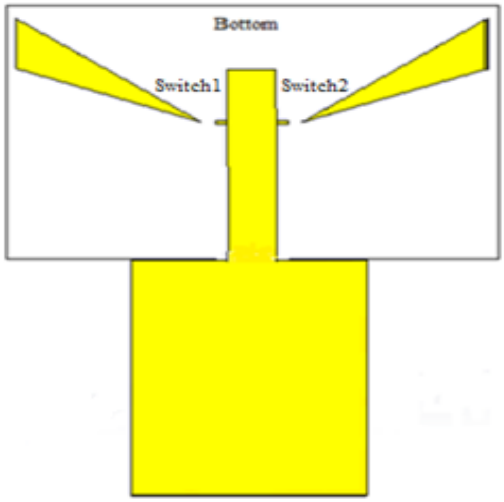

Figure(4.44): The proposed structure of state (0)

The simulated return loss S_{11} and radiation patterns of state (0) at different values of varactors and coupling varactors are shown in the following figures.

1) varactors =0.39 pF, coupling varactors=0.23 pF. The center frequency =2.75 GHz, bandwidth=0.48 GHz. The antenna operates at (2.44-2.93) GHz band.

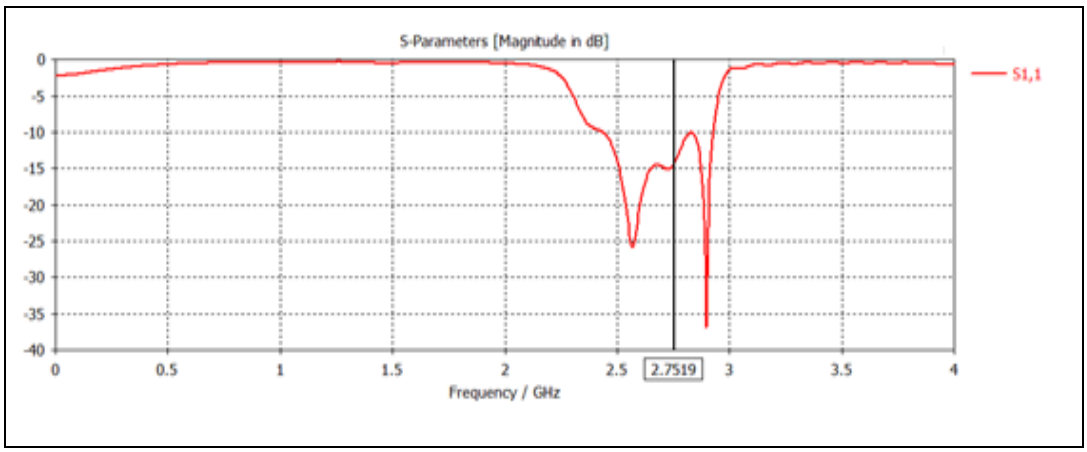

Figure(4.45): Simulated return loss S_{11} of state (0) at varactors=0.39 pF, coupling varactors=0.23 pF

The radiation patterns are shown in figure (4.46) at different frequencies of that band.

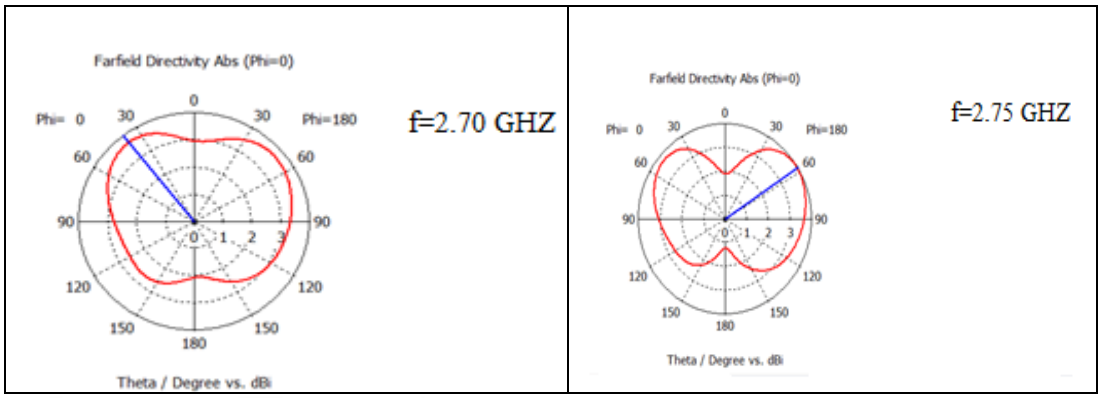

Figure(4.46): Simulated radiation patterns of state (0) at varactors=0.39 pF,coupling varactors=0.23 pF

2) varactors =0.45 pF , coupling varactors=0.23 pF. The center frequency =2.60 GHz , bandwidth=0.38 GHz. The antenna operates at (2.31-2.79) GHz band.

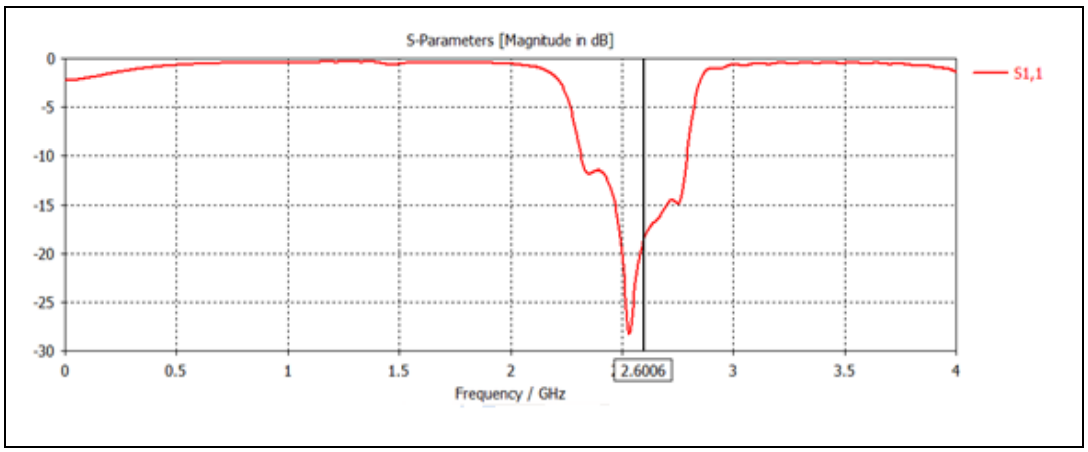

Figure(4.47): Simulated return loss S_{11} of state (0) at varactors=0.45 pF, coupling varactors=0.23 pF

The radiation patterns are shown in figure (4.48) at different frequencies of that band.

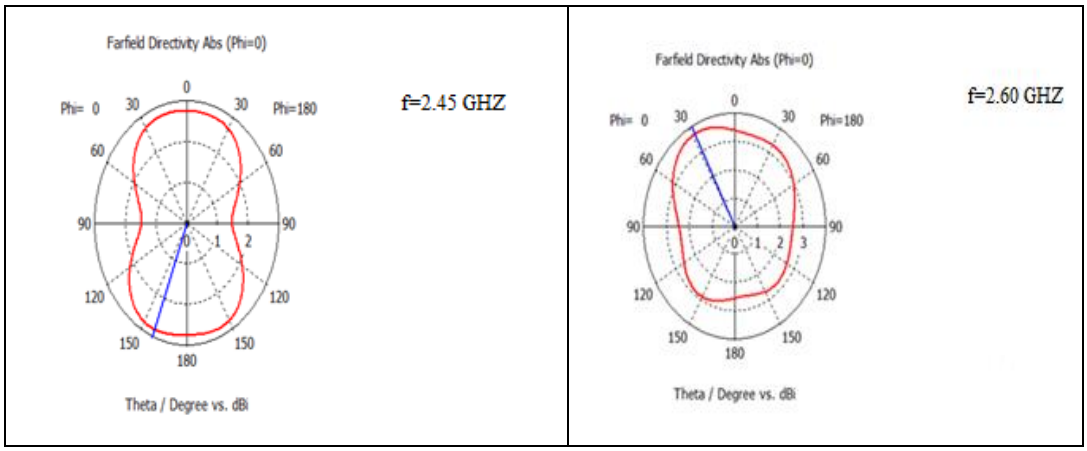

Figure(4.48): Simulated radiation patterns of state (0) at varactors=0.45 pF,coupling varactors=0.23 pF

3) varactors =0.64 pF , coupling varactors=0.29 pF. The center frequency =2.31 GHz , bandwidth=0.24 GHz. The antenna operates at (2.20-2.44) GHz band.

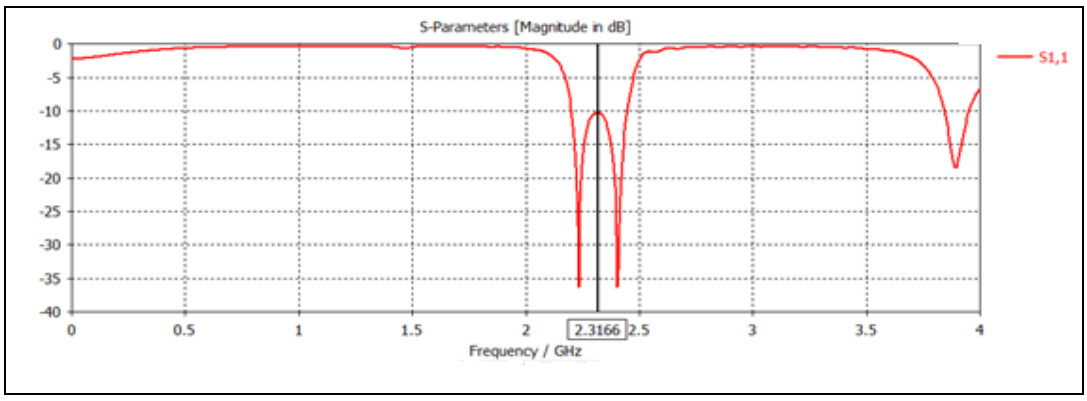

Figure(4.49): Simulated return loss S_{11} of state (0) at varactors=0.64 pF, coupling varactors=0.29 pF

The radiation patterns are shown in figure (4.50) at different frequencies of that band.

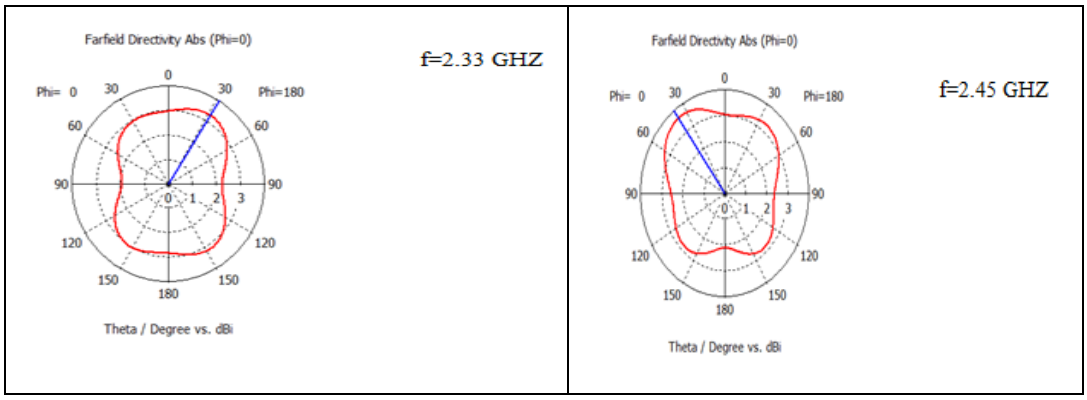

Figure(4.50): Simulated radiation patterns of state (0) at varactors=0.64 pF,coupling varactors=0.29 pF

For state (1) , switch1 is ON and switch2 is OFF at the bottom of substrate as shown in figure (4.51).

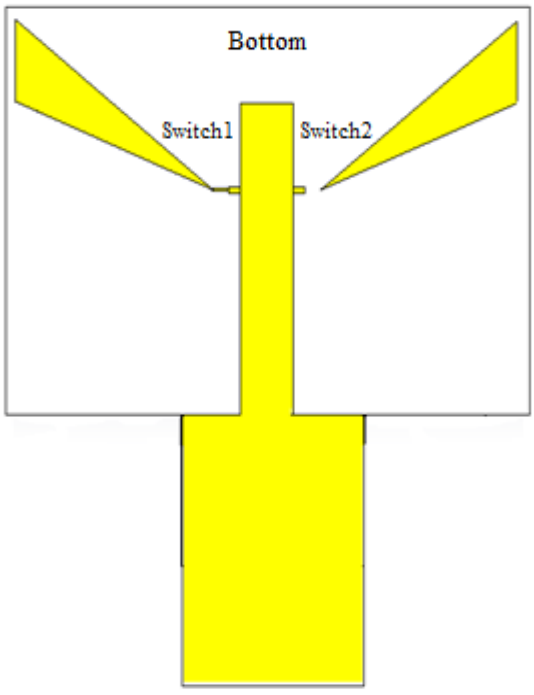

Figure(4.51): Proposed structure of state(1)

The simulated return loss S_{11} and radiation patterns of state (1) at different values of varactors and coupling varactors are shown in the following figures.

1) varactors =0.39 pF , coupling varactors=0.23 pF. The center frequency =2.75 GHz, bandwidth=0.54 GHz. The antenna operates at (2.38-2.92) GHz band.

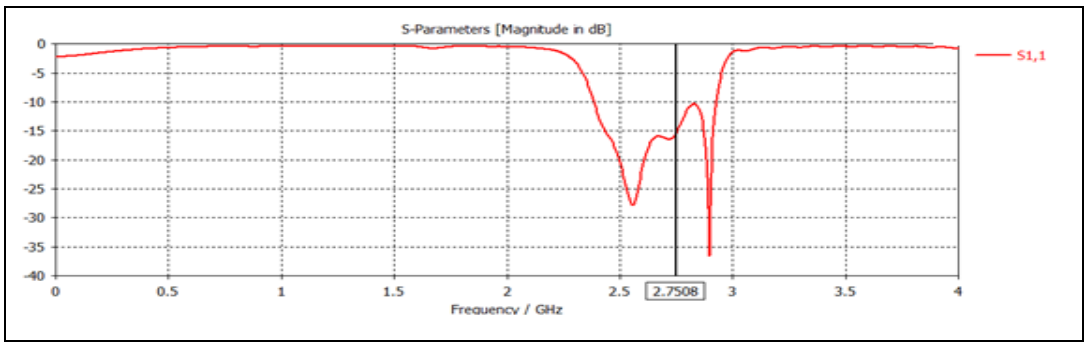

Figure(4.52): Simulated return loss S_{11} of state (1) at varactors=0.39 pF, coupling varactors=0.23 pF

The radiation patterns are shown in figure (4.53) at different frequencies of that band.

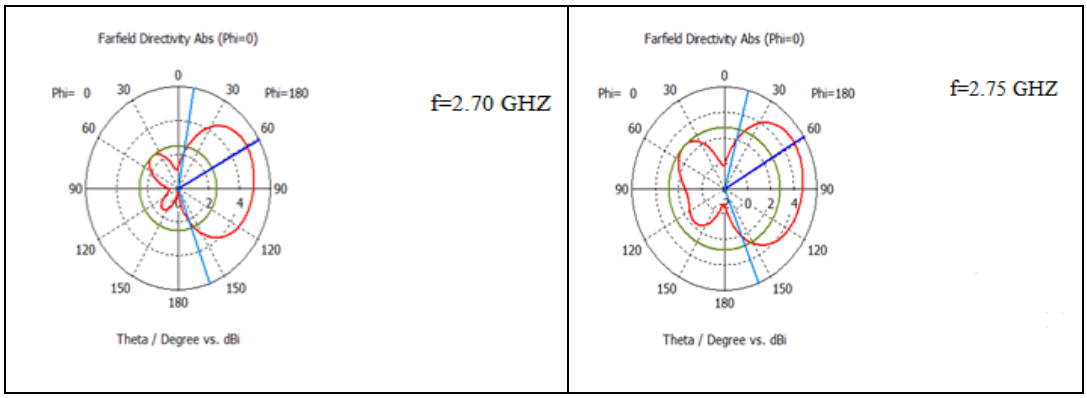

Figure(4.53): Simulated radiation patterns of state (1) at varactors=0.39 pF,coupling varactors=0.23 pF

2) varactors =0.45 pF , coupling varactors=0.23 pF. The center frequency =2.60 GHz , bandwidth=0.44 GHz. The antenna operates at (2.34-2.79) GHz band.

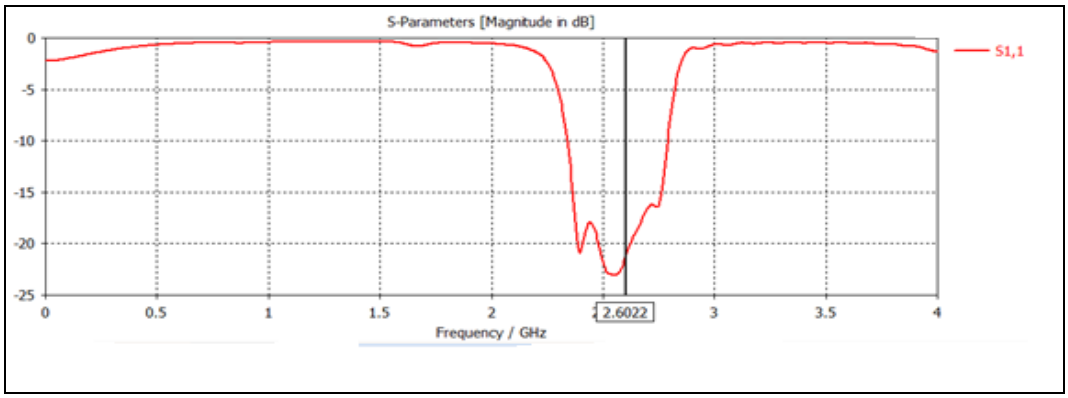

Figure(4.54): Simulated return loss S_{11} of state (1) at varactors=0.45 pF, coupling varactors=0.23 pF

The radiation patterns are shown in figure (4.55) at different frequencies of that band.

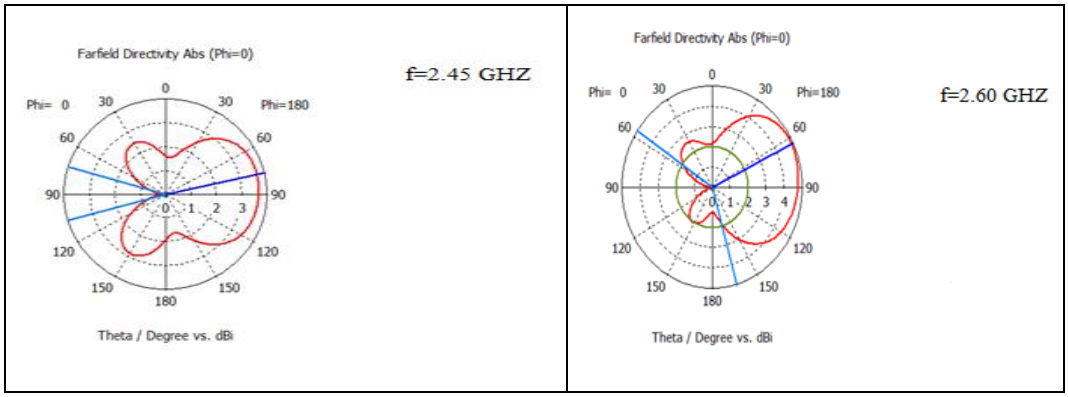

Figure(4.55): Simulated radiation patterns of state (1) at varactors=0.45 pF,coupling varactors=0.23 pF

3) varactors =0.64 pF , coupling varactors=0.29 pF. The center frequency =2.33 GHz , bandwidth=0.24 GHz. The antenna operates at (2.22-2.45) GHz band.

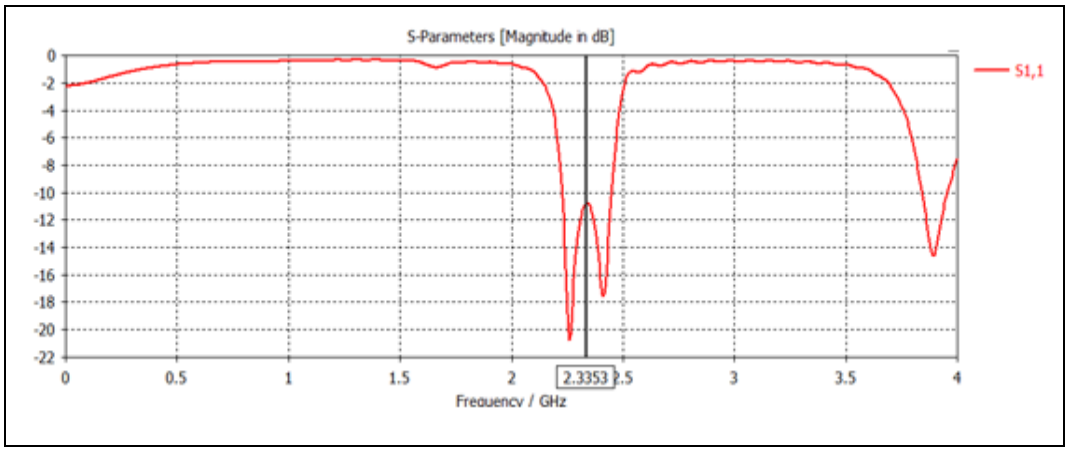

Figure(4.56): Simulated return loss S_{11} of state (1) at varactors=0.64 pF, coupling varactors=0.29 pF

The radiation patterns are shown in figure (4.57) at different frequencies of that band.

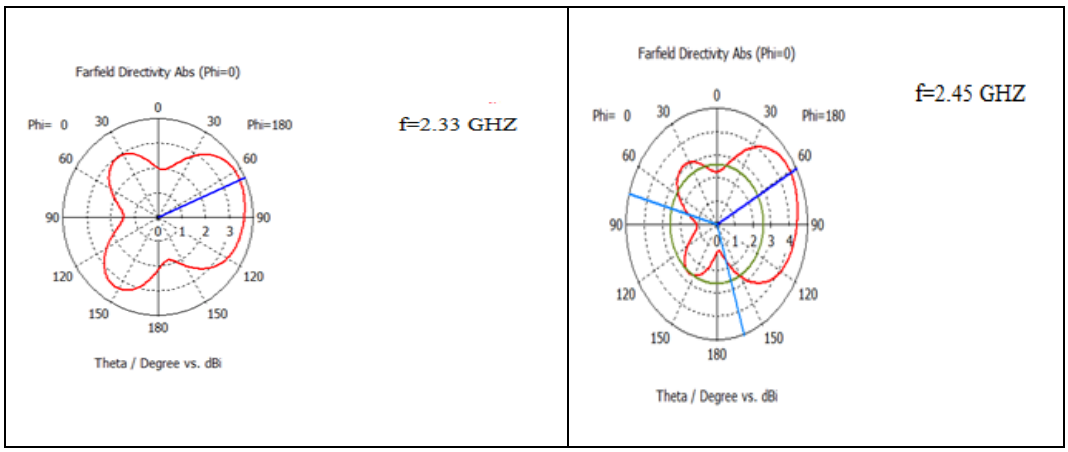

Figure(4.57): Simulated radiation patterns of state (1) at varactors=0.64 pF,coupling varactors=0.29 pF

For state (2) , switch1 is OFF and switch2 is ON at the bottom of substrate as shown in figure (4.58).

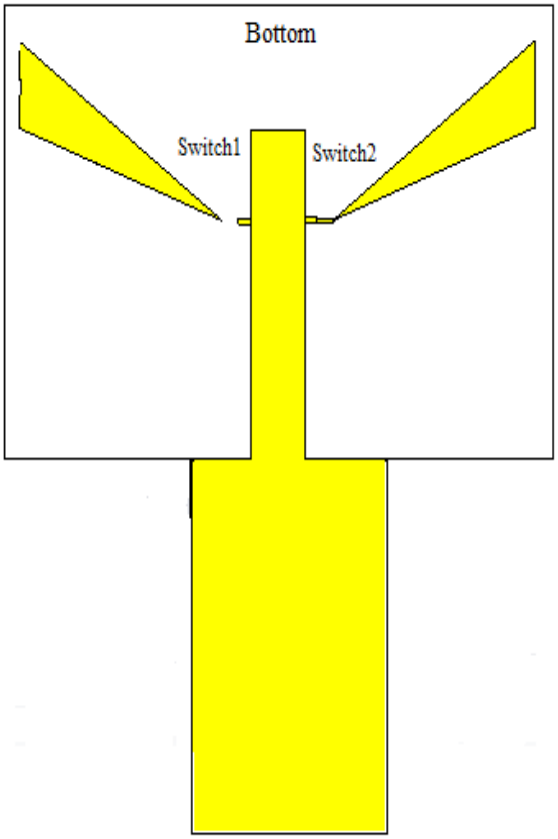

Figure(4.58): Proposed structure of state(2)

The simulated return loss S_{11} and radiation patterns of state (2) at different values of varactors and coupling varactors are shown in the following figures.

1) varactors =0.39 pF , coupling varactors=0.23 pF. The center frequency =2.75 GHz, bandwidth=0.54 GHz. The antenna operates at (2.38-2.92) GHz band.

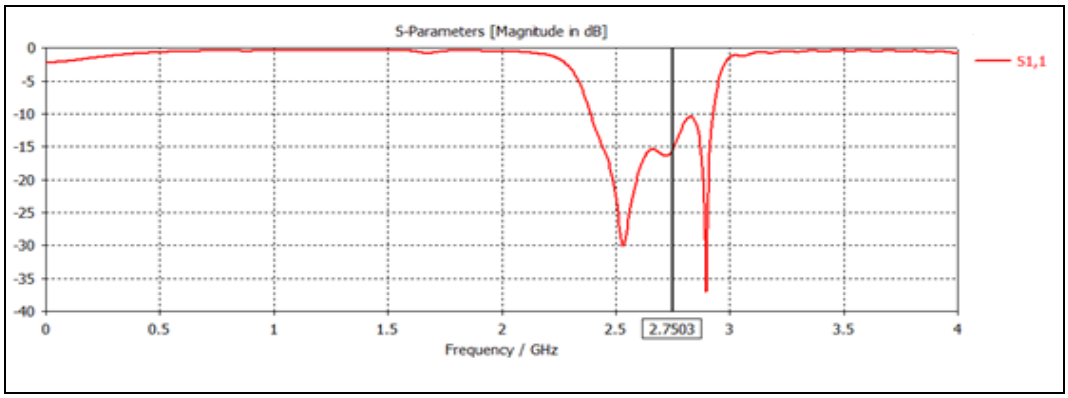

Figure(4.59): Simulated return loss S_{11} of state (2) at varactors=0.39 pF, coupling varactors=0.23 pF

The radiation patterns are shown in figure (4.60) at different frequencies of that band.

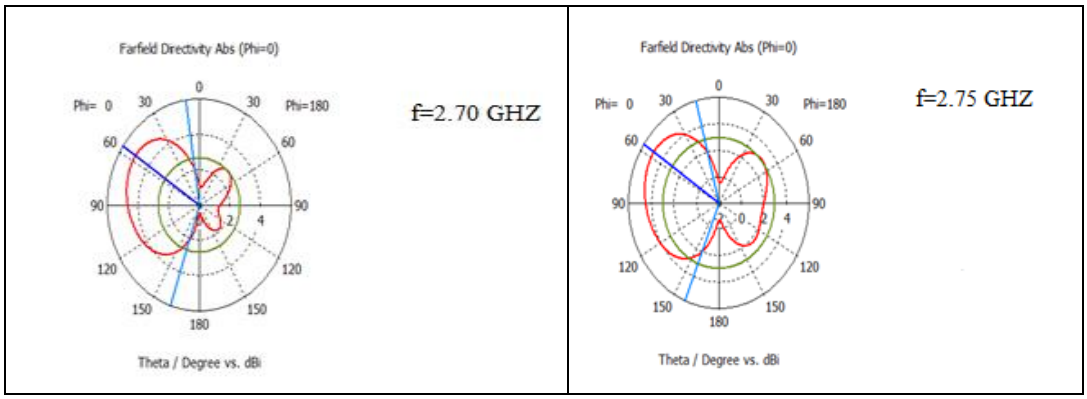

Figure(4.60): Simulated radiation patterns of state (2) at varactors=0.39 pF,coupling varactors=0.23 pF

2) varactors =0.45 pF , coupling varactors=0.23 pF. The center frequency =2.60 GHz, bandwidth=0.44 GHz. The antenna operates at (2.34-2.78) GHz band.

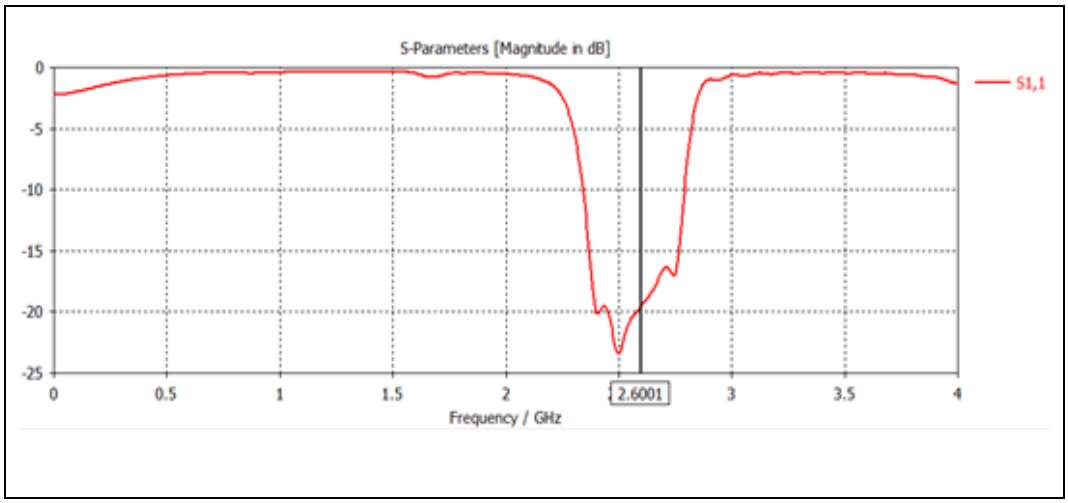

Figure(4.61): Simulated return loss S_{11} of state (2) at varactors=0.45 pF, coupling varactors=0.23 pF

The radiation patterns are shown in figure (4.62) at different frequencies of that band.

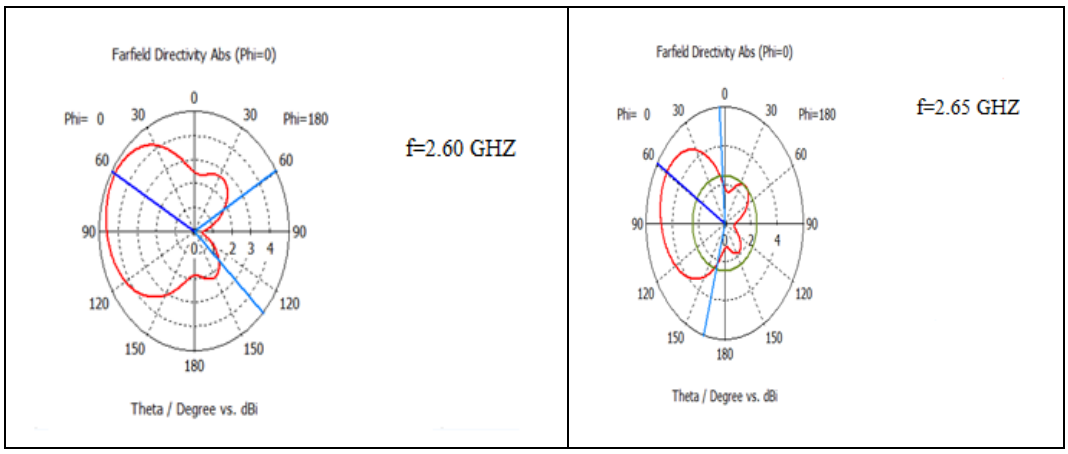

Figure(4.62): Simulated radiation patterns of state (2) at varactors=0.45 pF,coupling varactors=0.23 pF

3) varactors =0.64 pF , coupling varactors=0.29 pF. The center frequency =2.33 GHz, bandwidth=0.24 GHz. The antenna operates at (2.21-2.45) GHz band.

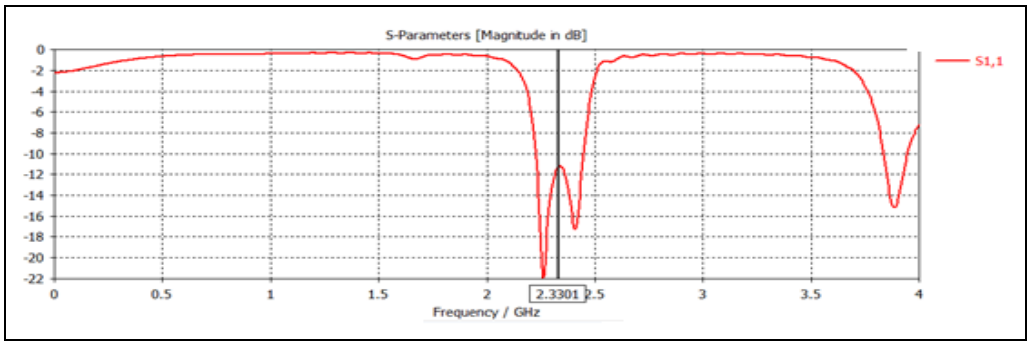

Figure(4.63): Simulated return loss S_{11} of state (2) at varactors=0.64 pF, coupling varactors=0.29 pF

The radiation patterns are shown in figure (4.64) at different frequencies of that band.

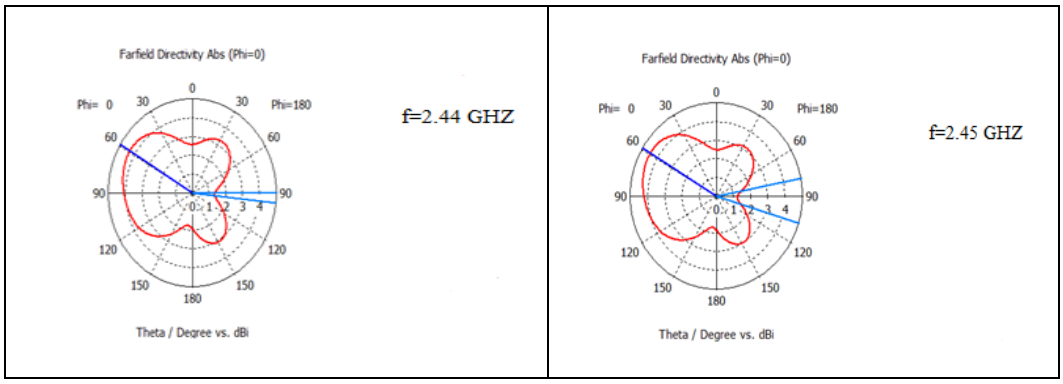

Figure(4.64): Simulated radiation patterns of state (2) at varactors=0.64 pF,coupling varactors=0.29 pF

4.7 Conclusion

In this chapter , pattern reconfigurable bow-tie antenna is successfully designed with several methods without affect on other antenna specifications. Also, frequency reconfigurable bow tie antenna is successfully designed. Pattern reconfigurable is achieved by adding microstrip segments to antenna that can be connected to the main antenna through switches to operate in many states. A microstrip 3^{rd} order filter is successfully designed, then it used for frequency reconfigurable by combining the antenna and the filter together. Finally, pattern and frequency reconfigurable bow-tie antenna is successfully designed.

Chapter 5

Conclusions and Future Work

Chapter 5

Conclusions and Future Work

Conclusions

A novel single element reconfigurable Bow-Tie antenna design was presented and it can be operated in frequency range (1.70-2.77) GHz. The antenna return loss, radiation pattern were simulated using CST simulation software .

Reconfigurable pattern capability has been added to the antenna by using extra microstrip triangular segments on top in one design and on bottom in another design. The radiation pattern can then be re-configured using PIN switches that connect the segments to the ground with switched to ON. By those switches the antenna can be operated in three states, in each state , the radiation patterns are reconfigured to different shapes. The antenna radiation patterns can be shaped to concentrate energy in specific directions while minimizing the gain in other unwanted directions without affecting the band width of the antenna. For the purpose of frequency reconfiguration, microstrip 3^{rd} order filter is successfully designed. The result of combining the antenna and the filter is pattern and frequency reconfigurable Bow-Tie antenna which it can be operated in multiple frequency ranges with radiation patterns reconfigurable on all frequency ranges.

Future Work

Fabricate and test the proposed structures using PIN switches and compare the results with the simulation results.

The reconfigurable single-element antenna can be arranged in an array. Reconfigurable arrays can be used to enhance the performance of future wireless networks at fraction of the cost of using complex phased arrays.

Work on other pattern and frequency reconfigurable Bow-Tie antenna models to further reduce the size.

References

References

Zuo, S., Wu, W. J., & Zhang, Z. Y. (2013). A simple filtering-antenna with compact size for WLAN application. *Progress In Electromagnetics Research Letters*, *39*, 17-26.

Xuelin, L. I. U., Xiaolin, Y. A. N. G., & Fangling, K. O. N. G. (2015). A Frequency-Reconfigurable Monopole Antenna with Switchable Stubbed Ground Structure. *Radioengineering*, *24*.

Ou Yang, J. (2008). A novel radiation pattern and frequency reconfigurable microstrip antenna on a thin substrate for wide-band and wide-angle scanning application. *Progress In Electromagnetics Research Letters*, *4*, 167-172.

Majid, H. A., Abd Rahim, M. K., Hamid, M. R., & Ismail, M. F. (2014). Frequency reconfigurable microstrip patch-slot antenna with directional radiation pattern. *Progress In Electromagnetics Research*, *144*, 319-328.

Kaushal, A., & Tyagi, S. (2015). MICRO STRIP PATCH ANTENNA ITS TYPES, MERITS DEMERITS AND ITS APPLICATIONS.

John, M., Shynu, S. V., & Ammann, M. J. (2010, April). A pattern reconfigurable slot antenna with hybrid feed. In *Antennas and Propagation (EuCAP), 2010 Proceedings of the Fourth European Conference on* (pp. 1-4). IEEE.

Yuan, X. (2012). Multi-Functional Reconfigurable Antenna Development by Multi-Objective Optimization.

Nikolaou, S., Bairavasubramanian, R., Lugo, C., Carrasquillo, I., Thompson, D. C., Ponchak, G. E., ... & Tentzeris, M. M. (2006). Pattern and frequency reconfigurable annular slot antenna using PIN diodes. *IEEE Transactions on Antennas and Propagation*, *54*(2), 439-448.

Ndujiuba, C. U., & Oloyede, A. O. (2015). Selecting Best Feeding Technique of a Rectangular Patch Antenna for an Application. *International Journal of Electromagnetics and Applications*, *5*(3), 99-107.

Singh, G., & Singh, J. (2012). Comparative Analysis of Microstrip Patch Antenna With Different Feeding Techniques. In *International Conference on Recent Advances and Future Trends in Information Technology, iRAFIT*.

Girase, N., Tiwari, R., Sharma, A., & Singh, H. (2014). Design and Simulation of Slotted Rectangular Microstrip Patch Antenna. *International Journal of Computer Applications*, *103*(17).

Hong, J. S. G., & Lancaster, M. J. (2004). *Microstrip filters for RF/microwave applications* (Vol. 167). John Wiley & Sons.

Roslee, M., Subari, K. S., & Shahdan, I. S. (2011, December). Design of bow tie antenna in CST studio suite below 2GHz for ground penetrating radar applications. In *RF and Microwave Conference (RFM), 2011 IEEE International*(pp. 430-433). IEEE.

Johari, E., & Singh, H. K. Comparative Study of Bow-tie and Bow-tie Slot Antenna for Ku band Application.

Sayidmarie, K. H., & Fadhel, Y. A. (2013). A planar self-complementary bow-tie antenna for UWB applications. *Progress in Electromagnetics research C*, *35*, 253-267.

Pan, K. C., Brown, D., Subramanyam, G., Penno, R., Jiang, H., Zhang, C. H., ... & Cerny, C. (2012). A reconfigurable coplanar waveguide bowtie antenna using an integrated ferroelectric thin-film varactor. *International Journal of Antennas and Propagation*, *2012*.

Pratishthan, V. (2012). Design of bow-tie microstrip antenna with fractal shape for W-Lan application. *Int. J. Electron. Commun. Technol. IJECT*, *3*(4), 445-449.

Chakravarthy, J. I., Akram, P. S., & Ramana, T. V. Design of Bowtie Antenna for Wideband Applications. *vol*, *2*, 858-861.

Harchandra, B., & Singh, R. Analysis and Design of Bowtie Antenna with Different Shapes and Structures.

El-Aziz, D. A., Abouelnaga, T. G., Abdallah, E. A., El-Said, M., & Abdo, Y. S. (2016). Analysis and Design of UHF Bow-Tie RFID Tag Antenna Input Impedance. *Open Journal of Antennas and Propagation*, *4*(02), 85.

Alqaisy, M. A., Chakrabraty, C., Ali, J., Alhawari, A. R., & Saeidi, T. (2016). Reconfigurable Bandwidth and Tunable Dual-Band Bandpass Filter Design for Ultra-Wideband (UWB) Applications. *Electromagnetics*, *36*(6), 366-378.

Akkaraekthalin, P., Hongdamnuen, S., & Vivek, V. (2006, December). A bandpass filter with cross-coupled L-shape folded resonators for compact size and spurious suppression. In *Microwave Conference, 2006. APMC 2006. Asia-Pacific* (pp. 1162-1165). IEEE.

Marimuthu, J., Abbosh, A., & Henin, B. (2013, July). Compact bandpass filter with sharp cut-off using grooved parallel coupled microstrip lines. In *Antennas and Propagation Society International Symposium (APSURSI), 2013 IEEE* (pp. 792-793). IEEE.

Goyal, A., & Kaur, A. Analysis and Design of Microstrip Bandpass Filter.

Ilchenko, M. E., Sizranov, V. A., Pereverzeva, L. P., & Poplavko, Y. M. (1999, September). Bandpass compact microstrip filters for wireless communication. In *Microwave Conference, 1999. Microwave & Telecommunication Technology. 1999 9th International Crimean [In Russian with English abstracts]* (pp. 238-240). IEEE.

AHMED, E. S. (2013). Design of Tri-Band Bandpass Filter Based On Quad-Sections SIR Resonator for Wireless Applications. *Wseas Transactions on Communications*, *12*(12), 641-650.

Fathelbab, W. M. (2008). A new class of reconfigurable microwave bandpass filters. *IEEE Transactions on Circuits and Systems II: Express Briefs*, *55*(3), 264-268.

NASRAOUI, H., MOUHSEN, A., & EL AOUFI, J. A New Design of a Band pass Filter at 2.45 GHz Based on Microstrip Line Using the Property of the Double Negative Metamaterials.

Tu, W. H. (2010). Switchable microstrip bandpass filters with reconfigurable on-state frequency responses. *IEEE Microwave and Wireless Components Letters*, *20*(5), 259-261.

Cansever, C. (2013). Design of a Microstrip Bandpass Filter for 3.1-10.6 GHz Uwb Systems.

Tu, W. H. (2010, May). Switchable microstrip bandpass filters with reconfigurable frequency responses. In *Microwave Symposium Digest (MTT), 2010 IEEE MTT-S International* (pp. 1488-1491). IEEE.

Lugo, C., & Papapolymerou, J. (2006). Six-state reconfigurable filter structure for antenna based systems. *IEEE Transactions on Antennas and Propagation*, *54*(2), 479-483.

Perruisseau-Carrier, J., & Pardo-Carrera, P. (2010, April). Recent developments on reconfigurable band-filtering antennas. In *Antennas and Propagation (EuCAP), 2010 Proceedings of the Fourth European Conference on* (pp. 1-4). IEEE.

Qin, P. Y., Wei, F., & Guo, Y. J. (2015). A wideband-to-narrowband tunable antenna using a reconfigurable filter. *IEEE Transactions on Antennas and Propagation*, *63*(5), 2282-2285.

Zamudio, M., Tawk, Y., Costantine, J., Kim, J., & Christodoulou, C. G. (2011, April). Integrated cognitive radio antenna using reconfigurable band pass filters. In *Antennas and Propagation (EUCAP), Proceedings of the 5th European Conference on* (pp. 2108-2112). IEEE.

Tawk, Y., Christodoulou, C. G., Zamudio, M., Nassar, E., & Costantine, J. (2013, July). The integration of reconfigurable filters for the matching of wideband antennas. In *Antennas and Propagation Society International Symposium (APSURSI), 2013 IEEE* (pp. 2211-2212). IEEE.

Tawk, Y., Zamudio, M. E., Costantine, J., & Christodoulou, C. G. (2012, March). A cognitive radio reconfigurable "filtenna". In *Antennas and Propagation (EUCAP), 2012 6th European Conference on* (pp. 3565-3568). IEEE.

Tawk, Y., Costantine, J., & Christodoulou, C. G. (2012). A varactor-based reconfigurable filtenna. *IEEE Antennas and Wireless Propagation Letters*, *11*, 716-719.

Zamudio, M. E., Tawk, Y., Christodoulou, C. G., & Costantine, J. (2012, July). Embedding a reconfigurable band-pass/band-stop filter into an antenna. In *Antennas and Propagation Society International Symposium (APSURSI), 2012 IEEE* (pp. 1-2). IEEE.

Kumar, N., Raju, P. A., & Behera, S. K. (2015, April). Frequency reconfigurable microstrip antenna for cognitive radio applications. In *Communications and Signal Processing (ICCSP), 2015 International Conference on* (pp. 0370-0373). IEEE.

Brito-Brito, Z., Llamas-Garro, I., Pradell-Cara, L., & Corona-Chavez, A. (2008, October). Microstrip switchable bandstop filter using PIN diodes with precise frequency and bandwidth control. In *Wireless Technology, 2008. EuWiT 2008. European Conference on* (pp. 286-289). IEEE.

Mansoul, A., & Ghanem, F. (2013, July). Frequency and bandwidth reconfigurable monopole antenna for cognitive radios. In *Antennas and Propagation Society International Symposium (APSURSI), 2013 IEEE* (pp. 680-681). IEEE.

CAI, X. T., WANG, A. G., Ning, M. A., & Wen, L. E. N. G. (2012). Novel radiation pattern reconfigurable antenna with six beam choices. *The Journal of China Universities of Posts and Telecommunications*, *19*(2), 123-128.

Li, H. (2012). Design and simulation of pattern reconfigurable antenna based on RF-MEMS. In *SpaceOps 2012* (p. 1267444).

Christodoulou, C. G., Tawk, Y., Lane, S. A., & Erwin, S. R. (2012). Reconfigurable antennas for wireless and space applications. *Proceedings of the IEEE*, *100*(7), 2250-2261.